Tutor
Dr. José María Gutiérrez González
Departament Enginyeria Química i Química Analítica

Màster en Enginyeria Química

Treball Final de Màster

Design of a plant for polylactic acid polymer manufacture

Diseño de una planta de fabricación del polímero ácido poliláctico

Andrea Canzobre Silva

February 2020

UNIVERSITAT DE BARCELONA
Dos campus d'excel·lència internacional
B:KC Barcelona Knowledge Campus
HUBC Health Universitat de Barcelona Campus

To the optimist, the glass is half full. To the pessimist, the glass is half empty. To the engineer, the glass is twice as big as it needs to be.

Unknown

A todos los profesores, tanto de la Universidad de Santiago como la Universidad de Barcelona, que me han acompañado y aconsejado durante este largo recorrido. En especial a aquellos que han sabido transmitir su conocimiento de una manera distinguible y fomentar mi interés por la Ingeniería Química.

Especial mención al Dr. Gutiérrez tanto a nivel profesional como personal, por su dirección a lo largo de este proyecto.

A mis padres, hermanas e Isidro, por todo su tiempo y apoyo incondicional a lo largo de mi carrera universitaria.

Report

INDEX

SUMMARY

Over the last decades, plastic demand has grown increasingly at a level such that it is unavoidable for current society. Plastics versatility and unique properties makes them suitable for all kind of industries, which currently suppose a threat to both environment and human health at every stage, right from their production to their end-of-life scenario.

Bioplastics stand out in this way as a greener solution able to reduce carbon footprint, with high recycling value and complete biodegradability or compostability. In this regard, polylactic acid constitutes a biodegradable and bio-based bioplastic which is gaining attention in the recent years, as it possesses the potential to replace conventional fossil-based plastics in food packaging and other applications. Continuous research and development in this field has made possible the polylactic acid mass production at a competitive cost, promising a sustainable future and overcoming the accumulation of plastic waste in landfills.

The purpose of this project is the development of the Master's Degree Final Project with which it is intended to apply for the Master Degree in Chemical Engineering by the "Universidad de Barcelona"

The project is focused on the design of a plant for polylactic acid polymer manufacture from lactic acid solutions. Based on a comparison among different polylactic acid market players and the increasing demand reflected in the market analysis, the plant has a fixed annual production capacity of 60,000 tonnes and operates 330 days per year.

A selection of the most adequate synthesis of the manufacturing process, according to product necessities, is conducted through a bibliographic research. By means of mass and energy balances, stream flows and operating conditions of each equipment are determined in order to carry out the basic design of the plant, in which the main design parameters and dimensions are detailed.

A falling film evaporator type of reactor is selected for the condensation polymerization of lactic acid into polylactic acid of low molecular weight, as it provides the advantages required to optimize the polymer production due to its high surface area to volumetric hold up ratio, which reduces evaporation residence time. A detailed design of this equipment, based on heat transfer and mechanical design, is carried out and reflected in the equipment lay-out.

As a final point, the control system of the plant is studied in order to supress the influence of external disturbances, ensuring the stability of the chemical process and the optimization of the process performance. The control system stands for the discussion of the control philosophy and the establishment of the control loops of the plant, described through a P&I diagram which includes the engineering details of the equipment as well as instruments, piping, valves and fittings.

Keywords: *polylactic acid, biopolymer, packaging, production process, basic engineering.*

1. INTRODUCTION

It is needless to say that conventional fossil-based plastics have become an integral part of our daily lives, as plastics are designed in order to satisfy different human needs in thousands of end products, becoming its use unavoidable for current society. Its production has increased more than 357 million metric tons since 1950, and this can be explained if we take into consideration its unique properties such as durability, lightness or strength, together with their low production cost, allowing its use in several applications from all kind of industries. (Filho et al., 2020)

Out of all kind of plastics applications, packaging is seen as the most frequent of plastic use, representing more than 39% of the total demand. Polymers such as polyethylene, polypropylene or polyethylene terephthalate are remarkable in this field due to its low cost, which makes them suitable for the mass production of plastic packaging. (Brizga et al., 2020)

However, most of these plastics are of petrochemical origin and therefore depend on non-renewable sources such as natural gas, crude oil or coal, leading to significant environmental impacts. In addition, plastic pollution in soil and marine ecosystems due to a far from perfect management of plastic disposal pose a serious threat to not only living organisms, but also human health. The main problem is that durability, from this point of view, turns then into a disadvantage, in a way such that these non-degradable plastics end up in the environment for hundreds of years, slowly becoming microplastics and having its consequently negative and adverse effects.

Research into the development of renewable sources of raw materials for plastic production as well as better alternatives to plastic disposal is being encouraged in the recent years. In this way, bioplastics stand out as a good alternative to prevent these mentioned problems and address environmental concerns, being part of the BBI's programme to replace at least 30% of conventional plastics with bio-based and biodegradable plastics by 2030. (RameshKumar et al., 2019)

A common definition for bioplastic is a material that is bio-based and/or biodegradable, distinguishing three different categories of bioplastics:

- Bio-based and biodegradable materials
- Biodegradable materials of petrochemical origin
- Bio-based and non-biodegradable materials

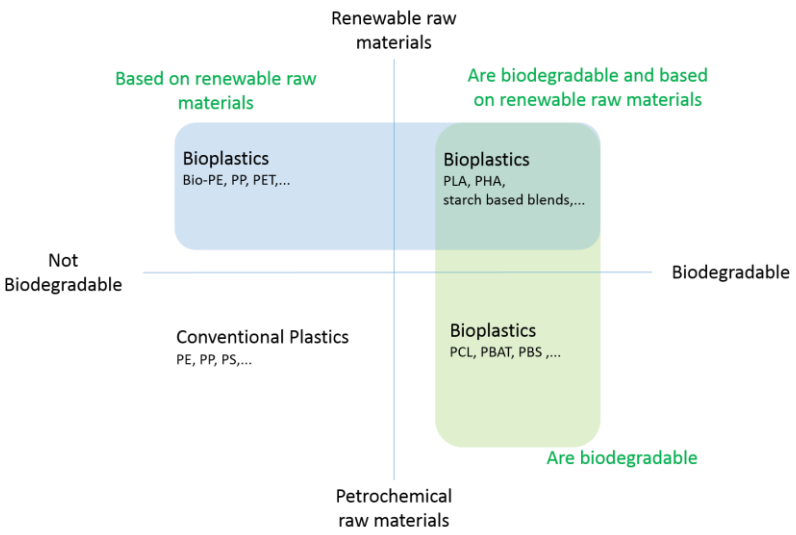

Figure 1. Bioplastic classification (University of Applied Science, 12/12/20 via Axipolymer)

Contrary to bio-based non-biodegradable plastics, fossil-based biodegradable plastics can be seen as a good alternative in a short-term reference as it may help to reduce landfill plastic problems and disposal. However, there is controversy as it is not environmentally friendly, and its production cost is sensitive to the fluctuation of crude oil. On the contrary, biodegradable and bio-based materials are polymers derived from sustainable sources with environmental credit, which is crucial for a sustainable future, especially in the packaging field, where products provide a short service life which leads to a wide range of environmental problems.

Bioplastics demand is experimenting a continuous growth over the last years fastened by government regulations and consumer preferences, yet its production still represents a small share in the global market due to the lack of scalability and productivity of production technologies in comparison to fossil-based routes, which increase its production cost and restrains its competitiveness.

Polylactic acid (PLA) is a biodegradable and bio-based aliphatic polyester derived from renewable sources. PLA is seen lately as the most viable polymer to replace non-degradable fossil-based polymers due to technological improvements in productivity and functionality, with current polymer processing technologies such as injection molding, extrusion, thermoforming and even 3D printing method.

Increasing production efficiency and competitive marketplace, linked to positive public perception, is driving PLA market over the years. Its orientation towards mass production at industrial scale at a competitive price slightly higher than conventional plastics, as well as its excellent properties makes it a suitable polymer able to replace well-known polymers such as polystyrene and polypropylene in packaging and other applications.

As there is an urgent need of substitution on fossil-fuel based plastics, the environmental impact of bioplastics is now in the spotlight. End-of-life phase and building

blocks production is a critical phase of these materials and LCA of bioplastics as well as greenhouse gases (GHG) measurement and non-renewable energy use is getting a major importance lately.

Regarding the environmental impact of PLA, if a comparison with conventional bioplastics is taken, LCA calculations reveals that long term PLA could become a CO_2 sink and contribute to a net reduction in GHG, since the CO_2 generated during the process is balanced with the CO_2 taken during the corn growing stage. (Henton et al., 2005)

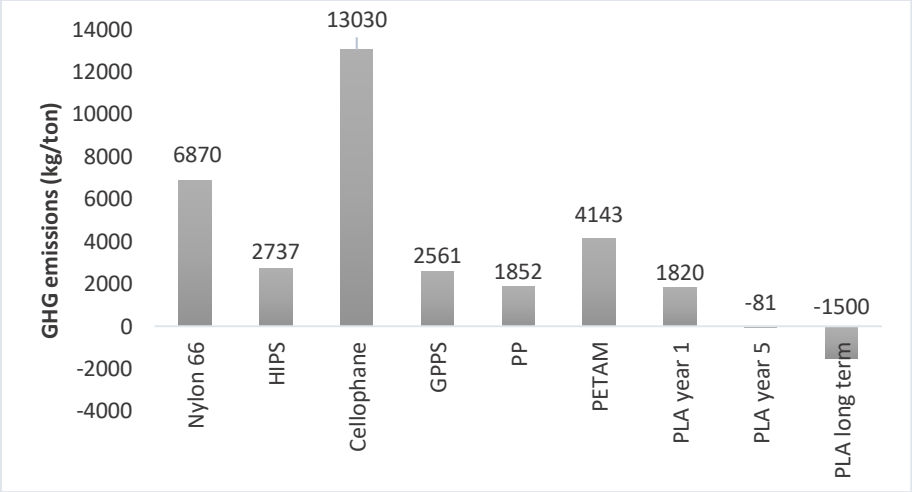

Figure 2. GHG emissions for production of different polymers (Henton et al., 2005)

On the contrary, benefits achieved by CO_2 uptake could be despised attending to water and land footprints. Substitution of all current conventional plastics production for packaging purposes with PLA bioplastic would require an extra 61 million ha of land and 388.8 billion m^3 of water, which could make PLA to be seen not suitable for fossil-based plastics substitution. (Brizga et al., 2020)

Nevertheless, PLA shows a greater recyclability than other type of plastics, as it can be hydrolysed with water to form its monomer, which can be later purified and polymerized again to remake PLA. Organic contamination in food packaging could also be seen as a restrain for PLA recycling cycle. However, this polymer can also be naturally composted with complete degradation in less than a few weeks under typical conditions. Moreover, the problematic of land and water use can also be solved with what so called second-generation bioplastics, which lies on the idea of being produced from renewable waste streams not suitable for food nor feed.

Bearing all the above mentioned in mind, it can be said efforts towards green chemistry will make possible the conventional plastic replacement with biopolymers in a near future. Technological advances in search of higher efficiencies and reduction of land and water footprint, together with further improvement of bioplastics end-of-life will lead to a positive impact not only economic, but also with environmental credit, which makes the design of a plant of this scale an interesting proposal making possible the transition to a production of sustainable bioplastics.

2. JUSTIFICATION AND OBJECTIVES

In search of a path towards the replacement of conventional plastics by bioplastics in the packaging field, the final objective of this project is to design a plant for polylactic acid polymer manufacture from lactic acid aqueous solutions.

The main motivation that has led to design of a plant of one of the most promising bioplastics is the positive impact of the process at environmental level, by producing not only a bio-based but also biodegradable material for its use in plastic packaging. In this way, the profitable and the sustainable vision of the chemical industry will act for the benefit of society and the planet.

In order to develop this main objective, the following chapters have been established:

1. **Market analysis**

   A market research is carried out in order to establish the production scale and annual capacity of the plant, the main properties and characteristics of raw materials and the quality of the final product, which are the main conclusions of this chapter.

2. **Selection of the production process**

   The synthesis of the manufacturing process will be selected on this chapter based on a bibliographic research in order to select the reaction pathway which is more adequate to the product necessities.

   Once selected, a comparative study among different patents of the selected method will be carried out with the objective of selecting the process conditions that best fit into the process.

   The main conclusions will be described through a PFD and the mass and energy balances of the process.

3. **Basic design of the production plant**

   In this chapter the main equipment is dimensioned. The main conclusions will be the equipment's specification sheets containing the main parameters and operating conditions as results.

4. **Instrumentation and control**

   The instrumentation and control stands for the discussion of the control philosophy and the establishment of the control loops. The main result will be the P&ID.

5. **Detailed design of a falling film evaporator**

   A detailed design of a falling film evaporator, where the polycondensation reaction takes place, is carried out. The lay-out, openings and dimensions will be detailed.

3. MARKET ANALYSIS

3.1. Scope of the study

The main objective of this market research is the analysis of the current economic situation, as well as the future forecast in the market, in order to previously justify the feasibility of carrying out the design project of a PLA manufacturing plant. These situations are determined by various factors that will be studied in this chapter, such as the evolution of the prices, market volatility, and the interaction between different continent markets or the factors that have caused such evolution.

In this chapter, a market study of bioplastics is introduced in order to enhance the importance of polylactic acid, the main product, out of the rest of bioplastics. Also a market study of lactic acid, used as a raw material for the production of polylactic acid, will be carried out in order to deduce the production and demand of polylactic acid.

All the information collected comes from various sources dedicated to in-depth study of the economic aspects that condition the products of interest.

3.2. Lactic acid market definition

Lactic acid is a compound manufactured either through chemical synthesis or biological fermentation, widely used as an acidulant, flavour enhancer, and shelf-life expender in foods and beverages. Lactic acid also acts as the raw material for ethyl lactate, an environmentally friendly solvent, and what is important to this chapter and it is witnessing significant attention since recent years, lactic acid also serves as a monomer for the manufacture of biodegradable polylactic acid. (IHS Markit, 2018)

In 2018, the global lactic acid market size valued at USD 2.64 billion and it is expected to grow at a compound annual growth rate (CARG) of 18.7% from 2019 to 2025. Out of the global lactic acid consumption, food and beverage applications accounted for the largest share in 2018 as lactic acid and its salts serve as acidulants and preservatives, respectively. PLA manufacture was the second in importance, expected to be leading application for lactic acid by 2023. (IHS Markit, 2018)

PLA manufacture accounted for 28.3% of the revenue share and this can be attributed to its rising use as a packaging material. Besides being a biodegradable bioplastic and being made from renewable sources, PLA also exhibits unique thermal and mechanical properties comparable to conventional plastics and so it is driving the market of lactic acid, expected to continue increasing over the forecast period. (Grandview Research, 2019)

Some market restraints are linked to the fluctuation in the cost of the raw material which has increased lactic acid prices and so hampering the industry growth over the forecast period. However, as commented above, production of biodegradable polymers as well as lactate solvents coming from renewable sources, combined with limited supply of

petrochemical feedstock will rise lactic acid demand in the future. (Grandview Research, 2019)

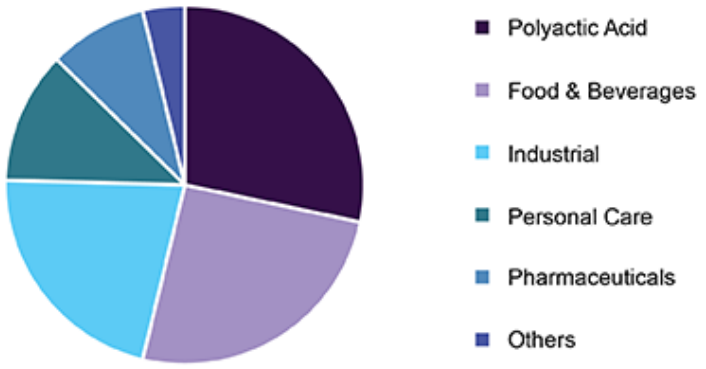

Figure 3. Global lactic acid market revenue by application, 2018 (Grandview Research, 2019)

If we take a region insight, North America emerged as the largest consumer of lactic acid in 2018. PLA manufacture was the largest segment in this region, followed by food and beverages, industrial and pharmaceutical end uses. (IHS Markit, 2018)

Asia and Oceania are the next on the list of lactic acid consuming region. It is food and beverages applications the ones that drive the consumption while PLA production and industrial applications play smaller roles. Despite this situation, consumption of lactic acid for PLA manufacture in this region is expected to grow at double-digit rates during 2018-2023. (IHS Markit, 2018)

Food and beverages end use is also driving Western Europe lactic acid consumption. This is due to a limited PLA production capacity despite it is expected to grow in the forecast period. (IHS Markit, 2018)

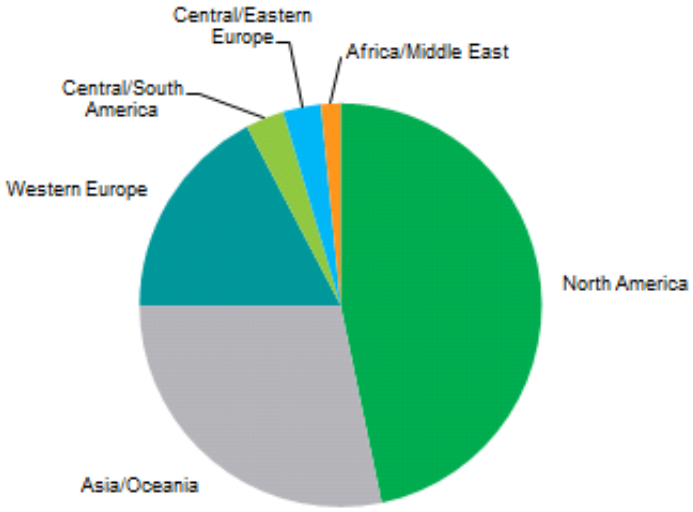

Figure 4. World consumption of lactic acid, 2018 (IHS Markit, 2020)

Companies tend now to invest in research and development for manufacturing lactic acid which is driving market conditions. Some of the key companies and market players are Corbion, which attained the first market position in 2018, followed by NatureWorks LLC, Galactic, Henan Jindan Lactic Acid Technology Co., Ltd. and Synbra Technology BV. (Grandview Research, 2019)

3.3. Bioplastics market definition

As it has been mentioned before, bioplastics are plastics that are bio-based, biodegradable or have both of these properties. We can highlight among all bioplastics, those that are bio-based and biodegradable plastics, such as polylactic acid (PLA), polybutylene succinate (PBS) and polyhydroxyalkanoates (PHA), and those that are bio-based and non-biodegradable such as polyethylene (PE) or polyethylene terephthalate (PET). This bio-based plastics are derived from renewable feed-stocks and so are eco-friendly which tends to shift the manufacturer for production of bioplastics.

As we can see in Figure 5, bioplastics are present in a variety of industries including packaging, textile, consumer goods, electrical and electronics amongst others. Packaging lead the global market with a share of 62.4% in 2019 and this is due to particular bioplastic properties such as gloss, antistatic behaviour and good printability which are driving the market. (Grandview Research, 2020)

More specifically, biodegradable polymer market is focused in the food packaging, dishes, cutlery and plastic bags market, which are the segments that are majorly driving the global market demand, and those responsible for the expected growth in the coming years. (IHS Markit, 2018)

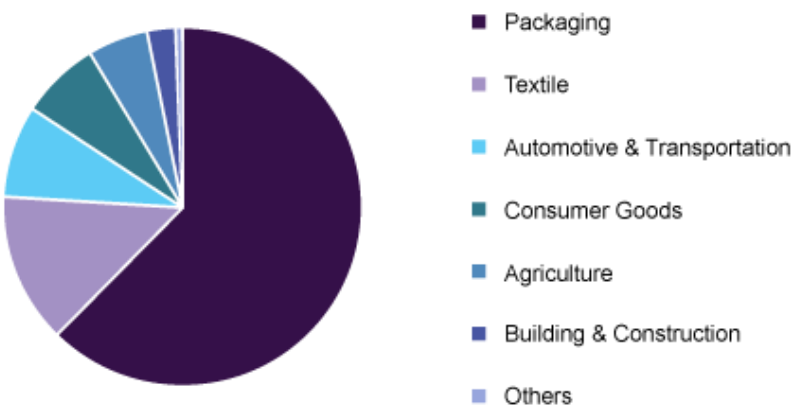

Figure 5. Global bioplastics market share by application, 2019 (Grandview Research, 2020)

In 2019, the global bioplastics market size was valued at USD 8.3 billion in 2019 and it is expected to grow at a compound annual growth rate (CARG) of 16.1% from 2020 to 2027. (Grandview Research, 2020)

On one hand, non-biodegradable plastics represented a share of 54.96% in 2019 and it is expected to maintain its leading position over the forecast years. This is due to its similar

properties to conventional plastics which led to its applications in a wide range of products increasing its demand. On the other hand, biodegradable plastics are expected to register the fastest CARG from 2020 to 2027, leading PLA and starch compounds the global consumption of biodegradable polymers accounting for 46% and 42%, respectively, in 2017. (Grandview Research, 2020)

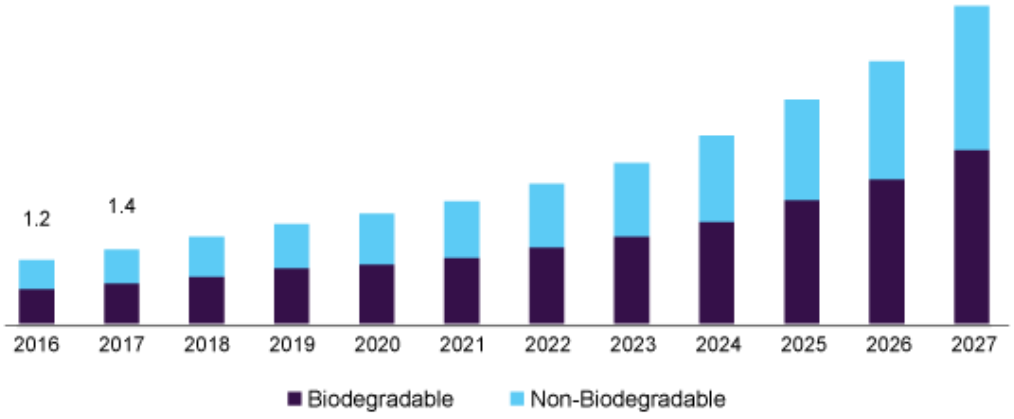

Figure 6. U.S. bioplastics market size by product, 2016-2027 (Grandview Research, 2020)

Biodegradable polymers are much higher priced than the commodity polymers typically used in packaging applications and so the industry is currently working towards bringing down the cost of manufacturing biodegradable polymers by increasing production capacity, improving process technology, and using low-cost feedstocks. Rising investments in R&D by private as well as public organizations is likely to support the growth of the bioplastics market. (Plastics Insight, 2017)

Moreover, growing consumer awareness about sustainability, recyclability and green packaging and this together with government policies for cleaner environment and taxes on conventional plastics are the main basis for driving the market of bioplastics. Because of this, manufacturers are focused on the search for alternatives that come from renewable sources and low price volatility, contrasting conventional plastics. (Plastics Insight, 2017)

3.4. Polylactic acid market definition

Polylactic acid is a biodegradable thermoplastic derived from renewable sources such as sugarcane and corn starch. It has multiple applications like the production of plastic films, plastic bottles or automotive parts, but most significant in food packaging and medical devices. This is due to its biodegradability as well as its unique properties such as remarkable resistance to oil, grease and UV rays and its better printability as compared to conventional plastics, driving the demand of PLA in food packaging applications. (Transparency Market Research, 2020)

PLA is the efficient alternative as packaging material to plastics derived from petroleum which prices fluctuate continuously. Not only it is a lightweight material that reduces GHG

emissions in its manufacture as compared to conventional plastics, but also it is one of the most efficient biopolymer in terms of feedstock efficiency (defined as the conversion ratio of feedstock weight to plastic polymer weight), as it can be seen in Figure 7. (Plastics Insight, 2020)

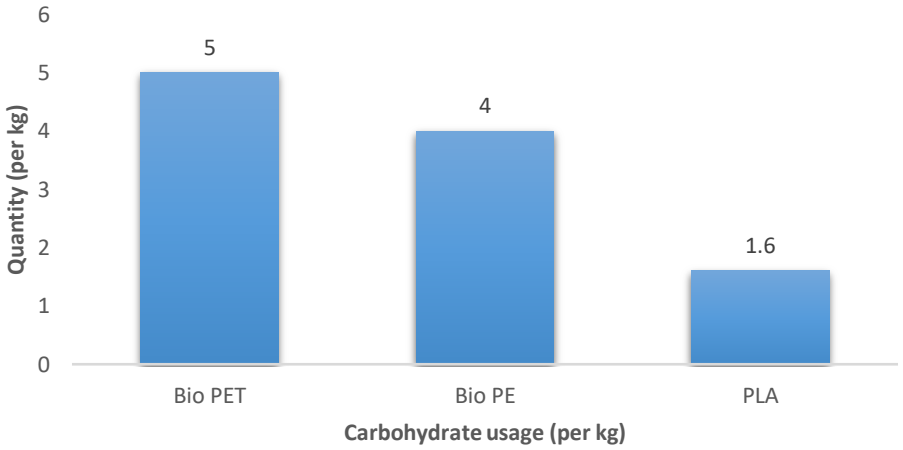

Figure 7. Feedstock efficiency score for PLA, 2016 (Institute for Bioplastics and Biocomposites, 2019)

The global polylactic acid market size was valued at USD 535.6 million in 2019 and is expected to grow at a compound annual growth rate (CAGR) of 15.9% from 2020 to 2027. (Grandview Research, 2020) Growing consumer awareness about sustainability, recyclability and green packaging, combined with favourable regulations related to the use of bio-based materials and the reduction of the consumption of single-use plastic products and the easy availability of raw materials is expected to give an impetus to the market growth and the demand of PLA as a sustainable packaging material for food and beverages, segment that accounted for more than 35% share of the global revenue in 2019. (Grandview Research, 2020)

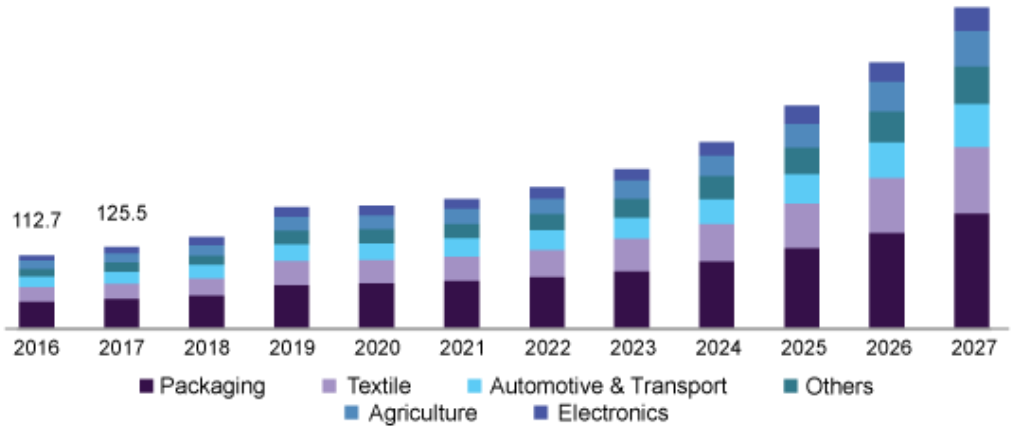

Figure 8. U.S. PLA market size by end use, 2016-2027 (Grandview Research, 2020)

The textile industry is also increasing the demand of PLA as it offers smooth 7 pleasant fabrics while in the automotive industry PLA is used in such a variety of interior parts due to its bio-based source and that it reduces the overall weight of the vehicles, becoming an effective

alternative over conventional plastics as it reduces the carbon footprint and the overall transportation costs. (Grandview Research, 2020)

One of the main market restraints that are hampering the growth of PLA market is the elevated price of PLA over conventional plastics such as PP and PS. As we can see in Figure 9, PLA price in 2017 varies from approximately 1,900 US$/ton to 5,200 US$/ton depending on the region (Plastics Insight, 2020). Reduction of the price gap between PLA and oil-based polymers due to R&D advances is promoting the market of this biopolymer. NatureWorks LLC polylactic acid is currently priced at a range of 1,800-2000 US$/ton while prices for PP and PS are in a range of 1,980 – 2,020 US$/ton and 2,000 – 2,060 US$/ton, respectively. (ICIS, 2011)

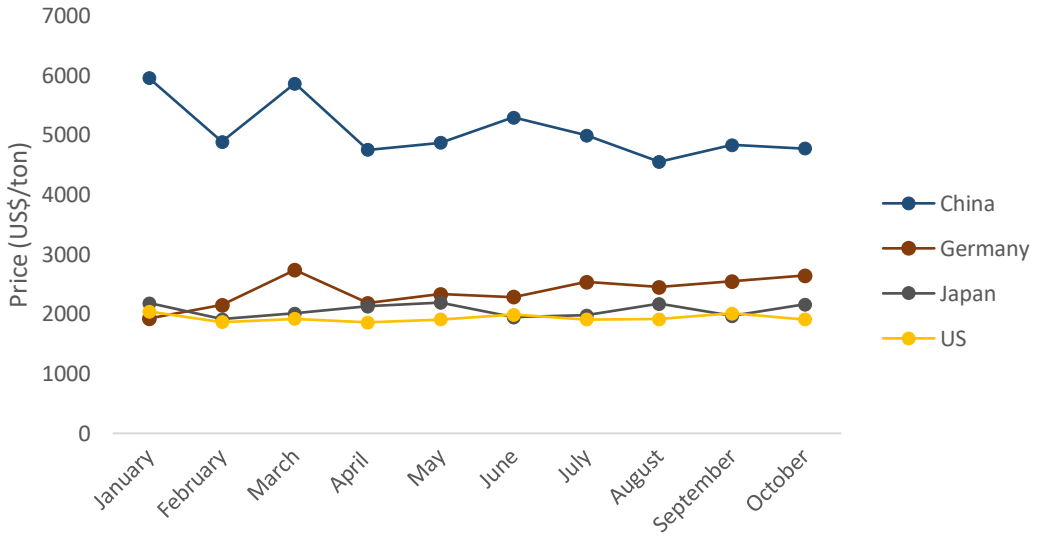

Figure 9. PLA price by month, 2017 (Plastics Insight, 2017)

Despite being an unforeseen situation, it is also necessary to analyse the situation created by the disease COVID-19 caused by coronavirus, which is leading to a widespread perception that in comparison to the reusable substitutes, new and single-use products are more hygienic.

In such situation, this current year governments have started to reverse bans and regulations on single-use plastics taking into consideration that many reuse habits considered to be environmentally friendly are now feared due to improper cleaning and disinfection measures. (Plastics Insight, 2020)

It is undeniable that the COVID-19 pandemic has affected the market to a great extent and PLA packaging market is not an exception to this. However, a recent report by consulting firm Bloomberg NEF mentions that concerns around food hygiene due to COVID-19 could increase plastic packaging intensity (Plastics Insight, 2020) and since PLA is based on biodegradable properties, it is expected that its market will have a lucrative value during the forecast period, even though in the current year it is expected to go through the minimum value. (Transparency market research, 2020). Moreover, rising demand for personal protective apparel

is expected to fuel the textile industry and so propel the demand of PLA in this segment. (Grandview Research, 2020)

In 2019, North America lead the PLA market accounting a 40% share of the global revenue and representing one of the major exporting countries. Its market is driven essentially by the demand for sustainable bioplastics in the food packaging segment and it is of significant importance the high availability of raw materials as well as the presence of major manufacturers of PLA that characterize the regional market. (Grandview Research, 2020)

Asia Pacific and Europe were respectively situated as the second and third largest regional market and the demand in these regions is expected to increase at a high rate in the next years. However, increasing COVID-19 cases are hampering the product demand in some of the main sectors such as electronics, appliances or automotive industry. (Grandview Research, 2020)

It is important to look after the main market players along with the market share in order to establish the capacity production of the plant.

NatureWorks LLC shows the highest production capacity among all other leading manufacturers with a 150,000 tonnes/year facility in Blair, Nebraska. As the mayor leader, this plant competes on the basis of technology and raw materials as well as the PLA quality offered, focusing on advancement in order to gain a competitive edge in the market. This facility releases 60% less GHG and uses 50% less non-renewable energy than conventional plastics like PS and PET. (ICIS, 2011)

NatureWorks LLC is followed by joint venture Total Corbion, which built a 75,000 tonne/year PLA production facility in Thailand, as sugar quota policy in Europe hinders the production process. (ICIS, 2018)

An increasing number of players have been carried away by the growing popularity of biodegradable plastics in recent years. Among all others, Pyramid technologies stand out with a yearly production capacity of 60,000 tonnes, and WeforYou and Synbra with a 50,000 tonnes/year facility. Some other market players are Mitsui Chemicals, Inc., Hitachi, Ltd., BASF SE, Braskem. (Plastics Insight, 2017)

The production capacity of these companies have been increasing over the years as the demand for consumption on yearly basis increased. They compete for low production costs which along with favourable government restrictions on one-single use plastics, is driving the PLA market. The global bioplastics production capacities are difficult to estimate and are usually based on forecast because of continuously emerging range of bio-based and biodegradable polymers and rising interests on investing in bioplastics sector.

Is for this reason it has been decided to design a facility plant which will operate continuously during 330 days/year and with a fixed production capacity of 60,000 tonnes of PLA per year.

4. SELECTION OF THE PRODUCTION PROCESS OF PLA

4.1. Lactic acid

Lactic acid, also known as 2-hydroxypropanoic acid, was first isolated by the Swedish chemist Carl Wilhelm in 1780 from sour milk. Its industrial production started in 1881 by the fermentation process. Lactic acid can also be produced by chemical synthesis, but bacterial fermentation of carbohydrates is the preferred process for major producers as chemical synthesis has many limitations such as limited production capacity, inability to produce the desired isomer as it results in a racemic mixture of L-lactic acid and D-lactic acid, and high manufacturing costs. On the contrary, bacterial fermentation process allows the specific production of the desired isomer either L-lactic acid or D-lactic acid by using the appropriate bacteria. (Castillo Martinez et al., 2013)

Physical properties of a lactic acid are listed in the following Table 1

Table 1. Physical properties of lactic acid (Henton et al., 2005)

Chemical formula	$C_3H_6O_3$
Chemical name	2-hydroxy-propanoic acid
Molecular weight	90.08
Physical appearance	Aqueous solution
Melting point (ºC)	53
Boiling point (ºC)	>200
Solubility in water	Miscible
Dissociation constant (Ka)	$1.38 \cdot 10^{-4}$
Density (kg/m^3)	1316
Viscosity (kg/ms)	$4.363 \cdot 10^{-2}$
Cp (J/kgºC)	2497

This organic acid is the basic monomer for the fabrication of PLA. It is of interest its chemical behaviour which is mainly determined by its physico-chemical properties:

- **Asymmetric optical activity of C2**. Lactic acid is a chiral molecule and so exists as two stereoisomers L-lactic acid and D-lactic acid, as shown in Figure 10. The existence in the form of two enantiomers makes lactic acid such a versatile compound as different optical lactic acids or the racemic mixture can lead to applications in different fields.

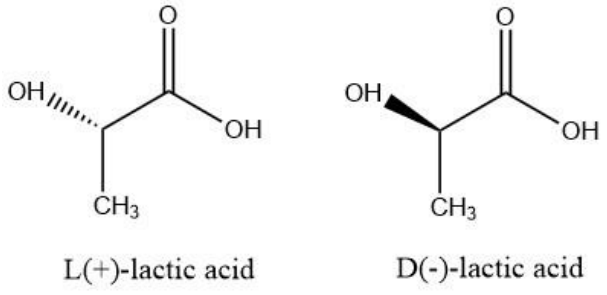

Figure 10. Structure of L(+) and D(-) isomers of the lactic acid

More important is the fact that while L-lactic acid can be metabolized by enzyme action of the human body, D-lactic acid or the racemic mixture is not degraded by human body's enzymes and so should not be present in applications that involve oral intake of lactic acid.

For this reason, food and pharmaceutical applications require high optical purity of L-lactic acid so it can attain the necessities for oral intake, while D-lactic acid is commonly used in non-food related applications such as the fabrication of solvents or biopolymers. (Castillo Martinez et al., 2013)

The optical purity of lactic acid also affects mechanical or thermal properties of PLA. High purity L-lactic acid is essential in the production of high molecular weight PLA for its use in biomedical and packaging applications, due to its excellence in mechanical properties and its low toxicity for human intake.

- **High solubility in water**: Because of this property and referring to what has been mentioned above, a small intake of D-lactic acid can be considered as safe as the high solubility of D-lactic acid promotes hydrolysis in body fluids which can break down the bulk of poly(D-lactide) and eventually be eliminated from the human system.

  Also because of its solubility and its carboxyl group, lactic acid may show corrosive properties as it can react with active metals, which has to be taken into account for material selection of the equipment in the process. (Castillo Martinez et al., 2013)
- **Bifunctional reactivity associated with the presence of a carboxyl and hydroxyl group**: Lactic acid is a three-carbon molecule which contains a carboxyl and hydroxyl group, and so a self-reactant compound by following esterification exothermic reactions. This groups react with each other in order to polymerize and form dimers of lactic acid.
- **Acidic character in aqueous medium**: As shown in Figure 11, lactic acid dissociation equilibrium in water leads to H+ and lactate ions which turns the pH of its solution acid.

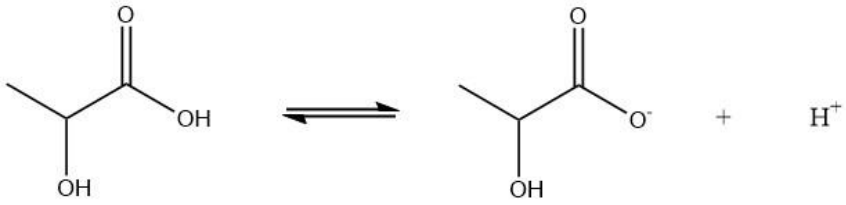

Figure 11. Dissociation equilibrium of lactic acid to lactate ions

Optical activity of lactic acid can affect PLA properties like melting point, mechanical strength and degradability, so selectivity of a single optical lactic acid is essential for quality control. As commented previously, high optical purity of L-lactic acid is required for food and pharmaceutical applications in order to attain the strict requirements for oral intake.

This grade of purity (99%) is achieved by the addition of complex nutrients and typical technologies used for lactic acid purification including electrodialysis, reverse osmosis, liquid

extraction, ion-exchange acidification, ion-exchange purification, distillation, insoluble salt processes or esterification. (Tin Sin, L. et al., 2013)

However, taking into account the high possibility of converting L-lactic acid and D-lactic acid into each other when exposed to extreme conditions and due to the fact that these purification technologies rise significantly the cost of production, crude lactic acid will be used as raw material for the process. High purity lactic acid is sold at US$1000-1500 per ton while industrial grades tend to be 20% less expensive depending on the final application. (Castillo Martinez et al., 2013)

4.2. Polylactic acid

Polylactic acid is an aliphatic polyester, biodegradable and bio-based, derived from its monomer lactic acid, which comes from renewable sources such as corn sugar, potato and sugar cane. PLA was first synthesized by Carothers in 1932, although only low molecular weight with lack of applications was obtained by heating lactic acid under vacuum while the condensed water was removed. (Jamshidian et al., 2010)

Currently, PLA can be synthesized by different polymerization routes like polycondensation, azeotropic dehydration or ring-opening polymerization. However, only high molecular weight PLA have reach the market in different industries as it provides suitable mechanical, thermal and barrier properties comparable with conventional plastics such as polypropylene, polystyrene or polyethylene terephthalate.

NatureWorks LCC stands out as the major producer of PLA derived from corn with a facility plant of 150,000 metric ton of high molecular weight PLA per year of capacity in Blair, Nebraska. Other market players such as Corbion are moving towards a more sustainable production of PLA through its production from biomass waste. (Castro-Aguirre et al., 2016)

Out of different bioplastics with competitiveness in the current market, polylactic acid is distinguished because of its eco-friendly properties. Not only it is derived from renewable sources, but it is also a biodegradable, recyclable and compostable polymer, which makes it a good alternative to replace fossil-based plastics providing a positive public perception, as it reduces environmental problems and plastic disposal problem in landfills offering different end-of-life scenarios, especially in food packaging or agricultural mulch films, where plastics become highly contaminated and are difficult to recover through recycling

Moreover, polylactic acid has a minor competitive cost out of other bioplastics and provides a better processability compared to similar polymers such as poly(hydroxyl alkanoate) (PHA), poly(ethylene glycol) (PEG) and poly(γ-caprolactone) (PCL).

High molecular weight PLA can be processed by well-known polymer manufacturing techniques used for similar properties polymers such as injection molding, sheet and film extrusion, blow molding, foaming thermoforming, fiber spinning or film forming. Melt

processing is the main technique used for mass production of PLA for different applications in several industries such as packaging, textile and fibers, medical or automotive. Quality requirements include the low presence of meso-lactide, as it may cause deteriorative changes in the crystallinity and biodegradation properties. (Castro-Aguirre et al., 2016)

Food packaging for short-life products is the leading application for PLA, covering the 70% of the market, as it is seen as a green alternative over conventional plastics. The textile industry, however, is gaining attention over the recent years. Biomedical applications are also remarkable as PLA provides biocompatibility with the human body, thus fits perfectly for medical implants, surgical sutures and medical devices. Moreover, the US Food and Drug Administration (FDA) recognises polylactic acid as a Generally Recognized as Safe (GRAS) material, which together with its biodegradability, biosorbability and biocompatible properties with the human body, makes it a good alternative as a drug carrier in the pharmaceutical field. (Jamshidian et al., 2010)

4.3. Reaction pathway study

PLA was first produced in 1932 by Carothers via ring-opening polymerization of lactide. It was not until 1954 that Dupont developed the purification technique obtaining high molecular weights and leading to the mass production of PLA. (Tin Sin, L. et al., 2013)

As depicted in Figure 12, there are two well-known routes for the synthesis of lactic acid into high molecular weight PLA: the polycondensation route, which involves two reaction pathways, the direct polycondensation (DP) and the azeotropic dehydration (AD); and the ring-opening polymerization (ROP) route.

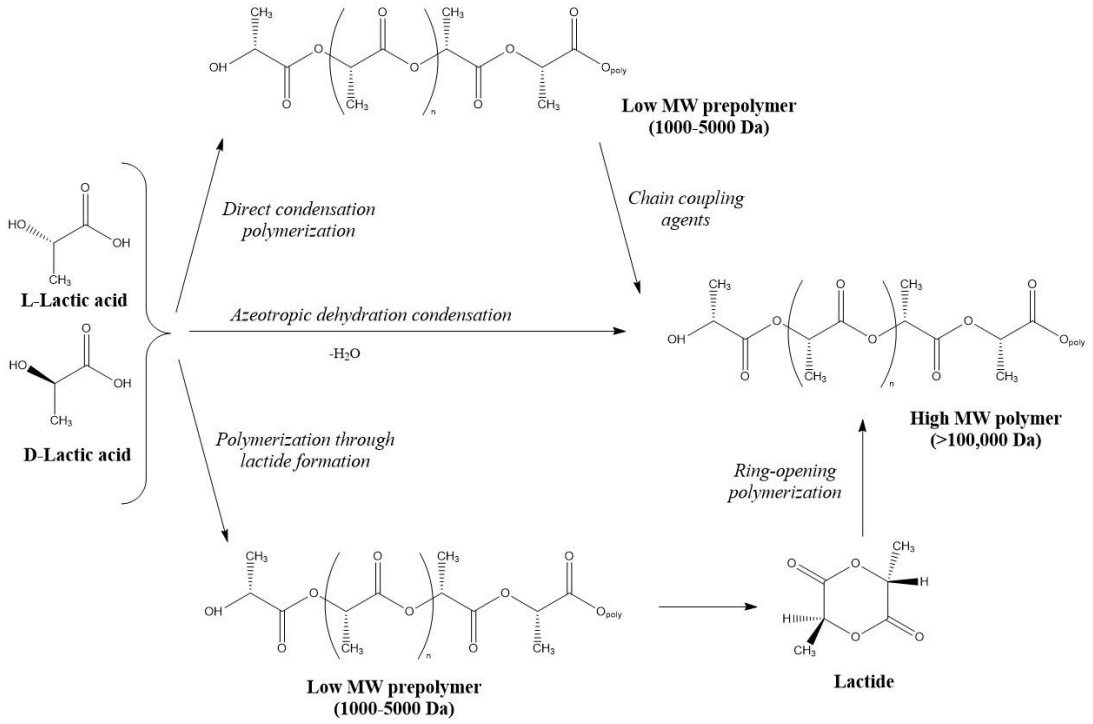

Figure 12. Synthesis methods for high molecular weight PLA (Garlotta, 2001)

4.3.1. Direct condensation polymerization

The direct polycondensation route is the simplest and least expensive way for producing PLA. As it can be seen in Figure 13, the carboxylic acid and hydroxyl groups of lactic acid react with each other in order to produce polylactic acid and water. It is important to consider the need of removal of the condensation water in order to proceed the reaction towards the right side. The removal of water as well helps to improve selectivity and thus to reduce side reactions that can take part during polymerization reactions. Due to the inherent equilibrium of the polymerization reaction, a depolymerization reaction also takes place forming ring structures such as lactide ring, lowering polymer's molecular weight. (Tin Sin, L. et al., 2013)

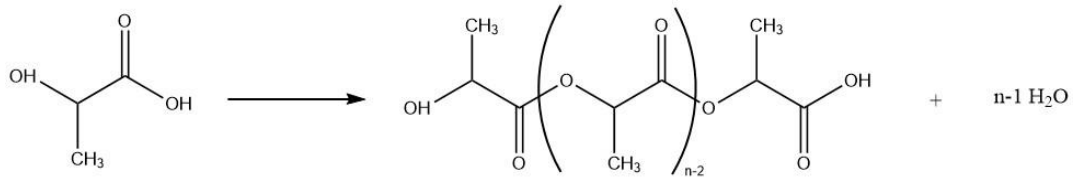

Figure 13. Condensation polymerization of lactic acid.

One of the drawbacks of this method is that the condensation polymerization in a solvent-free system leads to a low molecular weight (Mw= 1000-5000), glassy and brittle polymer which makes it unusable for any applications. This is due to various reasons such as the high viscosity of the melt polymer, the presence of impurities, the lack of reactive end-groups (-COOH and -OH groups), the excess of water and the equilibrium reaction to lactide formation. (Garlotta, 2001)

For this reason, it is needed the usage of external coupling agents as chain extenders or esterification-promoting adjuvants that can rise the molecular weight by reacting with either the hydroxyl or carboxyl groups, which leads to an elevation of the cost and complexity of the process. (Garlotta, 2001)

4.3.2. Azeotropic dehydration condensation polymerization

The azeotropic dehydration polymerization is a technique that allows to obtain high molecular weight polymers greater than 300,000 g/mol. This method was first commercialized by Mitsui Toatsu Chemicals, introducing a process where lactic acid and catalyst are azeotropically dehydrated under reduced pressures to obtain PLA while removing the majority of the condensation water. (Tin Sin, L. et al., 2013)

The main drawbacks of this method are the usage of solvents and the residual catalyst due to high levels required for suitable reaction rates. Catalyst impurities are the cause of many problems such as undesirable degradation or uncontrolled hydrolysis rates that affect further processing properties, or catalyst toxicity in the case of biomedical applications. This problem could be solved by the addition two equivalents of acid to divalent tin catalyst in order to deactivate the catalyst, or it could also be precipitated and filtered by the addition of strong acids such as sulfuric acid. (Garlotta, 2001)

4.3.3. ROP: Lactide formation and ring opening polymerization

The ring opening polymerization method consist in the production of high molecular weight PLA via ring-opening of lactide. Lactide is an intermediate substance obtained under reduced pressure by the depolymerization of low molecular weight PLA. It leads to a mixture of L-lactide, D-lactide or meso-lactide, with the percentages being dependent on lactic acid isomer feedstock, temperature and catalyst. (Tin Sin, L. et al., 2013)

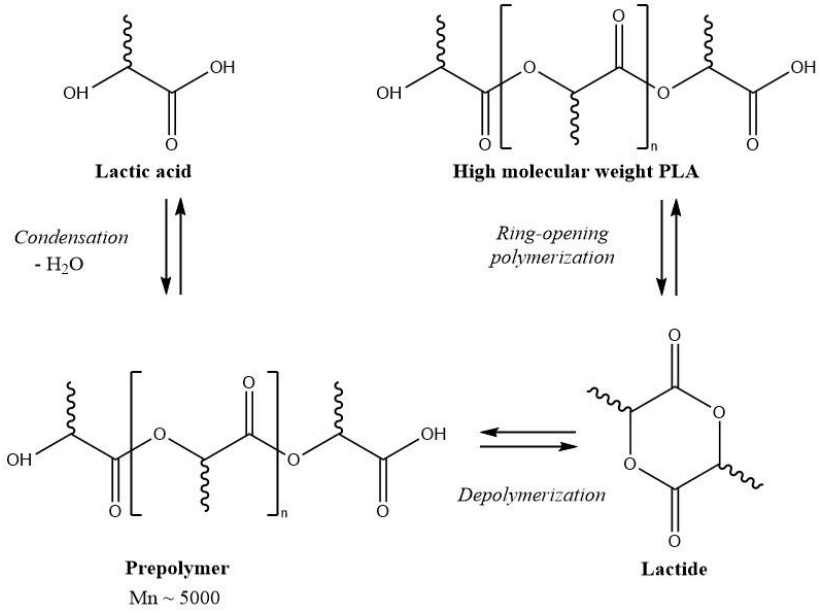

Figure 14. High molecular weight PLA production via ROP

PLA can undergo either cationic or anionic ring polymerization, depending on the initiator type, in a solvent-based system, allowing the formation of high molecular weight polymer as the formation of free radicals with the action of initiators upon the functional groups elevates the propagation of chain reactions. (Garlotta, 2001)

However, this anionic and cationic initiations are susceptible to racemization, transesterification and high impurity levels and thus for large-scale manufacture it is preferable the use of lower levels of nontoxic catalysts. The use of tin, zinc, aluminium and other heavy metal catalysts, highlighting the importance of tin (II) and zinc, are demonstrated to easily polymerize high molecular weight PLA with the absence of the problems above mentioned, yielding a high molecular weight polymer suitable for its use in food packaging and biomedical applications. This is due to their covalent metal-oxygen bonds and free p or d orbitals. (Garlotta, 2001)

4.3.4. Justification of the selected alternative

In this section, a comparison among the reaction routes explained above will be carried out in order to select the one that is most appropriate for the development of the project. Once selected, a comparison among different patents of the selected method will be carried out with the objective of selecting the process conditions that best fit into the process.

Direct polycondensation is the simplest way and at first the least expensive route to polymerize lactic acid. However, the yield of polymer PLA produced has a relatively low-molecular-weight (Mw=1000-5000) and also is poor in mechanical properties as compared to other reaction pathways, limiting the range of applications of PLA. The use of coupling agents leads to reaction byproducts which must be later removed, giving the advantage of a final product highly purified and free of impurities, avoiding undesired degradation of the product. On the contrary, this coupling agents increase the cost of production and the number of reaction and purification steps of nonrecoverable byproducts.

Azeotropic dehydration leads to a higher molecular weight PLA than the previous method, but with high catalyst impurities due to the high levels needed for suitable reaction rates, which could cause many problems during further processing. Azeotropic dehydration proceeds in solvent medium increasing the complexity of the process as it is difficult to separate from the final product, besides being a high time-consuming method with a higher energetic consumption. These conditions makes this method less attractive from an economic point of view, as the PLA produced would compete in the market at a higher price in comparison with PLA produced from more economic methods.

This entails selecting the ROP route as the most favourable alternative according to the evaluation criteria. Even though ROP also comprises the step of fabricating lactic acid prepolymer, the polymerization through lactide formation can be carried out without the usage of coupling agents. The extremely effective catalyst used in this method provide the advantage to guarantee the safety of PLA when used in food packaging and in biomedical applications, two of the major applications for PLA nowadays, as the stereoisomery can be controlled and so the specific stereoisomer L-lactic acid can be produced. Moreover, this method yields high molecular weight (>250,000) PLA polymer providing greater mechanical and biodegradability properties.

4.4. Production process study

Until 1931, processes for the manufacture of resins from lactic acid led to polymers of limited value based on physical characteristics and desirable film forming properties. The final product could only be purified by repeated recrystallization, leading to such low yields that the possibility of large-scale production was discarded.

It was not until this year that Dorough (Dorough, 1935) disclosed a new invention for the production of new lactide resins from lactic acid solutions. This method consisted in the concentration of the solution by distillation of water, followed by polymerization of the hydroxyl acid by intermolecular condensation and finally the removal of the lower molecular weight materials by distillation at reduced pressure, in order to lower the boiling point of this compounds and thus preventing the degradation of the high molecular weight polymer

produced. However, this technique was limited to a low molecular weight (Mw = 4000 g/mol) in comparison to newer techniques due to the presence of water and impurities, but mainly due to the competing depolymerisation reaction in which lactide is produced, which decelerates the rate of polymerization and thus limits the increase in molecular weight.

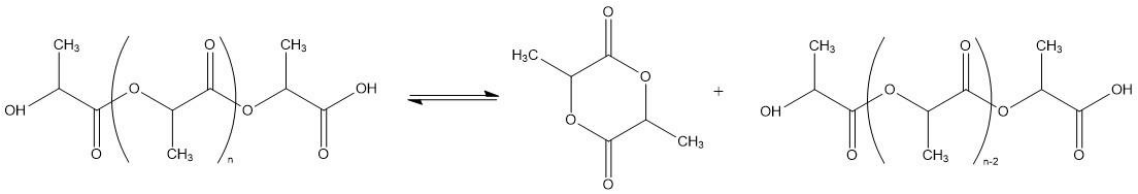

Figure 15. Depolymerization reaction scheme

Processes prior to 1989 kept using recrystallization steps for purification of crude lactide prior to polymerization. By that time, the significant losses of lactide and thus the relative low yield of this technique was overlooked as the high margin provided by biomedical applications and the lack of alternatives lead the investigations to another standpoint. However, the need in the development of a process for large-scale manufacture of biodegradable polymers, in a market where products are cost-competitive, oriented DeVries (De Vries, 1989) to discover a way to increase the molecular weight of the final polymer by means of dissolving the lactide in an organic solvent, and the extraction of this solution with water. This method also managed to remove the impurities carried along with lactide prior to polymerization, which affected positively to the chain length of the final PLA.

Along with this line, Bathia (Bathia, 1989) also proposed a continuous system in which the crude lactide is swept using inert gas from prepolymer reactor into a solvent stripping system to remove, recrystallize and purify lactide. However, it is believed now that none of this methods disclosed a commercially viable overall process for large-scale production of polylactic acid nor a cost-effectively process adequate for replacing petrochemical-based polymers.

Muller (Muller, 1991) patented a process for the preparation of optically pure L(-)- or D(+)- lactide from a pure lactic acid feed on an industrial scale. A large number of patent specifications and disclosure documents proposed the preparation of optically active lactide on the laboratory scale until this year. Nevertheless, no direct scale-up to industrial scale managed to be successful due to the pour overall yield and the high cost of the processes. Muller et al. proposed the obtaining of pure lactide from lactic acid solution, which is heated under reduced pressure and with the appropriate catalyst. The lactide produced is distilled off and subjected to purification techniques such as recrystallization and subsequent precipitation. The purity of lactide achieved was up to 99% but the yield of the overall process was not higher than 80%, relative to the lactic acid feed.

In this same year, Gruber et al (Gruber et al., 1992) disclosed a continuous method for the manufacture of selected optical purity polylactic acid from crude lactic acid with little or no waste of raw material lactic acid feed. The innovative part of this methods relies on feeding

under reduced pressure the crude lactide vapour from the prepolymer reactor into a series of distillation columns as purifying method. Thereby, this process avoids the yield loss associated with the recrystallization steps traditionally used to purify lactide and yields pure lactide with less than 0.1% total impurities. The pure lactide is further fed into a polymerization system using a tin-based catalyst, completely eliminating the use of costly and environmentally unfriendly solvents. Improved variations of this method have been emerging through the years. Drysdale et al. (Drysdale et al., 1993) proposed a method in order to improve distillation efficiency by the partial condensation of the stream of crude lactide vapour prior to the entry into the distillation system.

Through the subsequent years, improving conditions on the ring-opening polymerization process were provided by many authors. In 1998, Oota (Oota et al., 1998) proposed a method for preparing polylactic acid in an efficient way under the mild conditions of low polymerization catalytic amount and low polymerization temperature by adding a cyclic imide compound to the polymerization reaction system. By this method, the depolymerization of the polymer was inhibited and the remains of the catalyst and colouring of the polymer due to high amounts used were avoided. Moreover, the overall cost of the process was efficiently reduced. Along with this method, in this same year Ohara et al. (Ohara et al., 1998) proposed the addition of phosphorous compounds capable of inactivating the catalyst used in ROP of the lactide once the reaction was completed.

There is an invention presented in 2009 by Ramakrishma et al. (Ramakrishma et al., 2009) which relates a cost effective and industrially scalable method for the production of polylactic acid in a more efficient way by using as feed material the fermentation of non-edible renewable agricultural feed-stocks such as molasses and cane bagasse. In this way, the costs associated to the energy intensive step of distillation of crude lactide would be palliated by the use of an otherwise waste product of sugar industries as raw materials.

4.4.1. Justification of the selected patent

The patent selected on which the plant design will be based has to be chosen taking into account several factors, both technological and socio-economical. The preferred overall process has to allow the continuous manufacture of polylactic acid at industrial-scale level and led to a controlled optical purity in order to provide a polymer capable of replacing conventional polymers as well as an adequate biodegradability.

Bearing all patents mentioned in mind, lactide purification seems to be a critical stage of the ring-opening polymerization route, as it controls the overall yield of the process as well as the optical purity of the polymer produced. Recrystallization steps, solvent extraction and distillation are the most common methods used for lactide purification.

Recrystallization is an operation mentioned in many of the patents compared as it provides the technical feasibility necessary for the purification of lactide at laboratory-scale. However, significant losses of lactide and thus relative low yield is linked to this alternative, which together with the solid handling feature, discards it as a method for large-scale manufacture. Furthermore, there is no evidence in existing patents that this methods leads to a polymer with a molecular weight highly enough to provide equivalent properties to conventional petroleum-based polymers.

Solvent extraction method manage to solve this problem as it is capable of removing the impurities carried along with lactide prior to polymerization, and thus increases the chain length of the final polymer. However, it is still not a cost-effectively method which makes it difficult for competition in the market. Moreover, it has to be taken into consideration the problems that come along in the use of flammable and toxic solvents and thus the safety design and control measures that needs to be taken into consideration.

On the contrary, distillation method leads to an optical purity of lactide >99% as well as it avoids the yield loss and the solid-handling problems associated with the recrystallization steps and eliminates the use of costly and environmentally unfriendly solvents. Cargill Dow LLC has also demonstrated that this method is valid for industrial-scale operations and it is a low-cost continuous process that combines the substantial environmental and economic benefits of synthesizing both lactide and PLA, providing a commercially viable biodegradable commodity polymer made from renewable resources.

The seventeen patents owned by Cargill, Inc. under the name of "*Continuous process for the manufacture of lactide and lactide polymers"*, being the most recent published US patent 6326458 B1 (Gruber et al., 2001), relates with accuracy the process conditions in order to highly purify lactide and thus carry out the process to obtain a crystalline polylactic acid with control of racemization.

It is a fact that recent patents have provided more economical ways to produce PLA as compared to this patent by reusing waste non-edible agricultural feed-stocks as raw material for the production of lactic acid. Nevertheless, the objective of this project is limited to the production of PLA from lactic acid solution and the fermentation process is out of the scope of the project.

Gruber et al. discloses a cost-competitive process for the production of a biodegradable polymer capable of replacing conventional plastics in packaging applications, efficiently using catalyst to reduce energy consumption and improve yield. This process makes it able to control racemization of the enantiomers by minimizing residence time of the equipment used and a rigorous control of the process conditions, leading to the obtaining of high molecular weight PLA and free of impurities, avoiding uncontrolled degradation and colouring problems.

5. BASIC DESIGN OF THE PRODUCTION PLANT

The plant is designed in order to provide a continuous process for the annual production of 60,000 tonnes of polylactic acid of selected optical purity and composition from a lactic acid solution feed. Five well differentiated stages can be distinguished in the process and will be explained in detail herein below. In *Appendix 1* it is detailed the Process Flow Diagram (PFD).

- Section 100: Polycondensation of low molecular weight PLA
- Section 200: Depolymerization of PLA and Lactide formation
- Section 300: Lactide purification
- Section 400: Polymerization of Lactide

5.1. Section 100: Polycondensation of low molecular weight PLA

5.1.1. Process description

As has been detailed in Chapter 4.1, the crude lactic acid feed is a commercially available solution of 15% (w/w) combination of the optical enantiomers L- and D- lactic acid and 85% water. This solution is due to the fact that the fermentation process is carried out in an aqueous medium. The feed enters to an evaporation system with the purpose of removing the water used as a carrier as well as the one produced as condensation reaction by-product in order to concentrate the crude lactic acid feed.

It has been studied the possibility of using concentrated lactic acid as a direct feed for the process, which with the appropriate storage conditions of pressure and temperature, would avoid the requirement of evaporating huge quantities of water and thus would reduce the size of equipment and energy requirements, as well as the residence time in the evaporator which controls racemization. However, it has been demonstrated that lactic acid undergoes intramolecular self-esterification to form higher oligomers at concentrations up to 20-30% (Vu et al., 2005) and only stays at monomeric form below this condition. Therefore the type of evaporator selected is a falling film evaporator, as it provides a high surface area to volumetric hold up ratio, which reduces the time required for evaporation and thus reduces racemization as well as controls optical purity. This configuration is the simplest and most commonly used type of film-evaporator, recommended for heat sensitive materials like lactic acid as it withstand a minimum of exposure to heat with high heat transfer coefficients and short residence times on the heated surface. It is also recommended for the concentration of viscous products and suitable for vacuum operation with minimum cost operation. (Richardson et al., 2002)

The alternative of combine both the evaporator system and the prepolymer reactor into a single system has been taken into account as fixed asset costs could be reduced. However, the advantages of separating this systems leads to the optimization of the process resulting in reducing operating costs and providing a better control of the process. In the first step, lactic acid is concentrated to a weight percent up to 85%. It is well known in literature that solutions

above this concentration would cause significant losses of lactic acid in the overhead stream and a higher level of lactic acid in the oligomer form would be produced during the concentration. (Quarderer et al., 2001) Thus in this stage lactic acid losses are considered negligible and the water vaporized that leaves the system can be readily discarded without further treatment. On the contrary, lactic acid and other impurities will be vaporize in the prepolymer reactor and thus recycle or further treatment will be necessary before discarded.

As high evaporation ratios are required to concentrate lactic acid from a weight percent of 15% to 85%, it could be studied the possibility of using multiple-effect configuration in order to reduce steam consumption and therefore increase the economy of the evaporators. In this way, the effects would operate at different pressures and therefore different boiling temperatures so that the steam generated in one effect supplies heat to the others resulting in operating cost reduction. However, falling film evaporators have de advantage of provide high evaporation ratios, up to 70% without recirculation, added to the fact that single-effect evaporators are preferred when expensive materials of construction must be used. At high concentrations, lactic acid may be corrosive to metal and thus more expensive materials such as stainless steel must be used.

The operation conditions in the falling film evaporator E-101 are those which helps to reduce racemization and therefore vacuum evaporation will be carried out at 0.47 bar and at a temperature of 80ºC. Vacuum operation is appropriate for heat sensitive liquids as it is necessary to work at low temperatures. During the evaporation, water and volatile impurities are removed. It is known by literature that racemization is strongly influenced by the presence of impurities and by the exposure of lactic acid for prolonged periods at temperatures above 180ºC. Thus racemization can be neglected at this stage, as well as condensation reaction can be neglected at this operating conditions. (Quarderer et al., 2001). A steam ejector will be needed in order for the evaporator to operate under vacuum.

Once operating conditions of the outlet stream 3 are adjusted, the concentrated solution enters the prepolymer reactor E-103 which is indeed a further evaporator. The prepolymer reactor configuration as well is operated to minimize racemization and thus the falling film configuration is selected.

A condensation reaction as shows Figure 16 takes place in this equipment. Water and high volatile impurities are removed so that lactic acid can polymerize to form a low molecular weight polymer (2200 g/mol). Molecular weights higher than 2400 g/mol are not recommended and at lower molecular weights, the lactic acid content in the prepolymer reactor would be too high which would result in the production of a crude lactide with higher chemical impurities in further operations, as at the elevated temperature of lactide synthesis reaction, lactic acid would evaporate off the system before lactide does. At 2200 g/mol chemical purity as well as the

optical purity of the crude lactide can be controlled in further operations, improving therefore the properties of the final polymer product. (Ehsani et al., 2014).

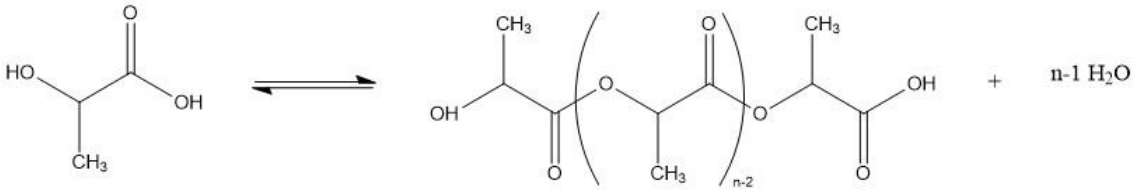

Figure 16. Condensation polymerization of lactic acid.

As the equilibrium dictates, a portion of the water vapour removed is the condensation reaction by-product, which shifts the equilibrium to the right increasing the reaction rate and the conversion. The vapour stream may contain lactic acid and therefore a further improvement and optimization of the process could consider the need of this stream to be condensed and recirculated to the first evaporator in order to prevent losses of feed material and increase the overall yield. As impurities are also being removed, a purge stream should also be needed in order to avoid accumulation.

The remaining liquid along with low volatility impurities, such as carbohydrates, amino acids and colour bodies, and part of the lactic acid that has not reacted is transferred to a hold tank which is maintained at a temperature of 160ºC in order to keep the prepolymer over the melting point.

5.1.2. Block diagram

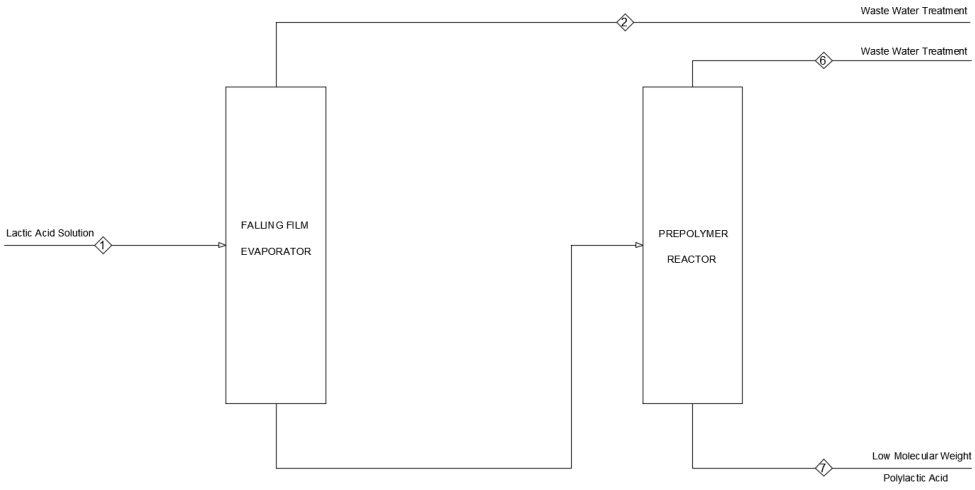

Figure 17. Block Diagram – Section 100

Table 2. Mass balance – Section 100

Stream (kg/h)	1	2	6	7
Lactic acid	13978.87	0.00	0.00	461.66
Water	83091.20	80819.84	4975.17	0.00
VI	488.77	488.77	0.00	0.00
NVI	195.51	0.00	0.00	195.51
PLA (LMW)	0.00	0.00	0.00	10813.39
Total	**97754.35**	**81308.62**	**4975.17**	**11470.56**

5.1.3. Equipment data sheet

Mass and energy balances of section 100, as well as sizing of the main equipment is detailed in *Appendix 2* and *Appendix 3*, respectively, in order to determine the basic design of each equipment. As a result, herein below are shown the specification sheet of each equipment containing the main features and operating conditions.

The prepolymer reactor E-103 is part of this section but its design is detailed in *Appendix 4*. Falling film evaporator E-101 also follows the same design procedure.

Heat exchanger E-102 is required to precondition stream 5 to the prepolymer reactor operating temperature and its design is reduced to calculate the required heat transfer area as well as low pressure steam requirements based on duty calculation from energy balance.

Pumps P-101 A/B and P-102 A/B are necessary to supply the required energy for liquid impulsion through streams 3 and 7, respectively. Its design is based on power requirement estimation based on the mechanical energy balance around suction and discharge conductions.

Table 3. E-101 specification sheet

Equipment label	E-101	Equipment name	Evaporator	
Process service	lps	Equipment type	Falling film evaporator	
OPERATING DATA				
	SHELL SIDE		TUBE SIDE	
Stream	lps		2	3
Fluid	Steam		Water vapour	LA solution
W (kg/s)	26.8		22.6	4.6
ρ (kg/m^3)	1.6		4.4	960.8
μ (kg/ms)	$1.33\cdot 10^{-5}$		$1.49\cdot 10^{-5}$	$2.91\cdot 10^{-4}$
C_p (J/kgK)	2410		2936	3141
k_f (W/mK)	$2.72\cdot 10^{-2}$		$3.13\cdot 10^{-2}$	$29.10\cdot 10^{-2}$
T (ºC)	133.6		80.0	80.0
P (kPa)	300		47	47
ΔP (kN/m^2)	47.8		36.3	0.48
v (m/s)	22.3		2.2	4.7
Nº of passes	1		1	
Q (kW)	58065.3			
U (W/m^{2}ºC)	653			
ΔT (ºC)	53.6			
A (m^2)	1659.0			
MECHANICAL DATA				
TUBES				
Material	Stainless steel	Pitch (mm)	25	
Nº tubes	5412	O.D. (mm)	20	
Length (m)	4.88	t (mm)	2	
SHELL				
Material	Carbon steel	I.D. (mm)	1950	
Length (m)	4.88	t (mm)	9.5	

Table 4. P-101 A/B specification sheet

Equipment label	P-101 A/B	Equipment type	Centrifugal pump
OPERATING DATA			
Type	Centrifugal		
Max. flow (m^3/h)	14.88		
ΔP (kPa)	40.3		
Theoretical Power (W)	67.4		
Pump Efficiency	0.75		
Power (W)	89.9		

Table 5. E-102 specification sheet

Equipment label	E-102	Equipment name	Heat exchanger
Process service	lps	Equipment type	Shell and Tubes heat exchanger
OPERATING DATA			
	SHELL SIDE		TUBE SIDE
Stream	Low pressure steam		Lactic acid solution
W (kg/s)	0.30		4.57
Q (kW)	629.10		
U ($W/m^2°C$)	750		
Δ*T* (°C)	42.1		
A (m^2)	19.94		

Table 6. P-102 A/B specification sheet

Equipment label	P-102 A/B	Equipment type	Positive displacement pump
OPERATING DATA			
Type	Positive displacement		
Max. flow (m^3/h)	10.24		
ΔP (kPa)	-94.6		
Theoretical Power (W)	100.7		
Pump Efficiency	0.75		
Power (W)	134.2		

5.2. Section 200: Depolymerization of PLA and Lactide formation

5.2.1. Process description

In hold tank HT-201 the catalyst is added in order to facilitate lactide formation. As disclosed by Muller, compounds such as tin dust, tin halide, tin oxide and organic tin compounds derived from C-C carboxylic acids can be utilized. (Muller, 1991) The amount and type of catalyst will affect the optical purity of the final polymer. Tin (II) chloride is selected as it is known by literature it provides the highest lactide conversion with the lowest degree of racemization. The catalyst is added to the hold tank at a rate which would ensure a 0.4 mol% of the feed stream to the depolymerization reactor. Higher concentrations would result in increased polymer polydispersity with higher possibilities of racemization. (Ehsani et al., 2014)

Also, a process phosphite-containing stabilizer to also facilitate lactide formation as well as to avoid degenerative lactic acid and lactide degradation reactions will be added to the hold tank. The catalyst and the stabilizer tris(nonylphenyl) phosphite are fed in this hold tank assuring an even distribution of the catalyst within the liquid and thus better controllability in the lactide reactor. It is known that the addition of process stabilizers affects negatively to the lactide formation rate. However, it can reduce the extent of racemization and thus control

optical purity of the lactide produced. This means the amount of stabilizer used, which is that which ensures a 0.15% weight percent in the feed stream to the reactor, depends on the optical purity of lactide selected as well as the operating conditions and amount and type of catalyst used.

A falling film evaporator type of reactor has been selected to carry out lactide formation, as this type of reactor provides the advantages required to optimize the lactide production. In this way, lactide can be vaporized and transfer to the purification step while shifting the equilibrium depolymerization reaction to the right. Moreover, this type of evaporator provides the minimum residence time as well as high heat transfer coefficient required, as PLA and lactic acid are heat sensitive materials which would sharply increase side degradation reactions when exposed to heat and therefore reducing lactide production yield. It assures to maintain a uniform film thickness which increases mass transfer rate in a way such that lactide rapidly forms and vaporizes favouring the equilibrium to the right side.

Lactide is produced from oligomeric PLA by back-biting reaction of the –OH end groups. Reaction temperature, time and pressure, as well as catalyst type and concentration and prepolymer molecular weight are the parameters that have to be optimized in order to achieve high lactide conversions with the lowest degree of polymerization. (Ehsani et al., 2014). Operating conditions of the reactor are those that favours the lactide production. Typical operating temperatures range from 180ºC to 300ºC. The reactor E-202 will be operating at a temperature of 210ºC as it helps to increase synthesis rate without increasing optical and chemical impurities in the crude lactide. Temperatures above 230ºC would derive in increasingly higher concentrations of meso-lactide.

The reactor will also operate under reduced pressure of 25 mmHg at steady-state operation. At higher pressure, the driving force for lactide evaporation is lower and thus the overall reaction rate. Outlet stream comprises a condenser in order to partially condensate lactide vapour prior to its entrance into the purification step. The remaining liquid stream contains polylactic acid that has not been converted, as well as residual catalyst and stabilizer and non-volatile impurities which came from the previous stage. In order to increase the overall yield of the process and reduce the catalyst and stabilizer inlet flow needed, this stream will be recirculated prior to the entrance into the hold tank. A purge stream is also needed to avoid accumulation of residual impurities with further degradation or colouring problems of the final product.

5.2.2. Block diagram

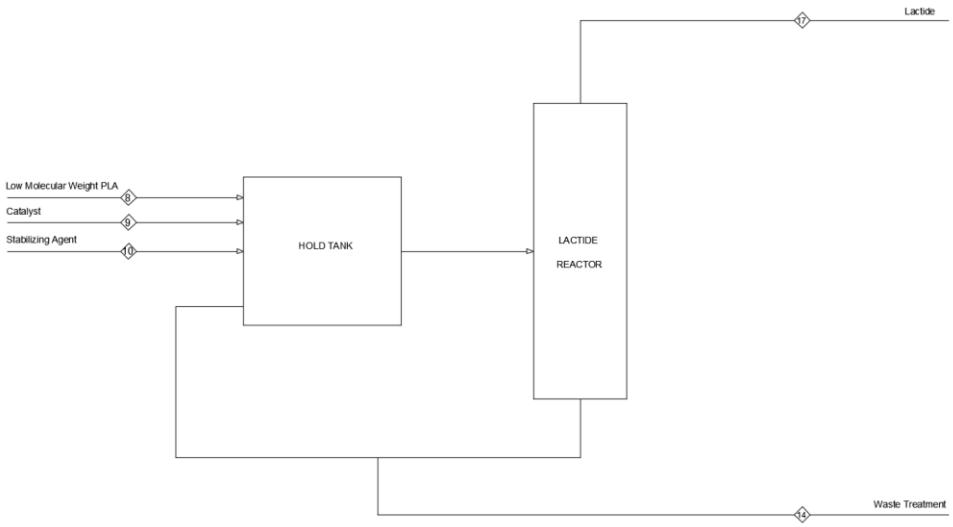

Figure 18. Block Diagram – Section 200

Table 7. Mass balance – Section 200

Stream (kg/h)	8	9	10	14	17
Lactic acid	461.66	0.00	0.00	0.00	39.89
Water	0.00	0.00	0.00	0.00	461.66
NVI	195.51	0.00	0.00	195.51	0.00
PLA (LMW)	10813.39	0.00	0.00	32.67	0.00
Catalyst	0.00	28.59	0.00	28.59	0.00
Stabilizing agent	0.00	0.00	39.10	39.10	0.00
Oligomers	0.00	0.00	0.00	0.00	1637.59
L-lactide	0.00	0.00	0.00	0.00	8650.76
D-lactide	0.00	0.00	0.00	0.00	329.58
Meso-lactide	0.00	0.00	0.00	0.00	122.90
Total	**11470.56**	**28.59**	**39.10**	**295.87**	**11242.38**

5.2.3. Equipment data sheet

Mass and energy balances of section 200, as well as sizing of the main equipment is detailed in *Appendix 2* and *Appendix 3*, respectively, in order to determine the basic design of each equipment. As a result, herein below are shown the specification sheet of each equipment containing the main features and operating conditions.

Hold tank HT-201 is used for a better controllability of the addition of catalyst and stabilizer previous to the lactide reactor, and it is maintained at an optimum temperature for storage of 160ºC in order to keep the prepolymer over the melting point. A basic design of this equipment includes size dimensions and energy requirements based on a continuous stirred tank design.

Pump P-201 A/B is necessary to supply the required energy for liquid impulsion and condition stream 15 to the hold tank operating conditions. Its design is based on power

requirement estimation based on the mechanical energy balance around suction and discharge conductions.

Heat exchanger E-201 is required to condition stream 11 to the depolymerisation reactor operating temperature of 210ºC and its design is reduced to calculate the required heat transfer area as well as medium pressure steam requirements based on duty calculation from energy balance.

A depolymerisation reaction takes place in the lactide reactor E-202. Lactide is produced through the depolymerisation of oligomeric low molecular weight PLA by back-bitting reactions of the carboxylic end groups and the ester bond of the chain back-bone, where a cyclic compound is formed, and by end-biting reactions, which involves the ring closure reaction to form lactide.

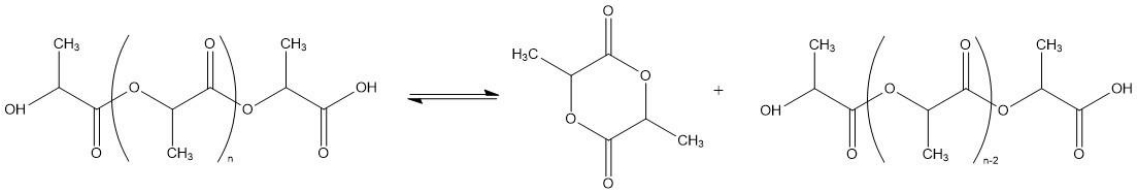

Figure 19. Depolymerization reaction

The depolymerisation reactor E-202 follows the same design procedure as reactor E-103, detailed in *Appendix 4,* adapted to the required operating conditions.

Table 8. HT-201 specification sheet

Equipment label	HT-201	Equipment name	Hold tank
Process service	cw	Equipment type	Continuous Stirring Tank Mixer
OPERATING DATA			
V (m^3)	2.00		
H (m)	1.28		
D (m)	0.85		
T (ºC)	160		
P (kPa)	101.3		
Q (kW)	9.35		
U ($W/m^2ºC$)	250		
ΔT (ºC)	130.5		
A (m^2)	0.29		
$W_{utility}$ (kg/s)	0.11		
TECHNICAL DATA			
Construction material	Stainless steel		
Agitator type	Turbine or Propeller		

Table 9. P-201 A/B specification sheet

Equipment label	P-201 A/B	Equipment type	Positive displacement pump
OPERATING DATA			
Type	Positive displacement		
Max. flow (m^3/h)	0.63		
ΔP (kPa)	-97.9		
Theoretical Power (W)	10.5		
Pump Efficiency	0.75		
Power (W)	14.0		

Table 10.E-201 specification sheet

Equipment label	E-201	Equipment name	Heat exchanger
Process service	mps	Equipment type	Shell and Tubes heat exchanger
OPERATING DATA			
	SHELL SIDE		TUBE SIDE
Stream	Low Mw PLA		Medium pressure steam
W (kg/h)	12228.62		17.34
Q (kW)	9.35		
U (W/m^{2}ºC)	600		
ΔT (ºC)	27.1		
A (m^2)	0.58		

Table 11.E-202 specification sheet

Equipment label	E-202	Equipment name	Depolymerization reactor	
Process service	hps	Equipment type	Falling film evaporator	
OPERATING DATA				
	SHELL SIDE		TUBE SIDE	
Stream	hps		17	13
Fluid	Steam		Lactide vapour	Low Mw PLA
W (kg/s)	1.08		3.12	0.27
ρ (kg/m^3)	16.6		1.2	1096.4
μ (kg/ms)	$1.75\cdot 10^{-5}$		$2.43\cdot 10^{-5}$	$3.05\cdot 10^{-2}$
C_p (J/kgK)	4347		1514	1894
k_f (W/mK)	0.038		0.039	0.195
T (ºC)	250.4		210	210
P (kPa)	4000		3.33	3.33
ΔP (kN/m^2)	19.6		1.1	86.6
v (m/s)	2.1		13.7	2.8
Nº of passes	1		1	
Q (kW)	1848.9			
U (W/m^{2}ºC)	158			
ΔT (K)	40.4			
A (m^2)	289.6			
MECHANICAL DATA				
TUBES				
Material	Stainless steel		Pitch (mm)	25
Nº tubes	946		O.D. (mm)	20
Length (m)	4.88		t (mm)	2
SHELL				
Material	Carbon steel		I.D. (mm)	914.4
Length (m)	4.88		t (mm)	9.5

5.3. Section 300: Lactide purification

5.3.1. Process description

The outlet stream of the depolymerisation reactor is composed of the mixture of lactide enantiomers (L-, D- and meso-lactide) as well as residual water, lactic acid and lactic acid dimers as condensation by-products. In order to obtain an optically pure and high molecular weight polylactic acid, it is of special importance the purification of lactide previous to its polymerization, as water and lactic acid can participate in ring-opening reactions with lactide, decreasing lactide yield and increasing acidity of the lactide product. (Meerdink et al., 2011)

Therefore this stream is fed directly to a distillation system composed by two packed distillation columns T-301 and T-302. A packed column helps to control racemization as it provides minimization of liquid hold-up compared to a plate column. (Gruber et al., 2001). Moreover, this configuration is preferred as for corrosive liquids a packed column is usually cheaper than the equivalent plate column, as well as packed columns should always be considered for vacuum operations (Sinnot, 2005). A thermosiphon is used as reboiler allowing to reduce the residence time of the bottom liquids.

The first column operates at 0.067 bar and it is used in order to remove volatile products such as water, lactic acid and low molecular weight oligomers as distillate stream while lactide enantiomers are obtained in bottoms. Traces of lactide may be removed as distillate product. A minimum reflux ratio is stablished in order to minimize the hold-up time in the column, which avoids racemization. Further improvements of this process could assess the possibility of recirculate the distillate to a previous stage of the process, such as the prepolymer reactor, to avoid raw material losses and therefore increase the overall yield of the process.

The second column operates at 0.013 bar and it is used to separate meso-lactide from L-lactide and D-lactide. Traces of lactic acid and oligomers from the previous column are removed with meso-lactide as distillate while L- and D- lactide are obtained in bottoms. Similarity in the boiling points of L- and D-lactide implies that the separation of both products cannot be obtained by distillation, even though the distillate stream is composed over a 96% of L-Lactide.

5.3.2. Block diagram

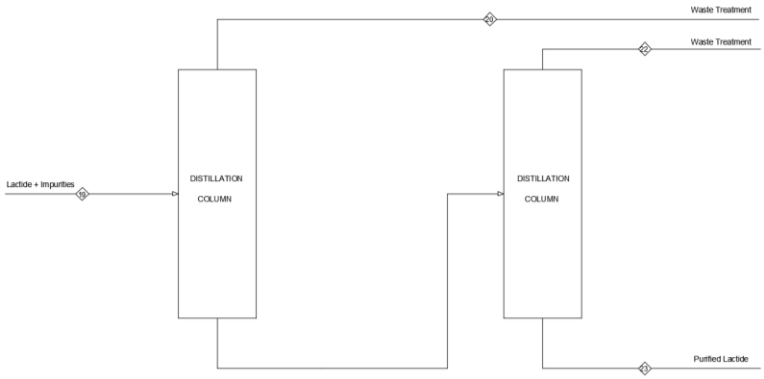

Figure 20. Block Diagram – Section 300

Table 12.Mass balance – Section 300

Stream (kg/h)	19	20	22	23
Lactic acid	39.89	39.09	0.80	0.00
Water	461.66	461.66	0.00	0.00
Oligomers	1637.59	1629.76	7.83	0.00
L-lactide	8650.76	86.51	85.64	8478.61
D-lactide	329.58	0.00	0.00	329.58
Meso-lactide	122.90	5.97	115.77	1.17
Total	**11242.38**	**2222.99**	**210.03**	**8809.36**

5.3.3. Equipment data sheet

Mass and energy balances of section 300, as well as sizing of the main equipment is detailed in *Appendix 2* and *Appendix 3*, respectively, in order to determine the basic design of each equipment. As a result, herein below are shown the specification sheet of each equipment containing the main features and operating conditions.

Condenser E-301 partially condensates stream 17 coming as vapour from the lactide reactor. Its design is reduced to calculate the required heat transfer area as well as cooling water requirements based on duty calculation from energy balance.

Pump P-301 A/B is necessary to supply the required energy for liquid impulsion and condition stream 18 to the distillation column T-301 operating conditions. Its design is based on power requirement estimation based on the mechanical energy balance around suction and discharge conductions.

Packed columns T-301 and T-302 are required to purify the outlet stream of the depolymerisation reactor in order to obtain an optically pure and high molecular weight polylactic acid in the polymerization section. Mass and energy balance of both packed columns have been simulated by Aspen Plus. A structured packing material is chosen over random packing so as to enhance contact between the vapour and liquid and to minimize the liquid hold-up, which results in a lower pressure drop over the column and in the minimisation of reactions between different species. A basic hydraulic design of both columns is carried out in order to determine the columns diameters which ensure an adequate pressure drop and avoid flooding conditions.

Table 13.E-301 specification sheet

Equipment label	E-301	Equipment name	Condenser
Process service	cw	Equipment type	Shell and Tubes heat exchanger
OPERATING DATA			
	SHELL SIDE		TUBE SIDE
Stream	Cooling water		Lactide
W (kg/s)	22.45		3.12
Q (kW)	1877.56		
U ($W/m^2°C$)	1250		
ΔT (°C)	139.0		
A (m^2)	10.80		

Table 14.P-301 A/B specification sheet

Equipment label	P-301 A/B	Equipment type	Centrifugal pump
OPERATING DATA			
Type	Centrifugal		
Max. flow (m^3/h)	8.45		
ΔP (kPa)	-3.3		
Theoretical Power (W)	44.4		
Pump Efficiency	0.75		
Power (W)	59.2		

Table 15. T-301 specification sheet

Equipment label	T-301	Equipment name	Distillation column
Process service	cw/mps	Equipment type	Packed column
OPERATING DATA			
	TOP		BOTTOM
Inside diameter (m)	0.778		0.778
V (kg/s)	0.617		0.617
L (kg/s)	2.505		2.505
T (ºC)	126		158
P (kPa)	6.67		6.67
% Flooding	39.6		39.6
Heating equipment	Condenser		Thermosiphon
m utility (kg/s)	14.99		0.01
Q (kW)	1253.6		800.3
U ($W/m^2ºC$)	350		1118
ΔT (ºC)	85.6		33.9
A (m^2)	41.8		21.1
TECHNICAL DATA			
Construction material	Carbon steel		
Packing type	Intalox 1T structured packing		
HETP	0.292		
Diameter (m)	0.778		
Height (m)	4.87		

Table 16. T-302 specification sheet

Equipment label	T-302	Equipment name	Distillation column
Process service	cw/mps	Equipment type	Packed column
OPERATING DATA			
	TOP		BOTTOM
Inside diameter	0.381		0.381
V (kg/s)	0.06		0.06
L (kg/s)	2.45		2.45
T (ºC)	137		146
P (kPa)	1.34		1.34
% Flooding	50.0		50.0
Heating equipment	Condenser		Thermosiphon
m utility (kg/s)	46.56		0.08
Q (kW)	3892.7		3688.7
U	350		1730
ΔT (ºC)	96.6		21.9
A (m^2)	115.1		97.3
TECHNICAL DATA			
Construction material	Carbon Steel		
Packing type	Intalox 1T structured packing		
HETP	0.292		
Diameter (m)	0.381		
Height (m)	7.46		

5.4. Section 400: Polymerization of Lactide

5.4.1. Process description

The purified lactide is transferred to a chain of two continuous stirred tank polymerization reactors R-401 and R-402 where high molecular weight polylactic acid is produced via ring-opening polymerization of lactide. The ROP can be catalysed by different tin,

lead, aluminium or zinc catalysts, among others. However, stannous octoate ($Sn(Oct)_2$) has been selected for many reasons, as it is soluble in lactide monomer, leading to high catalytic activity with yields over 90%; results in high molecular weight polymer, enhancing polymerization rate and leads to low degree of racemization. It is the most widely used catalyst in ROP of lactide at industrial levels due to its relatively low costs, besides it has low toxicity and it is accepted by the US Food and Drug Administration. (Metkar et al., 2019)

It is demonstrated conversion increases with the decrease of monomer to catalyst ratio. A 15,000 monomer to catalyst concentration ratio, which corresponds to a 0.018 wt% of catalyst in the feed stream, leads to the highest molecular weight and conversion, as reported by Yu et al. The lack of nucleophilicity of $Sn(Oct)_2$ in order to initiate the polymer chains makes the presence of an alcohol used as co-catalyst a necessity, in a way such that the catalyst will perform under the coordination insertion mechanism, where stannous octoate reacts with OH-bearing species to form an alkoxide which acts as the initiator of the polymerization reaction, enhancing the rate of reaction. (Yu et al., 2011)

The type and concentration of the alcohol is the responsible of the polymer chain microstructure characteristics and final PLA molecular weight. Dodecyl alcohol has been selected as it provides adequate properties to the system such as high melting point and thermal stability, as well as it has been demonstrated to improve the rate of polymerization and allow its use at the high temperatures needed for the reaction to occur. As the hydroxyl group acts as a chain initiation agent as well as chain transfer agent, its concentration is an important parameter that needs to be adjusted. A value of 17 for the alcohol to catalyst concentration ratio has been selected, as an increase in the concentration over this value would lead to higher rate of reaction but lower final molecular weight. (Yu et al., 2011)

The reaction temperature is also one of the most important parameters of the system as the polymerization rate and thus monomer conversion increases as temperature does. However, high temperatures over 180ºC and up to 230ºC lead to well-known degradation reactions such as transesterification and chain scission reactions, as the back-bitting reaction for the production of cyclic compounds is also catalysed by $Sn(Oct)_2$ and favoured at higher temperatures, leading to a decrease in final molecular weight. (Metkar et al., 2019) At the temperature stablished of 180 ºC and under the system conditions, the role of back-bitting reaction becomes important for residence times over 0.5 h, which is higher than the actual residence time of both reactors needed for the selected monomer conversion of 0.96. (Yu et al., 2011)

It is known monomer conversion also impacts polymerization rates as higher conversions leads to an increase in the polymer viscosity which decreases the rate of mass and heat transfer. At the final monomer conversion stablished of 0.96, a polymer of 115,973 g/mol with a polydispersity (Pd=Mw/Mn) of 1.9 is obtained.

5.4.2. Block diagram

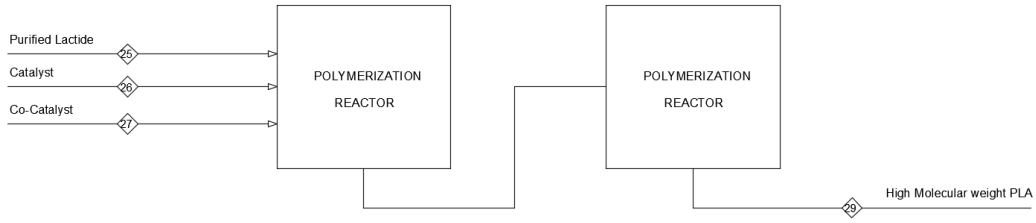

Figure 21. Block Diagram – Section 400

Table 17.Mass balance – Section 400

Stream (kg/h)	25	26	27	29
L-lactide	8478.61	0.00	0.00	332.43
D-lactide	329.58	0.00	0.00	12.92
Meso-lactide	1.17	0.00	0.00	0.05
PLA (HMW)	0.00	0.00	0.00	8463.96
Catalyst $Sn(Oct)_2$	0.00	1.65	0.00	1.65
Co-catalyst	0.00	0.00	28.06	28.06
Total	8809.36	1.65	28.06	8839.07

5.4.3. Equipment data sheet

Mass and energy balances of section 400, as well as sizing of the main equipment is detailed in *Appendix 2* and *Appendix 3*, respectively, in order to determine the basic design of each equipment. As a result, herein below are shown the specification sheet of each equipment containing the main features and operating conditions.

Pump P-401 A/B is necessary to supply the required energy for liquid impulsion and condition stream 23 to atmospheric condition in the polymerization reactor. Its design is based on power requirement estimation based on the mechanical energy balance around suction and discharge conductions.

Heat exchanger E-401 is required to condition stream 24 to the polymerization reactors operating temperature of 180ºC and its design is reduced to calculate the required heat transfer area as well as medium pressure steam requirements based on duty calculation from energy balance.

The reaction that takes place in this section is the ring-opening polymerization of L-Lactide based on the alkoxide initiation mechanism with $Sn(Oct)_2$ as catalyst (C) and dodecyl alcohol as co-catalyst (D) at 180ºC, as depicted in the following Figure 22.

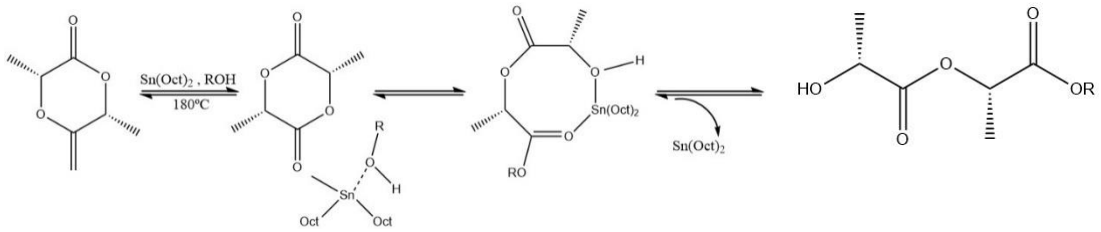

Figure 22. $Sn(Oct)_2$ catalysed ROP of L-Lactide in the presence of a hydroxylic initiator molecule

Taking into account both economical and mechanical aspects and attending to the Levenspiel diagram detailed in *Appendix 3*, a total number of 2 reactors is selected. The conversion achieved in the first reactor takes a value of 0.853 and it has been deduced by selecting the minimum total volume calculated as the sum of both volume reactors. A design procedure of a CSTR is carried out for both reactors, including size dimensions and energy requirements based on mass and energy balances.

Table 18.P-401 A/B specification sheet

Equipment label	P-401 A/B	Equipment type	Centrifugal pump
OPERATING DATA			
Type	Centrifugal		
Max. flow (m^3/h)	6.04		
ΔP (kPa)	-100.0		
Theoretical Power (W)	180.6		
Pump Efficiency	0.75		
Power (W)	240.8		

Table 19.E-401 specification sheet

Equipment label	E-401	Equipment name	Heat exchanger
Process service	mps	Equipment type	Shell and Tubes heat exchanger
OPERATING DATA			
	SHELL SIDE		TUBE SIDE
Stream	Medium pressure steam		Lactide
W (kg/h)	21.24		8809.36
Q (kW)	11.45		
U ($W/m^2°C$)	500		
ΔT (°C)	32.4		
A (m^2)	0.71		

Table 20.R-401 specification sheet

Equipment label	R-401	Equipment name	Polymerization reactor
Process service	cw	Equipment type	CSTR
OPERATING DATA			
Reactor type	Continuous Stirred Tank Reactor		
V (m^3)	2.33		
H (m)	1.36		
D (m)	0.91		
T (ºC)	180		
P (kPa)	101.32		
Viscosity (kg/ms)	580.8		
Q (kW)	390.9		
U ($W/m^2°C$)	400		
ΔT (°C)	140		
A (m^2)	6.98		
m utility (kg/s)	4.67		
TECHNICAL DATA			
Construction material	Stainless Steel		
Cooling system	Jacket system		
Agitator type	Anchor		

Table 21.R-402 specification sheet

Equipment label	R-402	Equipment name	Polymerization reactor
Process service	cw	Equipment type	CSTR
OPERATING DATA			
Reactor type	Continuous Stirred Tank Reactor		
V (m^3)	2.19		
H (m)	1.33		
D (m)	0.89		
T (ºC)	180		
P (kPa)	101.32		
Viscosity (kg/ms)	881.6		
Q (kW)	49.6		
U (W/m^2ºC)	400		
ΔT (ºC)	140		
A (m^2)	0.89		
m utility (kg/s)	0.59		
TECHNICAL DATA			
Construction material	Stainless Steel		
Cooling system	Jacket system		
Agitator type	Anchor		

6. INSTRUMENTATION AND CONTROL

Every chemical plant is exposed to a series of external influences or disturbances that makes it a necessity the continuous monitoring of the plant's operation and a control system in order to guarantee, in the most efficient and economical possible way, the satisfaction of certain requirements. This necessities are imposed by technical, economic and safety conditions for which the process is designed, such as production specifications, environmental regulations, economic and safety aspects, and operational conditions. (Stephanopoulus, 1984)

The control system of the plant will therefore allow to suppress the influence of these external disturbances, at the same time that it will ensure the stability of the chemical process and the optimization of the process performance.

6.1. Control types

There are different types of control determined by the relationship between the controlled variable (CV), which is the process variable measured by the sensor and whose value wants to be maintained under control, and the manipulated variable (MV), or the process variable in which the final control element acts in order to maintain the controlled variable in the Set Point.

At industrial scale, feedback control is the most commonly used as it allows an ease of implementation as well as it is sufficient for processes where the deviation from the SP is assumable. All control loops designed in this chapter will be feedback control loops.

A feedback controller measures directly the controlled variable and compares it with the set point established in order to generate a deviation error. This error, conditioned by the control algorithm PID, is provided to the final control element, conducting the appropriate corrective actions so that the manipulated variable reduces the deviation and brings the controlled variable back into the right direction to the sept point.

The main disadvantages of this type of control is that the action is taken after the deviation has been detected and thus the disturbance has already propagated throughout the process, which can present problems when the response time of the system is high. (Svrcek et al., 2014)

There are more complex types of control that help to reduce this problem by anticipating such as feedback-feedforward control, cascade or split range control but will not be object of study as they will not be used in the control system of the plant.

6.2. Elements of a control system

In every control loop configuration, the following elements in a SISO system (Single Input Single Output) can be distinguish: (Stephanopoulos, 1984)

- Sensor: Instruments in charge of measuring the controlled output variables. There are different types of sensor depending on the variable measured or on the construction characteristics.
- Transmissor: Secondary element that transforms the value of the variable into a signal understandable by the controller. It can be an electrical signal [4-20] mA or pneumatic [3-15] psi.
- Controller: It receives the signal of the transmitter and decides the action of the final control element by comparing the signal value with the set point.
- Final control element: Instrument that implements the action of the controller on the manipulated variable in order to bring the controlled variable back to the set point. Control valves are the most frequently encountered as final control elements.

6.3. Nomenclature

The ISA-5.1 Standard: *"Instrumentation Symbols and Identification"* nomenclature will be used to describe the control loops of the plant, in order to standardize the identification and representation of instruments and associated devices by introducing a designation system that follows the following pattern, where X is the controlled variable, YZ is the instrument function, A is the plant section and BB the loop number.

$$XYZ - ABB$$

The letters can have different meanings whether they are first or second letter. The following Table 22 sums up the most frequent letters used in a chemical process.

Table 22.P&ID nomenclature

Letter	First letter	Successive letters
A	-	Alarm
C	-	Control
F	Flow	-
H	-	High
I	-	Indicator
K	Time	-
L	Level	Low
P	Pressure	-
S	-	Switch
T	Temperature	Transmissor
V	-	Valve
Y	-	Conversor

6.4. Control loops of the process

Control loops of the plant will be described in this section. The P&I Diagram included in *Appendix 1* collects the engineering details of the equipment as well as instruments, piping, valves and fittings.

Control valves are selected as final control elements of the process. They will be provided with a bypass system in order to avoid the stoppage of the process in case of any type of failure as a safety measure. Also a drainage system is included to allow pressure relief in case the replacement of the valves is needed. The acronyms F.O and F.C refer to the state of valve in case of failure, fails open or fails closed, respectively, and it has been stablished based on security criteria. As a rule of thumb, outlet streams and cooling streams will remain open while inlet streams and heating streams will remain closed.

6.4.1. Section 100: Polycondensation of low molecular weight PLA

- **Falling film evaporator E-101 and Pump P-101 A/B**

A control system in the lactic acid solution feed flow is established in order to be able to define the production flow. In the falling film evaporator E-101 is evaporated part of the water of the feeding stream prior to the polycondensation of lactic acid. Control in operating conditions of temperature and pressure is required to attain the degree of evaporation specified, as well as a constant liquid level on the falling film evaporator that controls the residence time to avoid racemization.

This last control loop will also provide a stabilized flow to P-101 A/B avoiding cavitation problems of the pump. If the pump works at a flow rate lower than optimal or sucks a flow rate lower than the minimum it can cause the cavitation of the pump resulting in equipment damage. P-101 B is in standby mode and it is used during the maintenance operations of P-101 A or because its failure.

Control loop F-101 is a feedback type control loop that controls the inlet flow of the lactic acid solution by manipulating it, allowing the definition of the production flow at any given time. Its operation begins with the measurement of the stream 1 flow rate, which is the controlled variable, and the transmission of its signal through the flow transmitter FT-101 to the flow indicator and controller FIC-101. FIC-101 indicates the value of the signal received by the transmitter and, by comparing said value with the set point, controls the opening percentage of FV-101 control valve, final control element and actuator, manipulating the stream 1 flow rate, in a way such that if the flow rate is above or below the required value and selected as the set point, the valve closes or opens, respectively, in order to keep the inlet flow constant.

Control loop T-102 is a feedback type control loop that controls the temperature inside the evaporator by regulating the low pressure steam flow. Its operation begins with the measurement of the temperature inside the evaporator, which is the controlled variable, and the

transmission of its signal through the temperature transmitter TT-102 to the temperature indicator and controller TIC-102. TIC-102 indicates the value of the signal received by the transmitter and, by comparing said value with the set point, controls the opening percentage of TV-102 control valve, final control element and actuator, regulating the flow rate of the low pressure steam, which is the manipulated variable. The evaporator set point temperature is 80ºC, so that if this value increases or decreases, the valve closes or opens, respectively, in order to bring the temperature back to the set point.

Control loop P-103 is a feedback type control loop that controls the pressure of the vapour stream 2 in order to maintain a stable operating pressure, by manipulating the high pressure steam used in the ejector. Its operation begins with the measurement of the pressure in the vapour stream, which is the controlled variable, and the transmission of its signal through the pressure transmitter PT-103 to the pressure indicator and controller PIC-103. PIC-103 indicates the value of the signal received by the transmitter and, by comparing said value with the set point, controls the opening percentage of PV-103 control valve, final control element and actuator, regulating the flow rate of the high pressure steam, which is the manipulated variable, in a way such that if the pressure increases or decreases, the valve opens or closes, respectively, in order to bring the pressure back to the set point.

Control loop L-104 is a feedback type control loop that controls the liquid level inside the evaporator in order to maintain it stable by manipulating the discharge flow of pump P-101 A/B, avoiding this way cavitation problems of the pump. Its operation begins with the measurement of the liquid level inside the evaporator and the transmission of its signal through the LT-104 level transmitter to the LIC-104 level indicator and controller. LIC-104 indicates the value of the signal received by the transmitter and, by comparing said value with the set point, controls the opening percentage of the LV-104 valve, final control element and actuator, regulating the flow rate of the discharge stream 4. In this way, if the liquid level is above or below the set point, the valve opens or closes, respectively, in order to keep constant the liquid level.

- **Heat exchanger E-102**

Heat exchanger E-102 pre-heats the stream input prior to the prepolymer reactor E-103 in order to condition stream 5 to the reactor operating temperature. The control system in this equipment is needed in order to maintain a constant temperature previous to the entrance to the reactor at 130ºC

Control loop T-105 is a feedback type control loop that controls the temperature of the stream 5 that leaves the exchanger by regulating the low pressure steam flow. Its operation begins with the measurement of the temperature in stream 5, which is the controlled variable, and the transmission of its signal through the temperature transmitter TT-105 to the temperature

indicator and controller TIC-105. TIC-105 indicates the value of the signal received by the transmitter and, by comparing said value with the set point, controls the opening percentage of TV-105 control valve, final control element and actuator, regulating the flow rate of the steam, which is the manipulated variable. Stream 5 temperature is 130ºC, so that if this value increases or decreases, the valve closes or opens, respectively, in order to bring the temperature back to 130ºC.

- **Prepolymer reactor E-103 and pump P-102 A/B**

In the prepolymer reactor E-103 takes place the polycondensation of lactic acid to produce the prepolymer of low molecular weight. It is a requirement for the operating conditions of temperature and pressure to be constant in order to avoid side reactions as well as a constant liquid level on the falling film evaporator that controls the residence time, a critical parameter to control racemization.

In a similar way to the evaporator E-101, this last control loop will also provide a stabilized flow to P-102 A/B avoiding cavitation problems of the pump. If the pump works at a flow rate lower than optimal or sucks a flow rate lower than the minimum it can cause the cavitation of the pump resulting in equipment damage. P-102 B is in standby mode and it is used during the maintenance operations of P-102 A or because its failure.

Control loop T-106 is a feedback type control loop that controls the temperature inside the reactor by regulating the cooling water stream. Its operation begins with the measurement of the temperature inside the reactor, which is the controlled variable, and the transmission of its signal through the temperature transmitter TT-106 to the temperature indicator and controller TIC-106. TIC-106 indicates the value of the signal received by the transmitter and, by comparing said value with the set point, controls the opening percentage of TV-106 control valve, final control element and actuator, regulating the flow rate of the cooling water, which is the manipulated variable. The reactor set point temperature is 180ºC, so that if this value increases or decreases, the valve opens or closes, respectively, in order to bring the temperature back to the set point.

Control loop P-107 is a feedback type control loop that controls the pressure of vapour stream 6 in order to maintain a stable operating pressure, by manipulating the hps used in the ejector. Its operation begins with the measurement of the pressure in the vapour stream, which is the controlled variable, and the transmission of its signal through the pressure transmitter PT-107 to the pressure indicator and controller PIC-107. PIC-107 indicates the value of the signal received by the transmitter and, by comparing said value with the set point, controls the opening percentage of PV-107 control valve, final control element and actuator, regulating the flow rate of the high pressure steam, which is the manipulated variable, in a way such that if the pressure

increases or decreases, the valve opens or closes, respectively, in order to bring the pressure back to the set point.

Control loop L-108 is a feedback type control loop that controls the liquid level inside the reactor in order to maintain it stable by manipulating the discharge flow of pump P-102 A/B, avoiding this way cavitation problems of the pump. Its operation begins with the measurement of the liquid level inside the reactor and the transmission of its signal through the LT-108 level transmitter to the LIC-108 level indicator and controller. LIC-108 indicates the value of the signal received by the transmitter and, by comparing said value with the set point, controls the opening percentage of the LV-108 valve, final control element and actuator, regulating the flow rate of the discharge stream 8. In this way, if the liquid level is above or below the set point, the valve opens or closes, respectively, in order to keep constant the liquid level.

6.4.2. Section 200: Depolymerization of PLA and lactide formation

- **Hold Tank HT-201**

In the hold tank HT-201 besides the addition of catalyst and stabilizer up to the required concentration, the stream coming from the prepolymer reactor is cooled down to an optimum temperature for storage of 160ºC in order to keep the prepolymer over the melting point. The control system applied to this equipment maintains a stable liquid level on the inside avoiding any possible situation of flooding or emptying of the equipment, as well as controls the inside temperature.

Control loop T-201 is a feedback type control loop that controls the temperature inside the hold tank by regulating the cooling water stream. Its operation begins with the measurement of the temperature inside the tank, which is the controlled variable, and the transmission of its signal through the temperature transmitter TT-201 to the temperature indicator and controller TIC-201. TIC-201 indicates the value of the signal received by the transmitter and, by comparing said value with the set point, controls the opening percentage of TV-201 control valve, final control element and actuator, regulating the flow rate of the cooling water, which is the manipulated variable. The hold tank set point temperature is 160ºC, so that if this value increases or decreases, the valve opens or closes, respectively, in order to bring the temperature back to the set point.

Control loop L-202 is a feedback type control loop that controls the liquid level inside the hold tank in order to keep it stable by manipulating the flow rate of the outlet stream 11. Its operation begins with the measurement of the liquid level inside the mixer and the transmission of its signal through the LT-202 level transmitter to the LIC-202 level indicator and controller. LIC-202 indicates the value of the signal received by the transmitter and, by comparing said value with the set point, controls the opening percentage of the LV-202 valve, final control element and actuator, regulating the flow rate of the outlet stream. In this way, if the liquid level

is above or below the set point, the valve opens or closes, respectively, in order to keep the liquid level constant.

- **Heat exchanger E-201**

Heat exchanger E-201 pre-heats the stream input prior to the lactide reactor E-202 in order to condition stream 12 to the reactor operating temperature. The control system in this equipment is needed in order to maintain a constant temperature previous to the entrance to the reactor at 180ºC

Control loop T-203 is a feedback type control loop that controls the temperature of the stream 12 that leaves the exchanger by regulating the mps steam flow. Its operation begins with the measurement of the temperature in stream 12, which is the controlled variable, and the transmission of its signal through the temperature transmitter TT-203 to the temperature indicator and controller TIC-203. TIC-203 indicates the value of the signal received by the transmitter and, by comparing said value with the set point, controls the opening percentage of TV-203 control valve, final control element and actuator, regulating the flow rate of the steam, which is the manipulated variable. Stream 12 temperature is 180ºC, so that if this value increases or decreases, the valve closes or opens, respectively, in order to bring the temperature back to 180ºC.

- **Lactide reactor E-202 and pump P-201**

In the lactide reactor E-202 takes place the depolymerization reaction of the prepolymer into lactide. It is a requirement for the operating conditions of temperature and pressure to be constant in order to avoid side reactions as well as a constant liquid level that controls the residence time which in turn controls racemization. This last control loop will also provide a stabilized flow to P-201 A/B avoiding cavitation problems of the pump. If the pump works at a flow rate lower than optimal or sucks a flow rate lower than the minimum it can cause the cavitation of the pump resulting in equipment damage. P-201 B is in standby mode and is used during the maintenance operations of P-201 A or because its failure.

Control loop T-204 is a feedback type control loop that controls the temperature inside the reactor by regulating the high pressure steam flow rate. Its operation begins with the measurement of the temperature inside the reactor, which is the controlled variable, and the transmission of its signal through the temperature transmitter TT-204 to the temperature indicator and controller TIC-204. TIC-204 indicates the value of the signal received by the transmitter and, by comparing said value with the set point, controls the opening percentage of TV-204 control valve, final control element and actuator, regulating the flow rate of the high pressure steam, which is the manipulated variable. The reactor set point temperature is 210ºC, so that if this value increases or decreases, the valve closes or opens, respectively, in order to bring the temperature back to the set point.

Control loop P-205 is a feedback type control loop that controls the pressure of vapour stream 17 in order to maintain a stable operating pressure, by manipulating the high pressure steam used in the ejector. Its operation begins with the measurement of the pressure in the vapour stream, which is the controlled variable, and the transmission of its signal through the pressure transmitter PT-205 to the pressure indicator and controller PIC-205. PIC-205 indicates the value of the signal received by the transmitter and, by comparing said value with the set point, controls the opening percentage of PV-205 control valve, final control element and actuator, regulating the flow rate of the high pressure steam, which is the manipulated variable, in a way such that if the pressure increases or decreases, the valve opens or closes, respectively, in order to bring the pressure back to the set point.

Control loop L-206 is a feedback type control loop that controls the liquid level inside the reactor in order to maintain it stable by manipulating the discharge flow of pump P-201 A/B, avoiding this way cavitation problems of the pump. Its operation begins with the measurement of the liquid level inside the reactor and the transmission of its signal through the LT-206 level transmitter to the LIC-206 level indicator and controller. LIC-206 indicates the value of the signal received by the transmitter and, by comparing said value with the set point, controls the opening percentage of the LV-206 valve, final control element and actuator, regulating the flow rate of the discharge stream 16. In this way, if the liquid level is above or below the set point, the valve opens or closes, respectively, in order to maintain the liquid level constant.

6.4.3. Section 300: Lactide purification

- **Condenser E-301**

Condenser E-301 partially condensates stream 17 coming as vapour from the lactide reactor to a mass vapour fraction of 0.212. The control system in this equipment is applied in order to maintain a constant temperature previous to the entrance to the purification system of the process.

Control loop T-301 is a feedback type control loop that controls the temperature of the stream 18 that leaves the condenser by regulating the cooling water flow. Its operation begins with the measurement of the temperature in stream 18, which is the controlled variable, and the transmission of its signal through the temperature transmitter TT-301 to the temperature indicator and controller TIC-301. TIC-301 indicates the value of the signal received by the transmitter and, by comparing said value with the set point, controls the opening percentage of TV-301 control valve, final control element and actuator, regulating the flow rate of the cooling water, which is the manipulated variable. Stream 18 temperature is 150ºC, so that if this value increases or decreases, the valve opens or closes, respectively, in order to bring the temperature back to 150ºC.

- **Pump P-301**

The control in P-301 A and P-301 B pumps is applied in order to provide a stabilized flow to the equipment in case of no feeding supply or flow variation. If the pump works at a flow rate lower than optimal or sucks a flow rate lower than the minimum can cause the cavitation of the pump resulting in equipment damage. P-301 B is in standby mode and is used during the maintenance operations of P-301 A or because its failure.

As pump P-301 A/B is fed from the tubes of the condenser, an accumulator tank is placed prior to the pump to ensure a minimum liquid level controlled by manipulating the discharge stream of the pumps.

Control loop L-302 is a feedback type control loop that controls the liquid level inside the accumulator tank in order to maintain it stable by manipulating the discharge flow of pump P-301 A/B, avoiding this way cavitation problems of the pump. Its operation begins with the measurement of the liquid level inside the tank and the transmission of its signal through the LT-302 level transmitter to the LIC-302 level indicator and controller. LIC-302 indicates the value of the signal received by the transmitter and, by comparing said value with the set point, controls the opening percentage of the LV-302 valve, final control element and actuator, regulating the flow rate of the discharge stream 19. In this way, if the liquid level is above or below the set point, the valve opens or closes, respectively, in order to keep constant the liquid level.

- **Packed columns T-301 and T-302**

Distillation column T-301 is part of the purification system of lactide and has the main objective of separating the volatile components water, lactic acid and low molecular weight oligomers from the lactide. The control applied to this equipment is needed in order to maintain constant the degree of separation specified in distillate and bottoms subject to possible changes in flow or temperature. It is also necessary to control the bottom liquid level in order to guarantee the correct operation of the column, avoiding conditions of flooding or emptying of the equipment.

Control loop P-303 is a feedback type control loop that controls the pressure of vapour stream in order to maintain a stable operating pressure, and thus an adequate degree of separation, by manipulating the hps used in the ejector. Its operation begins with the measurement of the pressure in the vapour stream, which is the controlled variable, and the transmission of its signal through the pressure transmitter PT-303 to the pressure indicator and controller PIC-303. PIC-303 indicates the value of the signal received by the transmitter and, by comparing said value with the set point, controls the opening percentage of PV-303 control valve, final control element and actuator, regulating the flow rate of the high pressure steam,

which is the manipulated variable. in a way such that if the pressure increases or decreases, the valve opens or closes, respectively, in order to bring the pressure back to the set point.

Control loop F-304 is a feedback type control loop that controls the reflux flow rate of column T-301 by manipulating it to avoid a change in the degree of separation of the multicomponent column. Its operation begins with the measurement of the reflux stream flow rate, which is the controlled variable, and the transmission of its signal through the flow transmitter FT-304 to the flow indicator and controller FIC-304. FIC-304 indicates the value of the signal received by the transmitter and, by comparing said value with the set point, controls the opening percentage of FV-304 control valve, final control element and actuator, manipulating the reflux flow rate, in a way such that if the flow rate of the reflux stream is above or below the required value and selected as the set point, the valve closes or opens, respectively, in order to keep the flow constant.

Control loop L-305 is a feedback type control loop that controls the liquid level in the distillation tank in order to maintain it stable by manipulating the flow rate of the distillate stream 20 and thus avoiding flooding or emptying of the tank. Its operation begins with the measurement of the liquid level of the tank, which is the controlled variable, and the transmission of its signal through the level transmitter LT-305 to the level indicator and controller LIC-305. LIC-305 indicates the value of the signal received by the transmitter and, by comparing said value with the set point, controls the opening percentage of LV-305 control valve, final control element and actuator, manipulating the stream 20 flow rate, in a way such that if the liquid level is above or below the required, the valve opens or closes, respectively, in order to keep the liquid level constant.

Control loop T-306 is a feedback type control loop that controls the temperature inside the column by regulating the medium pressure steam flow from the thermosiphon. As distillation is based on liquid-vapour equilibrium, this control loop makes it possible to indirectly control the degree of separation achieved on the column. Its operation begins with the measurement of the temperature inside the column, which is the controlled variable, and the transmission of its signal through the temperature transmitter T-306 to the temperature indicator and controller TIC-306. TIC-306 indicates the value of the signal received by the transmitter and, by comparing said value with the set point, controls the opening percentage of TV-306 control valve, final control element and actuator, manipulating the steam flow in the thermosiphon, in a way such that if the temperature inside increases or decreases, the valve closes or opens, respectively, in order to bring the temperature back to its value.

Control loop L-307 is a feedback type control loop that controls the liquid level in the bottom part of the column by manipulating the flow rate of the bottom stream 21 and thus avoiding flooding or emptying of the column. Its operation begins with the measurement of the liquid level inside the column, which is the controlled variable, and the transmission of its signal

through the level transmitter LT-307 to the level indicator and controller LIC-307. LIC-307 indicates the value of the signal received by the transmitter and, by comparing said value with the set point, controls the opening percentage of LV-307 control valve, final control element and actuator, manipulating the stream 21 flow rate, in a way such that if the liquid level is above or below the required, the valve opens or closes, respectively, in order to keep the liquid level constant.

Control loops P-308, F-309, L-310, T-311 and L-312 carry out the same operation above explained, but corresponding to the distillation column T-302 operating conditions.

6.4.4. Section 400: Ring-opening polymerization of lactide

- **Heat exchanger E-401**

Heat exchanger E-401 heats the stream input prior to the polymerization reactor R-401 in order to condition stream 25 to the reactor operating temperature. The control system in this equipment is needed in order to maintain a constant temperature in order to guarantee an isothermal operation at the optimum temperature of 180ºC at which the reaction is carried out.

Control loop T-401 is a feedback type control loop that controls the temperature of the stream 25 that leaves the exchanger by regulating the mps steam flow. Its operation begins with the measurement of the temperature in stream 25, which is the controlled variable, and the transmission of its signal through the temperature transmitter TT-401 to the temperature indicator and controller TIC-401. TIC-401 indicates the value of the signal received by the transmitter and, by comparing said value with the set point, controls the opening percentage of TV-401 control valve, final control element and actuator, regulating the flow rate of the steam, which is the manipulated variable. Stream 25 temperature is 180ºC, so that if this value increases or decreases, the valve closes or opens, respectively, in order to bring the temperature back to 180ºC.

- **Polymerization reactor R-401 and R-402**

In reactors R-401 and R-402 the ring opening polymerization reaction takes place and the control system applied to these equipment is to assure an optimized refrigeration temperature and avoid any possible side reaction. Also a level control loop is needed to maintain a stable liquid level on the inside avoiding any possible situation of flooding or emptying of the equipment.

Control loop T-402 is a feedback type control loop that controls the temperature inside the reactor by regulating the cooling water stream. Its operation begins with the measurement of the temperature inside the reactor, which is the controlled variable, and the transmission of its signal through the temperature transmitter TT-402 to the temperature indicator and controller TIC-402. TIC-402 indicates the value of the signal received by the transmitter and, by comparing said value with the set point, controls the opening percentage of TV-402 control

valve, final control element and actuator, regulating the flow rate of the cooling water, which is the manipulated variable. The reactor set point temperature is 180ºC, so that if this value increases or decreases, the valve opens or closes, respectively, in order to bring the temperature back to the set point.

Control loop L-403 is a feedback type control loop that controls the liquid level inside the reactor in order to keep it stable by manipulating the flow rate of the outlet stream 28. Its operation begins with the measurement of the liquid level inside the reactor and the transmission of its signal through the LT-403 level transmitter to the LIC-403 level indicator and controller. LIC-403 indicates the value of the signal received by the transmitter and, by comparing said value with the set point, controls the opening percentage of the LV-403 valve, final control element and actuator, regulating the flow rate of the outlet stream. In this way, if the liquid level is above or below the set point, the valve opens or closes, respectively, in order to keep constant the liquid level.

Control loops T-404 and L-405 carry out the same operation, but it corresponds to the control of the reactor R-402.

6.5. Alarms of the process

Alarms as part of the control system act as a visual or auditory operating instruments with the main objective of alerting operators of possible deviations in operating conditions that can affect the plant safety. Alarms used in this process will help to increase the control system reliability and are listed in the following Table 23.

Table 23.Alarms identification code and function

Instrument identification	Function
PAH-101	High pressure in evaporator E-101
PAL-102	Low pressure in evaporator E-101
PAH-103	High pressure in prepolymer reactor E-103
PAL-104	Low pressure in prepolymer reactor E-103
PAH-201	High pressure in lactide reactor E-202
PAL-202	Low pressure in lactide reactor E-202
PAH-301	High pressure in column T-301
PAL-302	Low pressure in column T-301
LAH-303	High level in column T-301
LAL-304	Low level in column T-301
PAH-305	High pressure in column T-302
PAL-306	Low pressure in column T-302
LAH-307	High level in column T-302
LAL-308	Low level in column T-302

6.6. Indicators of the process

Indicators in the process are used in order to provide the operators the value of certain important variables of the process leading to a proper operation of the plant. The following Table 24 collects the indicators of the process.

Table 24.Indicators identification code and function

Instrument identification	Function
PI-101	Pressure indicator Pump 101-A
PI-102	Pressure indicator Pump 101-B
PI-103	Pressure indicator Pump 102-A
PI-104	Pressure indicator Pump 102-B
PI-201	Pressure indicator in hold tank HT-201
PI-202	Pressure indicator Pump 201-A
PI-203	Pressure indicator Pump 201-B
PI-301	Pressure indicator Pump 301-A
PI-302	Pressure indicator Pump 301-B
PI-401	Pressure indicator Pump 401-A
PI-402	Pressure indicator Pump 401-B
PI-403	Pressure indicator in reactor R-401
PI-404	Pressure indicator in reactor R-402
TI-405	Temperature indicator in stream 29

6.7. Safety valves of the process

Safety valves are pressure relief devices that guarantee the safety of the recipient when overpressure occurs in case of failure of the control system. The increase in pressure is given when mass or energy accumulates in a confined volume or space with restricted outlet flow.

Safety valves will be used in equipment where this situation can take place and are listed in the following Table 25.

Table 25.Safety valves identification code and function

Instrument identification	Function
PSV-101	Safety valve of evaporator E-101
PSV-102	Safety valve of prepolymer reactor E-102
PSV-201	Safety valve of hold tank HT-201
PSV-202	Safety valve of lactide reactor E-202
PSV-301	Safety valve of column T-301
PSV-302	Safety valve of column T-302
PSV-401	Safety valve of polymerization reactor R-401
PSV-402	Safety valve of polymerization reactor R-402

7. DETAILED DESIGN OF PREPOLYMER REACTOR

7.1. Selection of the equipment

It has been discussed previously in Chapter 5 the selection of a falling film evaporator type of reactor for the condensation polymerization of lactic acid into polylactic acid of low molecular weight, as it provides the advantages required to optimize the polymer production.

By using this configuration the water present in the solution and the water produced as byproduct of the reaction can be vaporized while shifting the equilibrium polymerization reaction to the right. Moreover, this type of evaporator provides the minimum residence time needed in order to avoid racemization, as well as high heat transfer coefficient required, as PLA and lactic acid are heat sensitive materials which would sharply increase side degradation reactions when exposed to heat, causing a reduction in PLA production yield. It assures to maintain a uniform film thickness which increases mass transfer rate in a way that polylactic acid and water rapidly forms and water vaporizes favouring the equilibrium to the right side.

In this equipment both phases, gas and liquid, flow in the same direction without mixing with each other. While the liquid flows by gravity as a thin film completely covering the walls of the reactor, the gas circulates in a turbulent regime at high speed through the reactor.

The configuration is similar to a shell and tubes heat exchanger, where the film is formed in the inner wall of each tube, and circulating cooling water outside them as the exothermic reaction provides the heat required to vaporize the water.

The following Figure 23 represents a scheme of the equipment E-103, where the lactic acid and water solution feed enters at the top of the evaporator through stream 5, flows down the long vertical tubes which comprises the heat transfer and reaction zone, and exists at the bottom of the tubes where vapour containing water exits the system through stream 6. Cooling water (cw) at 30ºC from the cooling tower circuit is used as refrigerant fluid as it will extract the necessary heat at a lower cost compared to other refrigerant fluids, exiting the system at 50ºC. The stream 7 comprises the 2200 g/mol polylactic acid, non-volatile impurities and unconverted portions of the lactic acid feed, leaving the system as liquid.

The film thickness in the falling film is a critical design parameter as on it depends mass and heat transfer through the system, and it is determined by the rate at which liquid flows down the tubes as a function of viscosity. A film thickness between 0.5 to 8 mm is recommended by Gruber et al. A value of 4 mm is selected considering that a thinner film helps to move heat more quickly across the film and more water molecules can vaporize in a shorter period of time, thus minimizing reactor residence time. Also this film thickness will help to avoid high temperature gradients across the film and thus charring or fouling is avoided. By stablishing this film thickness, Gruber et al. recommend the reactor mean residence time to be as low as possible in a range between 2.5 and 10 minutes favouring the avoidance of racemization. (Gruber et al., 2001)

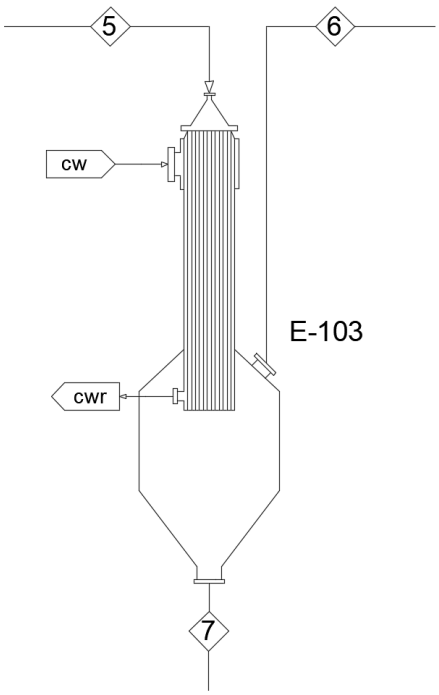

Figure 23. Falling film evaporator E-103 scheme

7.2. Mass and Energy balances

The reaction mechanism that takes place in the reactor is expressed as follow:

$$A(R_i)B + A(R_j)B \overset{k_1.k_{-1}}{\longleftrightarrow} A(R_{i+j})B + W$$

Where A and B represents – COOH and – OH groups, respectively, R is the repeating unit and water is represented by W. The subscripts i and j indicates the chain length of the molecules. The following Table 26 collects the mass balance results detailed in *Appendix 2.*

Table 26.Mass balance in prepolymer reactor E-103

Stream (kg/h)	5	6	7
Lactic acid	13978.87	0.00	461.66
Water	2271.35	4975.17	0.00
NVI	195.51	0.00	195.51
PLA (LMW)	0.00	0.00	10813.39
Total	16445.73	4975.17	11470.56

The energy balance in the reactor is expressed by the following equation 1:

$$Q = m_f \cdot \int_{T_i}^{T_r} Cp \cdot dT + n_{monomer} \cdot \Delta H_R + m_v \cdot \lambda_{vap} \qquad \text{[Eq.1]}$$

Where m_v stands for the water removed as vapor, m_f corresponds to the feed stream at a temperature T_i of 130ºC and T_r of 180ºC, and ΔH_R is the enthalpy of the reaction, expressed per mol of the monomer that has reacted. The exothermic behaviour of the reaction helps to evaporate the water present in the solution and the water produced as by-product of the reaction, therefore shifting the equilibrium polymerization reaction to the right. Cooling

water (cw) at 30ºC from the cooling tower circuit is used as refrigerant fluid as it will extract the necessary heat at a lower cost compared to other refrigerant fluids, exiting the system at 50ºC. Energy balance around reactor E-103 is detailed in *Appendix 2.*

Table 27.Heat transfer parameters E-103

Q (kW)	535.64
m_{cw} (kg/s)	6.41

7.3. Heat transfer and mechanical design

From energy balance it is obtained the heat that needs to be removed from the system, required in order to carry out the heat transfer design of the equipment. The general equation for heat transfer across a surface in an evaporator design is the following equation 2.

$$Q = U \cdot A \cdot \Delta T \qquad \text{[Eq.2]}$$

Where Q is the heat transferred per unit time calculated in *Appendix 2*, U is the overall heat transfer coefficient, A is the heat transfer area and ΔT is the mean temperature difference or driving force of the system. *Appendix 4* details the heat transfer design for this equipment, including shell and tubes definition, shell and tubes heat transfer coefficient and pressure drop calculation. Table 28 collects the main heat transfer parameters as results.

Table 28.Heat transfer parameters E-103

Q (kW)	535.64
$U_{o.ass}$ (W/m^{2}ºC)	34.58
ΔT (ºC)	114.1
A (m^2)	166.24

A mechanical design of the equipment has also been carried out and detailed in Appendix 4. The mechanical design of the prepolymer reactor E-103 follows the design for pressure vessels specified in ASME BPV. Section VIII Division.1.

By defining a design pressure and design temperature from the reactor operating conditions, and taking into account the required resistance to corrosion due to corrosive nature of lactic acid, as well as the main loads to which a process vessel can be subjected to, including pressure loads, wind load and loads due to the weight of the evaporator and internal accessories; the material of construction as well as material thickness that ensures the proper operation of the equipment has been determined. Also openings, as well as head and support type has been discussed, selected and dimensioned in this *Appendix 4.*

Table 29 corresponds to this equipment's specification sheet where the main features and operating conditions are collected, and it is followed by the prepolymer reactor layout, where main dimensions, tubes distribution and openings are detailed.

7.4. Prepolymer reactor E-103 – Specification sheet

Table 29.E-103 specification sheet

Equipment label	E-103	Equipment name	Prepolymer reactor	
Process service	cw	Equipment type	Falling film evaporator	
OPERATING DATA				
	SHELL SIDE		TUBE SIDE	
Stream	cw	cwr	7	6
Fluid	Cooling water	cw return	LMW PLA	Water vapour
W (kg/s)	6.41	6.41	3.19	1.38
ρ (kg/m^3)	995.2	991.8	1120.2	4.8
μ (kg/ms)	$7.97\cdot 10^{-4}$	$6.43\cdot 10^{-4}$	$3.05\cdot 10^{-2}$	$1.50\cdot 10^{-5}$
C_p (J/kgK)	4180	4180	137.6	1927.5
k_f (W/mK)	0.618	0.643	0.195	0.039
T (ºC)	30	50	180	180
P (kPa)	101.3	101.3	6.67	6.67
ΔP (kN/m^2)	36.5	36.5	75.6	2.0
v (m/s)	0.3	0.3	1.9	10.6
Nº of passes	1		1	
h (W/m^{2}ºK)	3448.17		60.84	283.37
h_f (W/m^{2}ºK)	4500		6000	
Q (kW)	535.6			
U (W/m^{2}ºK)	34.6			
ΔT_{lm} (K)	139.8			
F	0.82			
ΔT (K)	114.1			
A (m^2)	166.2			

MECHANICAL DATA			
Design P (psia)	16.1	Design T (ºF)	406
TUBES			
Material	SANDVIK 2RK65™	Pitch (mm)	25
k_w	16	Tubes arrangement	Triangular
Nº tubes	544	O.D. (mm)	20
Length (m)	4.88	t (mm)	2
SHELL			
Material	SANDVIK 2RK65™	I.D. (mm)	711.2
k_w	16	t (mm)	7
Length (m)	4.88	Bundle clearance	
Head	Torispherical	Support	Straight skirt

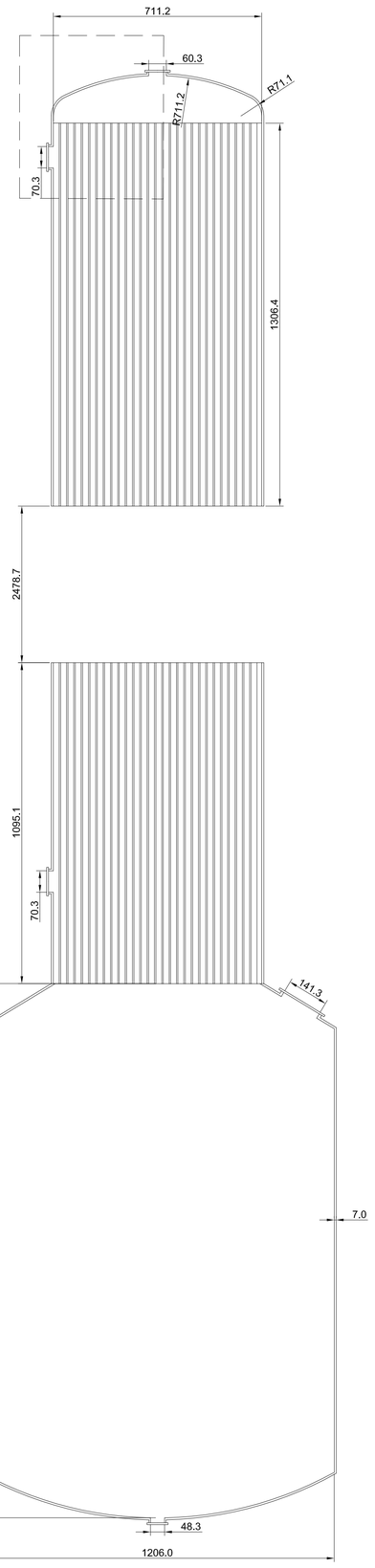

Cross section prepolymer reactor E-103
S: 1:10

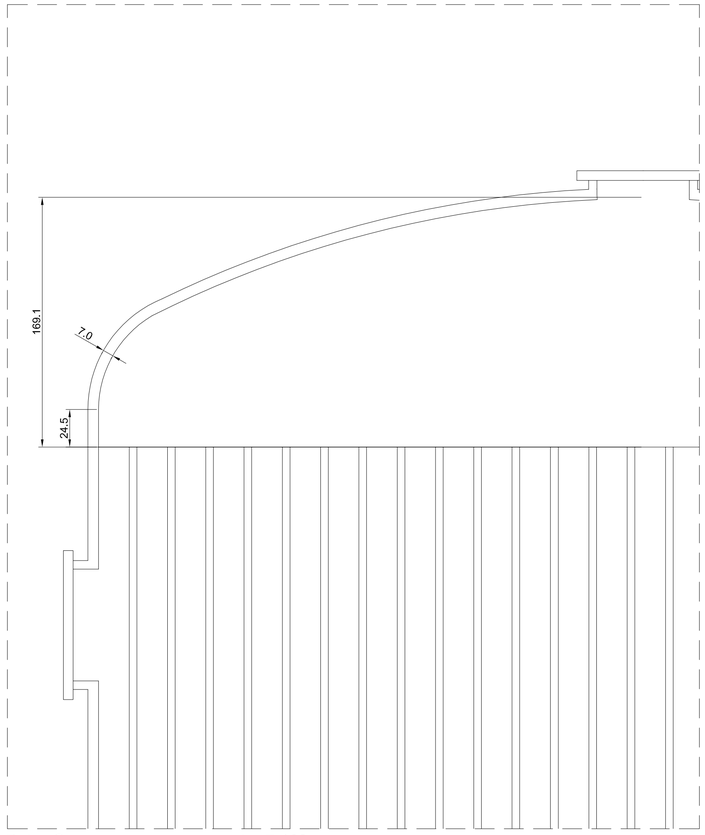

Detail Opening prepolymer reactor E-103
S: 200:1

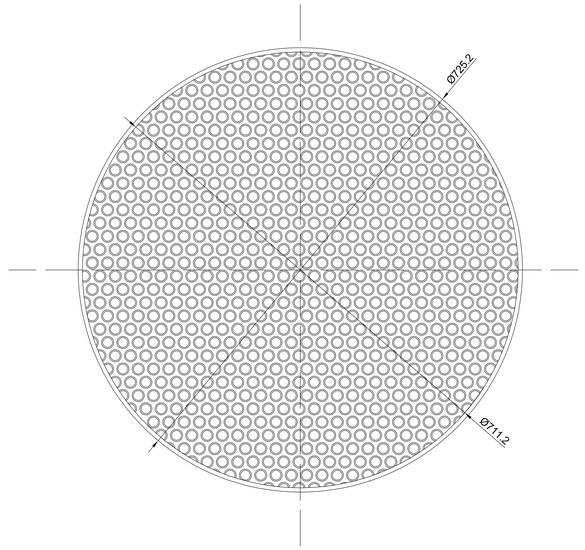

Detail tube sheet layout E-103
S: 1:5

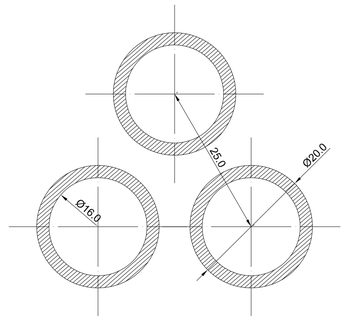

Detail Tubes distribution
S: 50:1

NOTES

- All dimensions are in millimetres and are duly justified in *Appendix 4. Detailed design - Prepolymer reactor*
- Material construction is high-alloy austenitic stainless steel SANDVIK 2RK65^{TM}
- Tubes arrangement follow a triangular pitch pattern. Number of tubes: 544
- Head type is torispherical
- Lenght of the reactor is cut to show both ends, where the greatest design complications lie

UNIVERSIDAD DE BARCELONA
FACULTAD DE QUÍMICA

Design of a plant of polylactic acid polymer manufacture

Diagram type: PREPOLYMER REACTOR E-103 LAYOUT

Author:	Scale:
Andrea Canzobre Silva	1:10 / 200:1 / 1:5 / 50:1

Date:	Signature:	Diagram Nº:
February 2021		1

8. CONCLUSIONS

Polylactic acid has been around since 1932, but it was not until getting the ability to mass produce at a large-scale that this biodegradable and bio-based polymer expanded its use in different applications. PLA stands out in this way as a greener solution with great potential and marketability to substitute conventional fossil-based commodity polymers, especially in food packaging of short life-time products, overcoming not only the accumulation of plastic waste in landfills but also reducing the emission of greenhouse gases and therefore helping to combat climate change and assuring a more sustainable future.

Government restrictions on single-use plastics, along with a positive public perception, is rapidly increasing polylactic acid demand all around the globe, which is generating greater interest in the search for further process improvements, orientated mainly towards the production of second generation polylactic acid, which means the use of biomass waste and crop residues for lactic acid production and therefore the reduction of all three carbon, land and water footprints.

It is concluded that the production of PLA via ring-opening of lactide is the most favourable technique for its use in food packaging and biomedical applications, as it provides crystalline polylactic acid of high molecular weight with excellent properties and at a competitive price.

Falling film evaporators are selected for the main reactions of the process, as besides providing the suitability for concentrating viscous products and for vacuum operations with the minimum cost, they provide the high surface area to volumetric hold up ratio required in order to reduce the evaporation residence times and thus racemization as well as optical purity control of the process compounds.

Feedback type control loops are selected for the control system as they allow an ease of implementation as well as an adequate alternative for processes where the deviation from the set point is assumable, being this type the most commonly used in industry. The control system of the plant intends to supress the influence of external disturbances, ensuring the stability of the chemical process and the optimization of the process performance.

By way of conclusion, polylactic acid has transcended from a minor-based biopolymer in a petroleum-based market to be considered as a part of a new solution towards a new greener economy based on a sustainable point of view, and efforts in this project has been directed with the objective of studying the viability, essentially technical, of a 60,000 tonnes per year polylactic acid production plant, ensuring the status of this compound as one of the major new bio-based polymers and attaining a positive impact not only economic, but also with environmental credit, towards the transition of a sustainable future.

REFERENCES AND NOTES

Ashby, M.F. *Materials selection in mechanical design.* 3rd edition, Elsevier Butterworth-Heinemann, 2005

Bathia, K.K. *Atmospheric pressure process for preparing pure cyclic esters*. U.S. Patent 4,835,293, May 1989

Brizga, J.; Hubacek, K.; Feng, K.; [Online] 2020. *The unintended side effects of bioplastics: Carbon, Land and Water footprints.* https://doi.org/10.1016/j.oneear.2020.06.016 (accessed Jan 22, 2021)

Castillo Martinez, F.A., Balciunas, E.M., Salgado, J.M., Domínguez González, J.M., Converti, A., Oliveira, R.P. de S., [Online] 2013. Lac*tic acid properties, applications and production: A review.* https://doi.org/10.1016/j.tifs.2012.11.007 (accessed Nov 5, 2020)

Castro-Aguirre, E.; Iñiguez-Franco, F.; Samsudin, H; Fang, X.; Auras, R. [Online] 2016. *Poly(lactic acid) – Mass production, processing, industrial applications and end of life.* https://doi.org/10.1016/j.addr.2016.03.010 (accessed Jan 23, 2021)

De Vries, K.S. *Preparation of polylactic acid and copolymers of lactic acids*. U.S. Patent 4,797,468, January 1989

Dorough, G. L. *Polymeric lactide resin*. U.S. Patent 1,995,970, March 1935

Drysdale, N.E.; Stambaugh, T.W.; Tarbell, J.V. *Solventless dimeric cyclic ester distillation process*. U.S. Patent 5,236,560, August 1993

Ehsani, M.; Khodabakhshi, K.; Asgari, M. [Online] 2014. *Lactide synthesis optimization: Investigation of the temperature, catalyst and pressure effects*. https://doi.org/10.1515/epoly-2014-0055 (accessed Dic 2, 2020)

Emel'yanenko, V.N.; Verevkin, S.P.; Pimerzin, A.A. [Online] 2008. *The thermodynamic properties of DL- and L-Lactides.* https://doi.org/10.1134/S0036024409120024 (accessed Dic 7, 2020)

Filho, W.L.; Salvia, A.L; Bonoli, A. et al. [Online] 2020. *An assessment of attitudes towards plastics and bioplastics in Europe,* Science of the Total Environment. https://doi.org/10.1016/j.scitotenv.2020.142732 (accessed Jan 21, 2021)

Garlotta, D. [Online] 2001. *A literature review of Poly(lactic acid). Journal of polymers and the environment*. https://doi.org/10.1023/A:1020200822435 (accessed Nov 5, 2020)

Global Asset Protection Services LLC. [Online] 2015. *GAPS Guidelines – Oil and Chemical plant layout and spacings.* https://docplayer.net/48710333-Oil-and-chemical-plant-layout-and-spacing.html (accessed Dic 26, 2020)

Grandview Research. *Lactic acid market size, Share & trend Analysis Report*. (2019) https://www.grandviewresearch.com/industry-analysis/lactic-acid-and-poly-lactic-acid-market (accessed Nov 2, 2020)

Grandview Research. *Polylactic acid market size, Share & trend Analysis Report*. (2020) https://www.grandviewresearch.com/industry-analysis/polylactic-acid-pla-market (accessed Nov 3, 2020)

Gruber, P.R.; Hall, E.S.; Kolstad J.J.; Iwen, M.L.; Benson, R.D.; Borchardt, R.L. *Continuous process for the manufacture of lactide and lactide polymers*. U.S. Patent 6,326,458 B1, December 2001

Gruber, P.R.; Hall, E.S.; Kolstad, J.J.; Iwen, M.L. Benson, R.D.; Borchardt, R.L. *Continuous process for manufacture of lactide polymers with controlled optical purity*. U.S. Patent 5,142,023, August 1992

Gutiérrez J.M.; *Simulación de una columna de paredes mojadas como reactor de sulfonación,* Universidad de Barcelona, 1984.

Harshe, Y.M.; Storti, G.; Morbidelli, M.; Gelosa, S.; Moscatelli, D. [Online] 2007. *Polycondensation kinetics of Lactic acid*. https://doi.org/10.1002/mren.200700019 (accessed Nov 27, 2020)

Henton, D.; Gruber, P.; Lunt, J.; Randall, J. [Online] 2005. *Polylactic acid technology*. https://doi.org/10.1201/9780203508206.ch16 (accessed Jan 20, 2021)

ICIS. *High polymer prices make PLA an attractive alternative – NatureWorks*. (2011) https://www.icis.com/explore/resources/news/2011/05/20/9462068/high-polymer-prices-make-pla-an-attractive-alternative-natureworks/ (accessed Nov 3, 2020)

ICIS. *Lactic acid market key to future PLA bioplastic success – Total Corbion*. (2018) https://www.icis.com/explore/resources/news/2018/12/04/10290595/lactic-acid-market-key-to-future-pla-bioplastic-success-total-corbion/ (accessed Nov 3, 2020)

IHS Markit. *Biodegradable Polymers – Chemical Economics Handbook.* (2018) https://ihsmarkit.com/products/biodegradable-polymers-chemical-economics-handbook.html (accessed Oct 30, 2020)

IHS Markit. *Lactic acid, its salts and esters – Chemical economics handbook*. (2018) https://ihsmarkit.com/products/lactic-acid-its-salts-chemical-economics-handbook.html (accessed Nov 2, 2020)

Institute for Bioplastics and Biocomposites. *Biopolymers facts and statistics.* (2019) https://www.ifbb-hannover.de/files/IfBB/downloads/faltblaetter_broschueren/f+s/Biopolymers-Facts-Statistics-2019.pdf (accessed Oct 30, 2020)

Jamshidian, M.; Tehrany, E.A.; Imran, M.; Jacquot, M.; Desobry, S. [Online] 2010. *Poly-lactic acid: Production, applications, nanocomposites and release studies.* https://doi.org/10.1111/j.1541-4337.2010.00126.x (accesed Jan 24, 2021)

Kister, H.Z. *Distillation Design*. McGraw-Hill, Inc, 1992

Kopinke, F.D.; Remmler, M.; Mackenzie, K.; Möder, M.; Wachsen, O. [Online] 1996. *Thermal decomposition of biodegradable polyesters – II. Poly(lactic acid*). https://doi.org/10.1016/0141-3910(96)00102-4 (accessed Dic 7, 2020)

Kulaniga R.G.; Lebedev, B.V.; Kiparisova Ye.G.; Lyudvig, Ye.B.; Barskaya, I.G. [Online] 1982. *Thermodynamics of dl-lactide, polylactide and polymerization of dl-lactide in the range of 0-430K.* https://doi.org/10.1016/0032-3950(82)90455-5 (accessed Dic 30, 2020)

Meerdink, J.; Sädergard, N.D.A.; *Purification process for lactide*. U.S Patent 8,053,584 B2, November 2011

Metkar, S.; Sathe, V; Rahman, I.; Idage, B.; Idage, S. [Online] 2019. *Ring opening polymerization of lactide: kinetics and modelling.* https://doi.org/10.1080/00986445.2018.1550395 (accessed Dic 14, 2020)

Mott, R. L.; Towler, G. *Mecánica de fluidos.* 6th edition, Pearson, 2006

Muller, M. Process for the preparation of lactide. U.S. Patent 5,053,522, October 1991

Ohara, H.; Sawa, S.; Ito, M.; Fujii, Y.; Oota, M.; Yamaguchi, H. *Method for producing polylactic acid*. U.S. Patent 5,770,682, June 1998

Oota, M.; Ito, M. *Process for preparing polylactic acid.* U.S. Patent 5,821327, October 1998

Plastics Insight. *Debate arises once again on ban of single-use plastics in time of Coronavirus.* (2020) https://www.plasticsinsight.com/debate-arises-once-again-on-ban-of-single-use-plastics-in-times-of-coronavirus/ (accessed Nov 3, 2020)

Plastics Insight. *Global bioplastics production capacity by type of materials.* (2017) https://www.plasticsinsight.com/global-bioplastics-production-capacity-type-materials/ (accessed Oct 31, 2020)

Plastics Insight. *Polylactic acid properties, production, price, market and uses*. (2017) https://www.plasticsinsight.com/resin-intelligence/resin-prices/polylactic-acid/ (accessed Nov 3, 2020)

Quarderer, G; Robbins, L.A.; Ryan, C.M. *Improved lactic acid processing, methods, arangements and products.* WO 01/38284 A1

Ramakrishma, S.V.; Rangaswamy, V.; Jain, D.; Jagdambalal, R.K.; Patel, P.S.; Kar, D.; Ramachandran, S.; Ganeshpure, P.A.; Satpathy, U.S. *Process for the production of polylactic acid (PLA) from renewable feedstocks*. U.S. Patent 7,507,561 B2, March 2009

RameshKumar, S.; Shaiju, P.; O'Connor, K.E.; Babu, R.P.; [Online] 2019. *Bio-based and biodegradable polymers – State-of-the-art, challenges and emerging trends.* https://doi.org/10.1016/j.cogsc.2019.12.005 (accessed Jan 22, 2021)

Richardson, J. F.; Harker, J. H.; Backhurst, J.; *Chemical Engineering - Particle technology and separation processes.* Vol.2., 5th edition; Butterworth-Heinemann, 2002

Safrit, B.T.; Schlager, G.E.; Li, Z.; [Online] 2013. *Modelling and simulation of polymerization of lactide to polylactic acid and co-polymers of polylactic acid using high viscosity kneader reactors.* (accessed Dic 23, 2020)

Sandvik. *Lactic acid corrosion tables.* https://www.materials.sandvik/es-es/materials-center/tablas-de-corrosion/lactic-acid/ (accessed Dic 30, 2020)

Seader, J.D.; Henley, E.J.; Roper, D.K.; *Separation process principles.* 3rd edition, John Wiley & Sons, Inc., 2011

Sinnot, R.K. *Chemical Engineering Design.* Vol.6, 4th edition, Elsevier Butterworth-Heinemann., 2005

Stephanopoulos, G. *Chemical process control: An introduction to theory and practice.* 1st edition, PTR Prentice Hall, 1984

Svrcek, W.Y.; Mahoney D.P.; Young B.R.; *A real-time approach to process control.* 3rd edition, John Wiley & Sons, 2014

Tin Sin, L.; Rahmat, A.; Rahman, W. *Polylactic acid – PLA Biopolymer Technology and Applications.* 1st ed.; Elsevier, 2013. ISBN: 978-1-4377-4459-0

Towler, G.; Sinnot, R. *Chemical Engineering Design. Principles, Practice and Economics of Plant and Process Design.* 2nd edition, Elsevier Butterworth-Heinemann., 2013

Transparency Market Research. *Lactic acid market and polylactic acid market size, share, trends, growth, export value, volume & trade, sales, pricing forecast.* (2018) https://www.transparencymarketresearch.com/pressrelease/lactic-poly-lactic-acid.htm (accessed Nov 3, 2020)

Transparency Market Research. *Polylactic acid (PLA) packaging market*. (2020) https://www.transparencymarketresearch.com/polylactic-acid-pla-packaging-market.html (accessed Nov 3, 2020)

Transparency Market Research. *Polylactic acid market.* (2020) https://www.transparencymarketresearch.com/polylactic-acid-market.html (accessed Nov 4, 2020)

Turton, R.; Bailie, R.C.; Whiting, W.B.; Shaeiwitz, J.A.;Bhattacharyya, D. *Analysis, Synthesis and Design of Chemical processes.* 4th edition, Prentice Hall, 2012

Vu, D.T.; Kolah, A.K.; Asthana, N.S.; Peereboom, L.; Lira, C.T.; Miller, D.J. [Online] 2005. *Oligomer distribution in concentrated lactic acid solutions.* https://doi.org/10.1016/j.fluid.2005.06.021 (accessed Nov 21, 2020)

Witzke, D.R.; Narayan, R.; Kolstad, J.J.; [Online] 1997. *Reversible kinetics and thermodynamics of the homopolymerization of L-Lactide with 2-Ethylhexanoic Acid Tin(II) salt.* https://doi.org/10.1021/ma970631m (accessed Dic 23, 2020)

Yu, Y.; Storti, G.; Morbidelli, M. [Online] 2011. *Kinetics of Ring Opening Polymerization of L,L-Lactide.* https://doi.org/10.1021/ma901359x (accessed Dic 14, 2020)

E-101	P-101 A/B	E-102	E-103	P-102 A/B	HT-201	P-201 A/B	E-201	E-202	E-301	P-301 A/B	T-301	E-302	E-303	T-302	E-304	E-305	P-401 A/B	E-401	R-401	R-402
EVAPORATOR	CENTRIFUGAL PUMP	HEAT EXCHANGER	PREPOLYMER REACTOR	CENTRIFUGAL PUMP	HOLD TANK	CENTRIFUGAL PUMP	HEAT EXCHANGER	LACTIDE REACTOR	CONDENSER	CENTRIFUGAL PUMP	PACKED COLUMN	CONDENSER	REBOILER	PACKED COLUMN	CONDENSER	REBOILER	CENTRIFUGAL PUMP	HEAT EXCHANGER	POLYMERIZATION REACTOR	POLYMERIZATION REACTOR

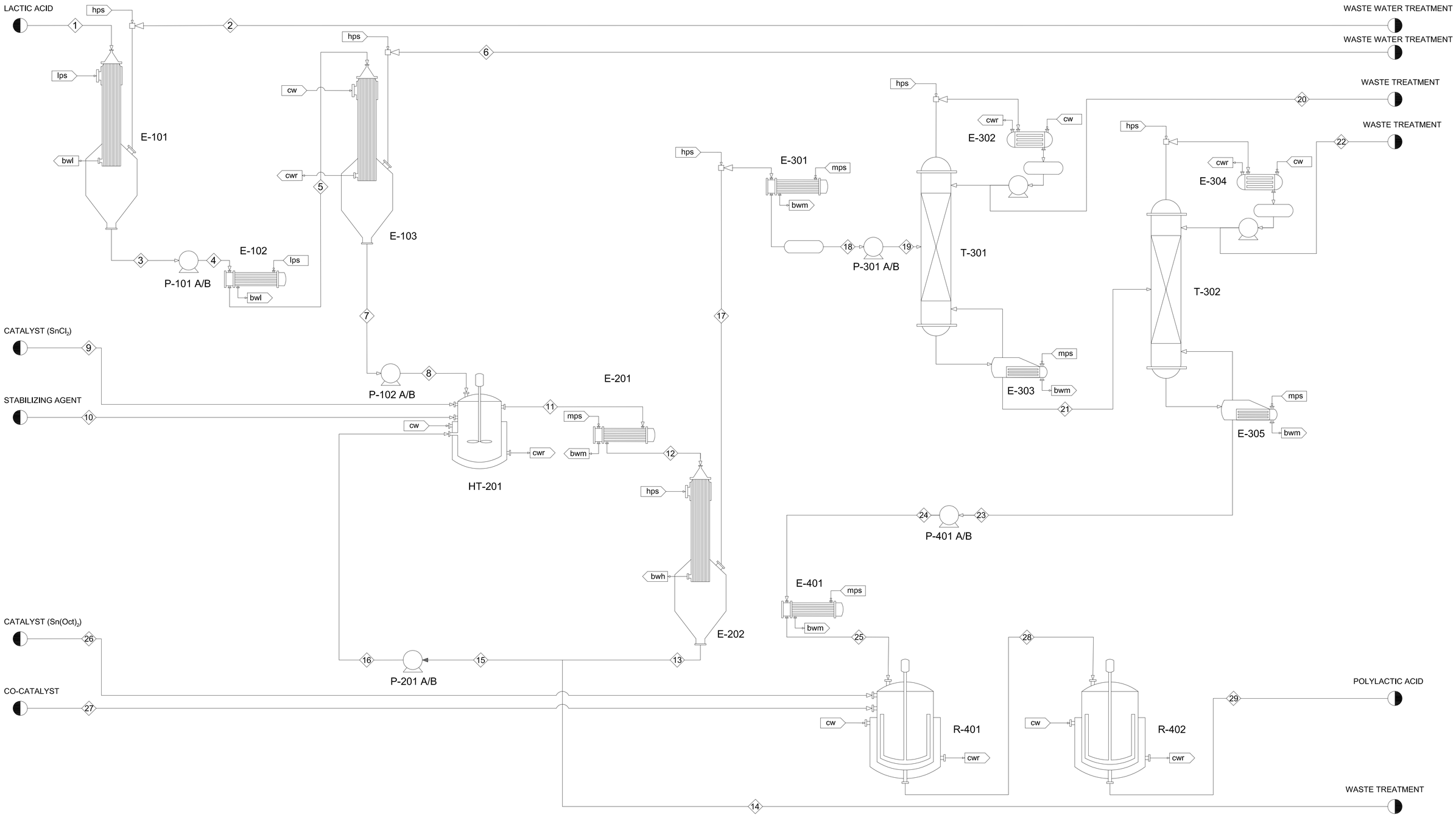

Stream	1	2	3	4	5	6	7	8	9	10	11	12	13	14	15	16	17	18	19	20	21	22	23	24	25	26	27	28	29
Temperature (ºC)	25	80	80	80	130	180	180	180	25	25	160	180	210	210	210	210	210	150	150	126	158	137	146	146	180	25	25	180	180
Pressure (bar)	1.013	0.470	0.470	0.067	0.067	0.067	0.067	1.013	1.013	1.013	1.013	1.013	0.034	0.034	0.034	1.013	0.034	0.034	0.067	0.067	0.067	0.013	0.013	1.013	1.013	1.013	1.013	1.013	1.013
Total mass flow (kg/h)	97754.35	81308.62	16445.73	16445.73	16445.73	4975.17	11470.56	11470.56	28.59	39.10	12228.63	12228.63	986.25	295.87	690.37	690.37	11242.38	11242.38	11242.38	2222.99	9019.39	210.03	8809.36	8809.36	8809.36	1.65	28.06	8839.07	8839.07
Total molar flow (kmol/h)	4778.66	4495.23	283.43	283.43	283.43	276.16	12.21	12.21	0.15	0.06	18.00	18.00	7.98	2.39	5.58	5.58	114.86	114.86	114.86	52.21	62.65	1.53	61.13	61.13	61.13	0.00	0.15	9.23	2.62
Component mass flow(kg/h)																													
Lactic acid	13978.87	0.00	13978.87	13978.87	13978.87	0.00	461.66	461.66	0.00	0.00	461.66	461.66	0.00	0.00	0.00	0.00	39.89	39.89	39.89	39.09	0.80	0.80	0.00	0.00	0.00	0.00	0.00	0.00	0.00
Water	83091.20	80819.84	2271.35	2271.35	2271.35	4975.17	0.00	0.00	0.00	0.00	0.00	0.00	0.00	0.00	0.00	0.00	461.66	461.66	461.66	461.66	0.00	0.00	0.00	0.00	0.00	0.00	0.00	0.00	0.00
VI	488.77	488.77	0.00	0.00	0.00	0.00	0.00	0.00	0.00	0.00	0.00	0.00	0.00	0.00	0.00	0.00	0.00	0.00	0.00	0.00	0.00	0.00	0.00	0.00	0.00	0.00	0.00	0.00	0.00
NVI	195.51	0.00	195.51	195.51	195.51	0.00	195.51	195.51	0.00	0.00	651.70	651.70	651.70	195.51	456.19	456.19	0.00	0.00	0.00	0.00	0.00	0.00	0.00	0.00	0.00	0.00	0.00	0.00	0.00
PLA (LMW)	0.00	0.00	0.00	0.00	0.00	0.00	10813.39	10813.39	0.00	0.00	10889.61	10889.61	108.90	32.67	76.23	76.23	0.00	0.00	0.00	0.00	0.00	0.00	0.00	0.00	0.00	0.00	0.00	0.00	0.00
Catalyst $SnCl_2$	0.00	0.00	0.00	0.00	0.00	0.00	0.00	0.00	28.59	0.00	95.31	95.31	95.31	28.59	66.72	66.72	0.00	0.00	0.00	0.00	0.00	0.00	0.00	0.00	0.00	0.00	0.00	0.00	0.00
Stabilizing agent	0.00	0.00	0.00	0.00	0.00	0.00	0.00	0.00	0.00	39.10	130.34	130.34	130.34	39.10	91.24	91.24	0.00	0.00	0.00	0.00	0.00	0.00	0.00	0.00	0.00	0.00	0.00	0.00	0.00
Oligomers	0.00	0.00	0.00	0.00	0.00	0.00	0.00	0.00	0.00	0.00	0.00	0.00	0.00	0.00	0.00	0.00	1637.59	1637.59	1637.59	1629.76	7.83	7.83	0.00	0.00	0.00	0.00	0.00	0.00	0.00
L-lactide	0.00	0.00	0.00	0.00	0.00	0.00	0.00	0.00	0.00	0.00	0.00	0.00	0.00	0.00	0.00	0.00	8650.76	8650.76	8650.76	86.51	8564.25	85.64	8478.61	8478.61	8478.61	0.00	0.00	1249.38	332.43
D-lactide	0.00	0.00	0.00	0.00	0.00	0.00	0.00	0.00	0.00	0.00	0.00	0.00	0.00	0.00	0.00	0.00	329.58	329.58	329.58	0.00	329.58	0.00	329.58	329.58	329.58	0.00	0.00	48.57	12.92
Meso-lactide	0.00	0.00	0.00	0.00	0.00	0.00	0.00	0.00	0.00	0.00	0.00	0.00	0.00	0.00	0.00	0.00	122.90	122.90	122.90	5.97	116.93	115.77	1.17	1.17	1.17	0.00	0.00	0.17	0.05
PLA (HMW)	0.00	0.00	0.00	0.00	0.00	0.00	0.00	0.00	0.00	0.00	0.00	0.00	0.00	0.00	0.00	0.00	0.00	0.00	0.00	0.00	0.00	0.00	0.00	0.00	0.00	0.00	0.00	7511.24	8463.96
Catalyst $SnOct_2$	0.00	0.00	0.00	0.00	0.00	0.00	0.00	0.00	0.00	0.00	0.00	0.00	0.00	0.00	0.00	0.00	0.00	0.00	0.00	0.00	0.00	0.00	0.00	0.00	0.00	1.65	0.00	1.65	1.65
Co-catalyst	0.00	0.00	0.00	0.00	0.00	0.00	0.00	0.00	0.00	0.00	0.00	0.00	0.00	0.00	0.00	0.00	0.00	0.00	0.00	0.00	0.00	0.00	0.00	0.00	0.00	0.00	28.06	28.06	28.06

UNIVERSIDAD DE BARCELONA
FACULTAD DE QUÍMICA

Design of a plant of polylactic acid polymer manufacture

Diagram type: PROCESS FLOW DIAGRAM (PFD)

Author: Andrea Canzobre Silva

Scale: S/E

Date: February 2021

Signature:

Diagram Nº: 2

E-101	P-101 A/B	E-102	E-103	P-102 A/B	HT-201	P-201 A/B	E-201	E-202	E-301	P-301 A/B	T-301	E-302	E-303	T-302	E-304	E-305	P-401 A/B	E-401	R-401	R-402
EVAPORATOR	CENTRIFUGAL PUMP	HEAT EXCHANGER	PREPOLYMER REACTOR	CENTRIFUGAL PUMP	HOLD TANK	CENTRIFUGAL PUMP	HEAT EXCHANGER	LACTIDE REACTOR	CONDENSER	CENTRIFUGAL PUMP	PACKED COLUMN	CONDENSER	REBOILER	PACKED COLUMN	CONDENSER	REBOILER	CENTRIFUGAL PUMP	HEAT EXCHANGER	POLYMERIZATION REACTOR	POLYMERIZATION REACTOR

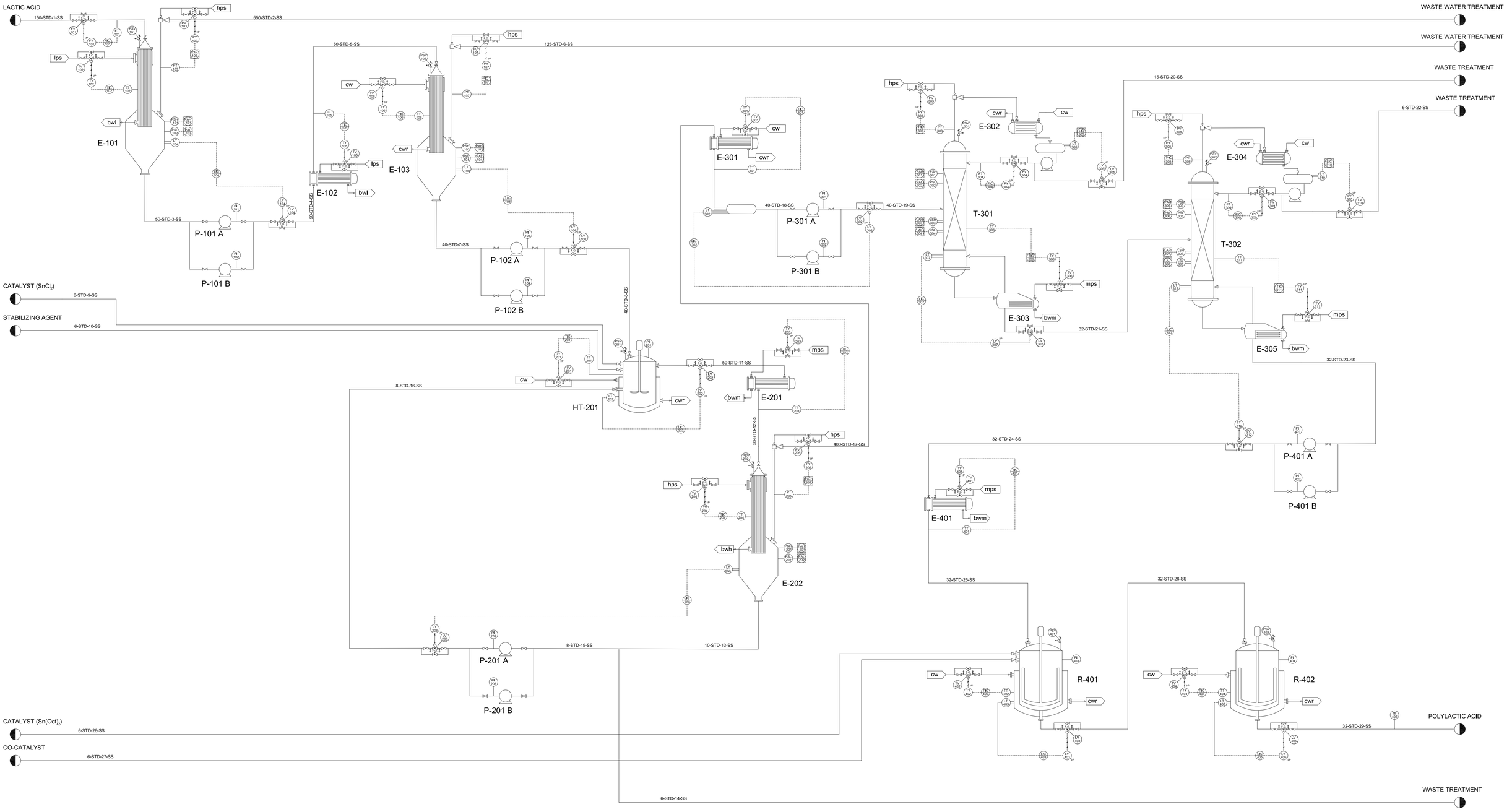

DIAGRAM REFERENCE

Diag. Núm.	Title	Sheet

VALVE SYMBOLS

Control valve	Drain valve	F.O. : Fails Open
Hand control valve	Safety valve	F.C. : Fails Closed

LINE SYMBOLS

- Connection to process
- Electric signal transmission
- Pneumatic signal transmission

NOTES

XYY ABB

X: First letter
YY: Successive letters
A: Plant section
BB: Loop number

First letter		Successive letters	
		A	Alarm
		C	Control
		H	High
		I	Indicator
F	Flow	L	Low
K	Time	S	Switch
L	Level	T	Transmissor
P	Pressure	V	Valve
T	Temperature	Y	Conversor

(*) The I/P symbol refers to the conversion of electrical to pneumatic signal

INTERLOCKING DESCRIPTION

———

UTILITIES

- mps - Medium pressure steam
- bwm - Boiling feed water (medium pressure)
- hps - High pressure steam
- bwh - Boiling feed water (high pressure)
- lps - Low pressure steam
- bwl - Boiling feed water (low pressure)
- cw - Cooling water
- cwr - Cooling water return

INSTRUMENT IDENTIFICATION

Location		Function	
XYY ABB	Field mounted instrument	XYY ABB	Discreet instrument
XYY ABB	Panel mounted instrument	XYY ABB	Field mounted shared display device with limited access to adjustments
		XYY ABB	Field mounted programmable logic controller (PLC)

UNIVERSIDAD DE BARCELONA
FACULTAD DE QUÍMICA

Design of a plant of polylactic acid polymer manufacture

Diagram type: PIPING AND INSTRUMENTATION DIAGRAM (P&ID)

Author:	Scale:
Andrea Canzobre Silva	S/E
Date: February 2021	**Signature:**
	Diagram Nº: 2

APPENDIX 2: MASS AND ENERGY BALANCES

2.1. Evaporator E-101

In order to size the evaporator operating under continuous flow and steady state conditions, a mass balance, energy balance and heat transfer calculation must be carried out. Some assumptions have been considered:

- Lactic acid does not vaporize at this operating conditions and water is the only one volatile component of the feed
- Perfect mixing is considered as boiling action on the surface agitates the solution in the evaporator enough to take this assumption. In this way, the solution temperature in the evaporator equals the exiting temperature of the concentrated lactic acid solution and the water vapour leaving the system.
- Bearing all the above mentioned in mind, the overall temperature difference which constitutes the driving force for heat transfer of the system is the difference between the temperature of the saturated steam used as heating medium and the boiling temperature of the solution.
- The driving force is sufficiently high in order to achieve nucleate boiling and short enough to not cause undesirable film boiling.
- Heat losses are considered negligible

In this way, the global mass balance and the mass balance on lactic acid are defined as:

$$m_f = m_v + m_l$$

$$m_f \cdot x_f = m_l \cdot x_l$$

The energy balance on the system is expressed as the sum of the heat needed to heat the feed up to 80ºC and the heat required to evaporate the water. Low pressure steam (lps) at 133.6 ºC and 3 bar is used as heating fluid.

$$Q = m_f \cdot Cp \cdot \Delta T + m_v \cdot \lambda_{vap,v} = S \cdot \lambda_{vap,s}$$

Table 30. Mass balances in falling film evaporator E-101

Stream (kg/h)	1	2	3
Lactic acid	13978.87	0.00	13978.87
Water	83091.20	80819.84	2271.35
Volatile impurities	488.77	488.77	0.00
Non-volatile impurities	195.51	0.00	195.51
Total	97754.35	81308.62	16445.73

Table 31. Energy balance in falling film evaporator E-101

Q (kW)	58065.29
C_p (J/kgºC)	3964
ΔT (ºC)	55.0
$\lambda_{vap.v}$ (kJ/kg)	2308.8
S (kg/h)	96604.2
$\lambda_{vap.s}$ (kJ/kg)	2163.8

2.2. Prepolymer reactor E-103

The reaction mechanism that takes place in the prepolymer reactor is expressed as follow:

$$A(R_i)B + A(R_j)B \overset{k_1.k_{-1}}{\longleftrightarrow} A(R_{i+j})B + W$$

Where A and B represents – COOH and – OH groups, respectively, R is the repeating unit and water is represented by W. The subscripts *i* and *j* indicates the chain length of the molecules. The mathematical model was determined under the following assumptions:

- The kinetic constants are independent of the polymer chain length.
- An open system with completed water removal is considered and only water is transferred from the reaction mixture to vapour phase through vaporization.
- The reversible nature of the reaction limits the extent of conversion of lactic acid to PLA and hence the degree of polymerization. However, as the by-product is continuously removed, side reaction depolymerisation reaction will not be considered as the reaction is completely shifted to the right. Therefore, an ideal irreversible polycondensation reaction is being considered.
- The water removed as vapor is the sum of the water present in solution from the previous stage and the one formed as by-product of the polycondensation reaction.
- Lactic acid and polylactic acid evaporation are neglected.
- The reaction mechanism defined leads to the limiting polydispersity value of 2.
- As the by-product is continuously removed, side reaction depolymerisation reaction is not considered as the reaction is completely shifted to the right.

Under these assumptions the rate of accumulation for polymer with chain length *i,* in terms of conversion, is expressed by Harshe et al. by the equation 3, where k_1 stands for the polymerization rate constant, $\lambda_{1.0}$ represents the initial total number of monomer units and *X* the conversion. (Harshe et al., 2007)

$$\frac{dX}{dt} = k_1 \lambda_{1.0} (1 - X)^2 \qquad \text{[Eq.3]}$$

By integrating this equation, the polymerization rate constant can be estimated based on the reaction time and the degree of polymerization DP.

$$k_1 = \frac{\overline{DP} - 1}{\lambda_{1.0} \cdot t} \qquad \text{[Eq.4]}$$

The degree of polymerization is defined by Harshe et al. in terms of moments by the following equation, where $\lambda_1$and λ_0 represent the total number of chains and of monomer units. respectively. (Harshe et al., 2007)

$$\overline{DP_n} = \frac{\lambda_1}{\lambda_0} = \frac{\lambda_{1.0}}{\lambda_0} \qquad \text{[Eq.5]}$$

Defining the conversion in terms of moments by equation 6 we can obtain the degree of polymerization in terms of conversion.

$$\overline{DP_n} = \frac{1}{1-X} \quad \text{[Eq.6]}$$

By taking into account the final average molecular weight of the polymer, 2200 g/mol the following results are obtained.

Table 32.Kinetic parameters in prepolymer reactor E-103

Average Mw (g/mol)	2200
$\overline{DP}$	30.3
x	0.967
k_1 (L/mol·h)	0.1629
t (h)	0.158

If an overall mass balance around the reactor is carried out, the following results are obtained:

Table 33.Mass balance in prepolymer reactor E-103

Stream (kg/h)	**5**	**6**	**7**
Lactic acid	13978.87	0.00	461.66
Water	2271.35	4975.17	0.00
NVI	195.51	0.00	195.51
PLA (LMW)	0.00	0.00	10813.39
Total	16445.73	4975.17	11470.56

The energy balance in the reactor is expressed by the following equation 7:

$$Q = m_f \cdot \int_{T_i}^{T_r} Cp \cdot dT + n_{monomer} \cdot \Delta H_R + m_v \cdot \lambda_{vap} \quad \text{[Eq.7]}$$

Where m_v stands for the water removed as vapor, m_f corresponds to the feed stream at a temperature T_i of 130ºC and T_r of 180ºC, and ΔH_R is the enthalpy of the reaction, expressed per mol of the monomer that has reacted.

Since there is no data available, the enthalpy of reaction is estimated by the Hess law as follows:

$$\Delta H_R = \Delta H_f^\circ + \int_{298}^{T_r} \Delta C_p(T) dT \quad \text{[Eq.8]}$$

$$\Delta H_f^\circ = \sum \Delta H_f^\circ (products) - \sum \Delta H_f^\circ (reactants) \quad \text{[Eq.9]}$$

The enthalpy of formation of the 2200 g/mol polymer is estimated with the Joback and Reid group contribution method from the lactic acid standard enthalpy of formation.

$$\Delta H_f^\circ \left(\frac{kJ}{mol}\right) = 68.29 \sum n_j \Delta_H \quad \text{[Eq.10]}$$

Table 34.Group contribution for the Joback and Reid method

Structural group	**-COOH**	**-CH_3**	**>CH-**	**-OH**	**=O**	**-O-**
Δ_H (kJ/mol)	-426.72	-76.46	29.89	-208.04	-247.61	-132.22

Table 35.Standard enthalpy of formation estimation

Component	ΔH_f° (kJ/mol)
Lactic acid	-613.04
Lactic acid monomer (n = 28.28)	-358.11
End chain monomer of polylactic acid (1)	-635.40
End chain monomer of polylactic acid (2)	-502.22
Polylactic acid	-11264.79

Lactic acid and water heat capacity has been estimated with ASPEN HYSYS software. Polylactic acid heat capacity has been estimated using the Joback method by group contribution based on lactic acid heat capacity, following the procedure above explained and by the following equation 11, where Cp is expressed in J/mol·K and T in K:

$$C_p = \sum n_j \Delta_A - 37.93 + \left(\sum n_j \Delta_B + 0.21\right)T + \left(\sum n_j \Delta_C - 3.91 \cdot 10^{-4}\right)T^2 + \left(\sum n_j \Delta_D + 2.06 \cdot 10^{-7}\right)T^3 \quad \text{[Eq.11]}$$

Table 36 resumes the data needed for the estimation of the polycondensation reaction enthalpy per mol of the monomer and Table 37 the results to obtain the heat that needs to be removed from the system.

Table 36.Heat capacities as a function of temperature

Cp (J/mol·K)	25ºC	130ºC	180ºC
Water	75.7	76.8	79.8
Lactic acid	224.9	247.5	264.2
Polylactic acid	302.8	345.3	372.0

Table 37.Energy balance in prepolymer reactor E-103

ΔH_R **(kJ/mol)**	-10937.5
λ_{vap} **(kJ/kg)**	2015.0
Q (W)	-535634

2.3. Depolymerization reactor E-202

A depolymerisation reaction takes place in this equipment. Lactide is produced through the depolymerisation of oligomeric low molecular weight PLA by back-bitting reactions of the carboxylic end groups and the ester bond of the chain back-bone, where a cyclic compound is formed, and by end-biting reactions, which involves the ring closure reaction to form lactide.

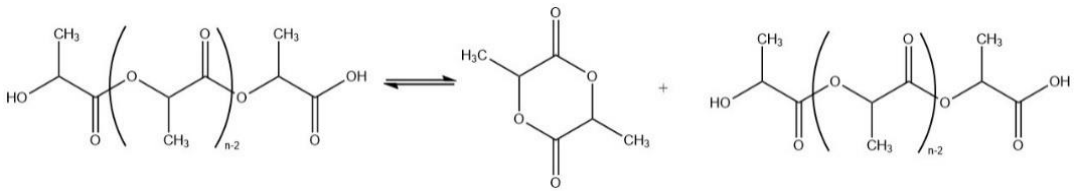

Figure 24. Depolymerization reaction

As the outlet liquid stream is recirculated in order to increase the overall yield of the process and recover the catalyst and stabilizer used in this stage, the mass balance shown herein below corresponds to the mass balance once the steady state has been reached in the system.

28.59 kg/h and 39.10 kg/h of catalyst and stabilizer, respectively, are needed continuously in order to obtain a concentration of 0.4 mol% and 0.15 weight% on the feed stream to the reactor, respectively, once steady-state has been reached. A purge stream is also needed to avoid accumulation of non-volatile impurities that are being recirculated to the feed tank.

As disclosed by Ehsani et al., at these operating conditions and a 0.4 mol% of $SnCl_2$ as catalyst, a 0.99% of crude lactide is produced over the initial PLA weight. This crude lactide is composed by a 15.19% of dimer concentrations, 0.37% of lactic acid, 1.14% of meso-lactide and 83.3% of L/D- lactide. Moreover, a 96.33% of L-lactic acid is obtained over the total amount of L, D and meso-lactide produced. (Ehsani et al, 2014)

The equilibrium reaction is assumed to be completely shifted to the right, as crude lactide is continuously evaporated and removed from the system. Side reactions such as degradation of the polymer may occur but will be neglected at these operating conditions. Only polycondensation of lactic acid into low molecular weight polymers such as dimers and trimers will be taken into consideration.

Table 38.Mass balance hold tank HT-201

Stream (kg/h)	8	9	10	11	16
Lactic acid	461.66	0.00	0.00	461.66	0.00
Water	0.00	0.00	0.00	0.00	0.00
NVI	195.51	0.00	0.00	651.70	456.19
PLA (LMW)	10813.39	0.00	0.00	10889.61	76.23
$SnCl_2$	0.00	28.59	0.00	95.31	66.72
Stabilizer	0.00	0.00	39.10	130.34	91.24
Oligomers	0.00	0.00	0.00	0.00	0.00
L-lactide	0.00	0.00	0.00	0.00	0.00
D-lactide	0.00	0.00	0.00	0.00	0.00
Meso-lactide	0.00	0.00	0.00	0.00	0.00
Total	11470.56	28.59	39.10	12228.63	690.37

Table 39.Mass balance depolymerization reactor E-202

Stream (kg/h)	12	13	17
Lactic acid	461.66	0.00	39.89
Water	0.00	0.00	461.66
NVI	651.70	651.70	0.00
PLA (LMW)	10889.61	108.90	0.00
$SnCl_2$	95.31	95.31	0.00
Stabilizer	130.34	130.34	0.00
Oligomers	0.00	0.00	1637.59
L-lactide	0.00	0.00	8650.76
D-lactide	0.00	0.00	329.58
Meso-lactide	0.00	0.00	122.90
Total	12228.63	986.25	11242.38

The energy balance in the reactor is expressed by a similar equation to the previous prepolymer reactor, taking into account that this time lactide is being removed from the system. Temperature inlet and inside the reactor are 180 and 210ºC respectively. The heating fluid is medium pressure steam at 15 bar and 198.3ºC.

$$Q = m_f \cdot \int_{T_i}^{T_r} Cp \cdot dT + n_{PLA} \cdot \Delta H_R + m_{lactide} \cdot \Delta H_{vap} = m_{steam} \cdot \lambda_{vap} \qquad \text{[Eq.12]}$$

To simplify calculations, as the feed stream to the reactor is mainly composed by polylactic acid (>90% w/w), the change of enthalpy for reactants entering the system has been calculated as that of PLA by Joback contribution method, as explained in the previous section. Enthalpy of reaction is expressed per mol of PLA that has reacted, and it has been obtained by literature (Kopinke et al., 1996) under the assumption of no variation to the operating conditions of the reactor. Enthalpy of vaporization of lactide has also been obtained by literature (Emel'yanenko et al., 2008). Enthalpy of side reaction has been estimated as the condensation reaction of lactic acid to form lactic acid dimers, following the previously explained to obtain polycondensation enthalpy of reaction to form PLA.

Table 40. Energy balance E-202

$m_f \cdot \int_{T_i}^{T_r} Cp \cdot dT$ **(kW)**	60.48
ΔH_R **(kJ/mol PLA)**	1221.0
n_{PLA}**(mol/h)**	4900.3
$\Delta H_{vap-lactide}$ **(kJ/kmol)**	56810.2
$n_{Lactide}$**(mol/h)**	74.80
$\Delta H_{R-side\ reaction}$ **(kJ/mol LA)**	-810.4
n_{LA}**(mol/h)**	4682
Q (kW)	**1848.93**

Table 41. Utility requirements in E-202

$\lambda_{vaporization}$ **(kJ/kg)**	1714.1
m_s **(kg/h)**	3883.2

2.4. Packed columns T-301 and T-302

As a multicomponent system is to be separated, mass and energy balance of both packed columns have been simulated in Aspen Plus, being the results collected in the following Table 42 and Table 43.

Table 42. Mass balance Column T-301

Stream (kg/h)	**19**	**20**	**21**
Lactic acid	39.89	39.09	0.80
Water	461.66	461.66	0.00
Oligomers	1637.59	1629.76	7.83
L-lactide	8650.76	86.51	8564.25
D-lactide	329.58	0.00	329.58
Meso-lactide	122.90	5.97	116.93
Total	11242.38	2222.99	9019.39

Table 43.Mass balance Column T-302

Stream (kg/h)	21	22	23
Lactic acid	0.80	0.80	0.00
Water	0.00	0.00	0.00
Oligomers	7.83	7.83	0.00
L-lactide	8564.25	85.64	8478.61
D-lactide	329.58	0.00	329.58
Meso-lactide	116.93	115.77	1.17
Total	9019.39	210.03	8809.36

2.5. Ring Opening Polymerization reactors R-401 and R-402

The reaction that takes place in both reactors is the ring-opening polymerization of L-Lactide based on the alkoxide initiation mechanism with $Sn(Oct)_2$ as catalyst (C) and dodecyl alcohol as co-catalyst (D) at 180ºC, as depicted in the following Figure 25.

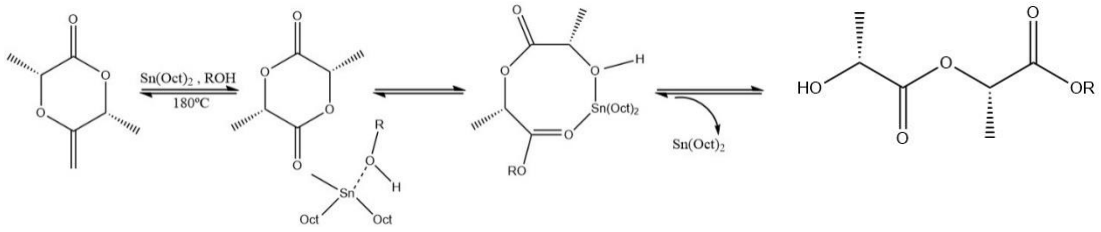

Figure 25. $Sn(Oct)_2$ catalysed ROP of L-Lactide in the presence of a hydroxylic initiator molecule

The kinetic scheme for the system considered is represented herein below, where A stands for the octanoic acid, R stands for the active species containing tin alkoxide and M for the monomer L-Lactide. G is the terminated PLA chains produced by non-radical chain scission reaction, which are being considered.

The kinetic scheme represents the reversible activation reaction (a), the reversible propagation (b), the reversible chain transfer (c) and intermolecular transesterification (d-f). Degradation reactions of the active, dormant and dead polymer chains, which are favoured in the presence of catalyst, will be neglected as at the conversion stablished the system is still living.

$$a.\quad C + D_n \underset{k_{a2}}{\overset{k_{a1}}{\rightleftharpoons}} R_n + A$$

$$b.\quad R_n + M \underset{k_d}{\overset{k_p}{\rightleftharpoons}} R_{n+2}$$

$$c.\quad R_n + D_i \underset{k_s}{\overset{k_s}{\rightleftharpoons}} R_i + D_n$$

$$d.\quad R_i + R_j \underset{k_{te}}{\overset{k_{te}}{\rightleftharpoons}} R_{i+j-n} + R_n$$

$$e.\quad R_i + D_j \underset{k_{te}}{\overset{k_{te}}{\rightleftharpoons}} R_{i+j-n} + D_n$$

$$f.\quad R_i + G_j \underset{k_{te}}{\overset{k_{te}}{\rightleftharpoons}} R_{i+j-n} + G_n$$

The following relationship can be applied considering a living system with reversible propagation and under the assumption that the reaction proceeds at a constant number of growing chains.

$$Y = \ln\left(\frac{M_0 - M_{eq}}{M - M_{eq}}\right) = k_p \cdot R^* \cdot t \quad \text{[Eq.13]}$$

$$M_n = \frac{M_0 \cdot X}{R^* + D} \cdot M_m \quad \text{[Eq.14]}$$

Where M stands for the monomer concentration, being the subscripts 0 for the initial and eq of the equilibrium, k_p is the propagation rate coefficient, R^* is the concentration of living chains, t is the reaction time and Y is the logarithm of the normalized conversion. M_n is the number average molecular weight, X is the monomer conversion, D is the dormant chains and M_m is the molecular weight of the monomer repeating unit, in this case lactoyl repeating unit, with a 72 g/mol molecular weight. As will be explained below, the sum of R^* + D corresponds to the initial co-catalyst concentration D_0

The conversion X is defined by the following equation 15.

$$X = \frac{M_0 - M}{M_0} \quad \text{[Eq.15]}$$

The material balance of the active chain R then can be defined by the following equation 16:

$$\frac{d[R^*]}{dt} = k_{a1}[C][D] - k_{a2}[R^*][A] \quad \text{[Eq.16]}$$

By integrating this equation and taking into account the following relationship between the species involved at any time ($[R^*] = [D_0] - [D] = [C_0] - [C] = [A] - [A_0]$), the concentration of all species can be evaluated by giving time evolution of one of them. Also, if we consider the linearity of Y vs time, it is demonstrated that all living and dormant chains are produced instantly once the reaction starts, maintaining a constant number during the polymerization, which means that equilibrium conditions are attained for reaction and thus the following expression for the material balance is obtained:

$$\frac{[R^*][A]}{[C][D]} = \frac{k_{a1}}{k_{a2}} = K_{eq.a} \quad \text{[Eq.17]}$$

Being $K_{eq.a}$ the equilibrium constant of the activation reaction. Following this, the final concentration of catalyst can be calculated as a function of the initial catalyst and activated concentration and the equilibrium constant of the activation reaction by the following expression:

$$[C] = \frac{-B + \sqrt{B^2 + 4[C_0](K_{eq.a} - 1)([C_0][A_0]}}{2(K_{eq.a} - 1)} \quad \text{[Eq.18]}$$

Where B is a parameter defined by the following equation 19:

$$B = [A_0] + 2[C_0] + K_{eq.a}([D_0] - [C_0]) \quad \text{[Eq.19]}$$

The kinetic parameters provided by Yu et al. are exposed in Table 44 and the following ratios over initial monomer concentration have been stablished in order to fulfil the material balance around the reactor, which are collected in Table 45. (Yu et al., 2011)

Table 44. Kinetic parameters of ROP reaction

$K_{eq,a}$ (-)	0.256
K_{a1} (L/mol·h)	10^6
K_p (L/mol·h)	37000
K_s (L/mol·h)	10^6
K_{te} (L/mol·h)	90
$[M_{eq}]$ (mol/L)	0.225

Table 45.Initial concentration ratios

$[M_0]$ (mol/L)	10.076
$[M_0]/[C_0]$	15000
$[D_0]/[C_0]$	17
$[A_0]/[C_0]$	0.36

Final conversion in R-401 is 0.853 as later will be explained. By stablishing a final conversion of 0.961 in R-402, where the system is still a living system, the following results collected in Table 46 are obtained.

Table 46.Molecular weight in R-401and R-402

	R-401	R-402
Mn	54167	61038
Mw	102919	115973

The next table 47 shows the inlet and outlet streams of the reactor R-401 and R-402. The weight percent of catalyst and co-catalyst concentration have been determined by its concentration and the feeding stream density determined by Aspen Plus ($\rho = 1.457\ g/cm^3$)

Table 47.Mass balance R-401and R-402

Stream (kg/h)	25	26	27	28	29
L-lactide	8478.61	0.00	0.00	1249.38	332.43
D-lactide	329.58	0.00	0.00	48.57	12.92
Meso-lactide	1.17	0.00	0.00	0.17	0.05
$Sn(Oct)_2$	0.00	1.65	0.00	1.65	1.65
Co-catalyst	0.00	0.00	28.06	28.06	28.06
PLA (HMW)	0.00	0.00	0.00	7511.24	8463.96
Total	8809.36	1.65	28.06	8839.07	8839.07

As the feed to the first reactor is already at operating conditions, the energy balance around the reactor can be expressed as follows, where ΔH_R is the enthalpy of the reaction expressed per mol of lactide that has reacted.

$$Q = n_{lactide} \cdot \Delta H_R \qquad \text{[Eq.20]}$$

Table 48.Energy balance in R-401 and R-402

	R-401	**R-402**
Q (kW)	-390.9	-49.6
$n_{lactide}$**(mol/s)**	14.48	1.84
ΔH_R **(J/mol)** (Kulaniga et al., 1982)	-27000	

APPENDIX 3: EQUIPMENT SIZING

3.1. Falling Film evaporators

Both falling film evaporators E-101 and E-201 will follow the design procedure explained for the prepolymer reactor E-103 in *Appendix 4*.

3.2. Packed columns

In packed bed columns the vapour liquid contact is continuous, not stage-wise, as in a plate column. The liquid flows down the column over the packing surface and the gas or vapour, counter-currently, up the column. A good liquid and vapour distribution is required through the packed bed in order to achieve a good performance of the column and thus its design is a critical factor for its operation.

The packing selection criteria is based on whether it provides a large surface area, this is, a high interfacial area between the gas and the liquid; low resistance to vapour flow and uniform vapour flow across the column and promotes an uniform distribution of the liquid through the packing surface. (Sinnot, 2005)

A structured packing material is chosen over random packing so as to enhance contact between the vapour and liquid and to minimize the liquid hold-up, which results in a lower pressure drop over the column and in the minimisation of reactions between different species. Even though random packing is a more economic option, structured packing is more efficient, which means a lower column height will be needed if structured packing is used over random packing. This type of packing also reduces the vapour pressure drop, which is a critical parameter that needs to be controlled in vacuum distillation. (Meerdink et al., 2011)

The advantage of structured packings over random packing is their low HETP (typically less than 0.5 m) and low pressure drop (around 100 Pa/m). (Sinnot, 2005) Intalox 1T structured packing provided by Koch-Glitsch has been selected as packing material. The following Table 49 collects the data provided by Kister. (Kister, 1992)

Table 49. Characteristics of Structured Packing INTALOX

Name	Number	Area (m^2/m^3)	HEPT (m)	F_p (m^{-1})	Vendor
INTALOX	1T	310	0.292	66	Koch-Glitsch

The capacity of a packed column is determined by its cross-sectional area. To estimate the column diameter, the flow factor F_{LV} vs a parameter K_4 is represented graphically in a generalised pressure-drop correlation in Figure 26. The flow factor is calculated by the following equation 21, where L_W and V_W are the liquid and vapour flow rates.

$$F_{LV} = \frac{L_W}{V_W} \cdot \sqrt{\frac{\rho_V}{\rho_L}} \qquad \text{[Eq.21]}$$

$$K_4 = \frac{13.1 \cdot (V_W^*)^2 \cdot F_p \cdot \left(\frac{\mu_L}{\rho_L}\right)^{0.1}}{\rho_V \cdot (\rho_L - \rho_V)} \qquad \text{[Eq.22]}$$

Where V_W^* is the vapour mass flow-rate per unit column cross-sectional area (kg/m^{2}s) and F_p is the packing factor, characteristic of the size and type of packing.

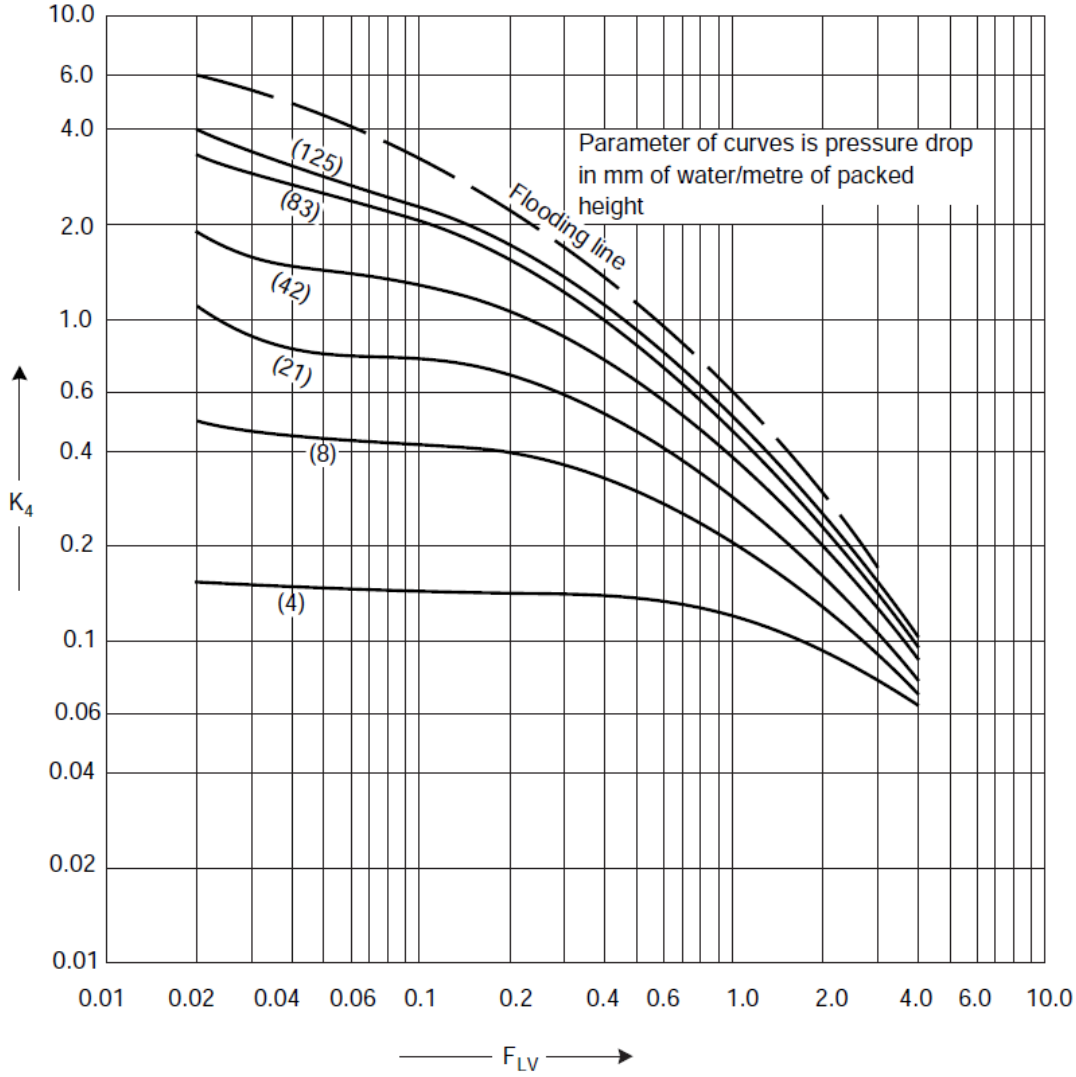

Figure 26. Generalised pressure drop correlation

Table 50. Design calculations of T-301 and T-302

	T-301	**T-302**
F_{LV} **(-)**	0.078	0.366
ΔP **(mmH2O/m)**	10.21	10.21
K_4 **(-)**	0.55	0.40
F_p **(m^{-1})**	66	66
V_W^* **(kg/m^{2}s)**	1.30	0.51

Therefore, the column area required and the diameter can be calculated by the following equations 23 and 24.

$$A_{cross} = \frac{V_W}{V_W^*} \quad \text{[Eq.23]}$$

$$D_c = \sqrt{\frac{4}{\pi} \cdot A_{cross}} \quad \text{[Eq.24]}$$

Table 51. Diameter calculation T-301 and T-302

	T-301	**T-302**
A_{cross} **(m^2)**	0.475	0.114
D_c **(m)**	0.778	0.381

It should be ensured that the percentage of flooding at the selected diameter, which will be rounded to standard dimensions, is between the recommended values for packed bed distillation columns of [40-80] %. (Sinnot, 2005)

$$\%\ Flooding = \sqrt{\frac{K_4}{K_{4,flooding}}} \cdot 100 \qquad \text{[Eq.25]}$$

Table 52.Flooding percentage T-301 and T-302

	T-301	**T-302**
$K_{4.flood}$	3.5	1.6
% $Flooding$	39.6	50.0

3.3. Continuous Stirred Tank Reactors (CSTR)

The general design equation for an ideal CSTR is expressed by equation 26, where the subscript A stands for the limiting reactant.

$$\frac{V}{F_{Ao}} = \frac{X_A}{-r_A} \qquad \text{[Eq.26]}$$

As shows Figure 27, if the Levenspiel diagram is plotted for the system to be considered in order to determine the require volume of the chemical reactor, it can be deduced more than one reactor will be needed if high conversions are intended to be achieved.

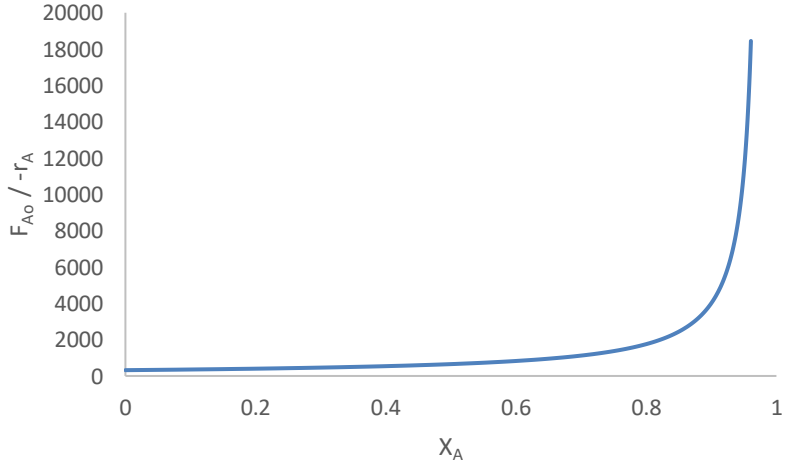

Figure 27. Levenspiel diagram

For the system considered, the equation 26 can be expressed as follows by equation 27 if the feed enters partially converted.

$$V = \frac{F_{Ao} \cdot (X_{A_f} - X_{Ai})}{k_p \cdot [R^*] \cdot [M] - k_d \cdot [R^*]} \qquad \text{[Eq.27]}$$

Taking into account both economical and mechanical aspects, a value of 2 reactors will be needed. The conversion achieved in the first reactor takes a value of 0.853 and it has been deduced by selecting the minimum total volume calculated as the sum of both volume reactors.

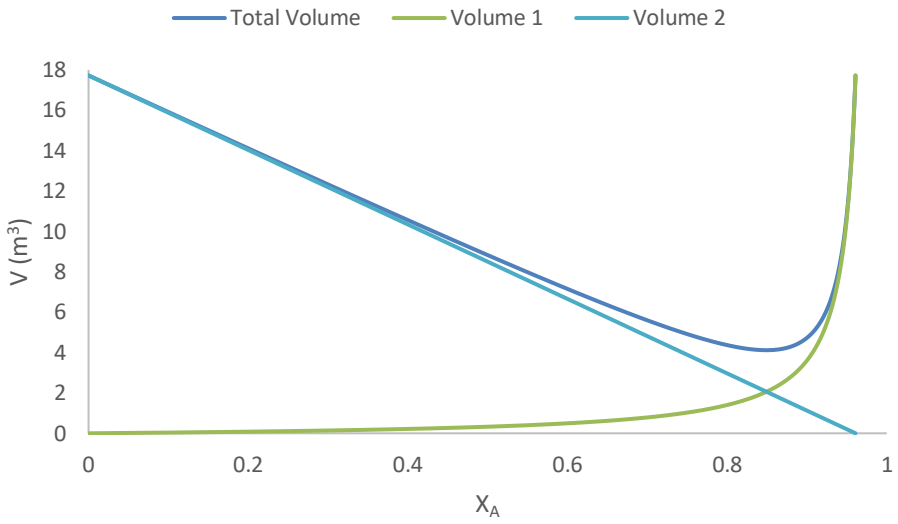

Figure 28. Total volume as a function of conversion

Table 53.Final conversion estimation

	R-401	**R-402**
V_{ideal} **(m^3)**	2.123	1.995
F_{Ao} **(mol/h)**	61125.17	61125.17
$-r_A$ **(h^{-1})**	24.54	3.31
X_{Ai}	0	0.853
X_{Af}	0.853	0.961

The sizing both reactors R-401 and R-402 will be determined based on heuristic relationships for the design of CSTR type of reactor through the following equations 28 and 29. In addition, a 10% oversizing over the reactor ideal volumes will be increased as a safety measure against expansion.

$$V_{real} = \pi \cdot \frac{D_r^2}{3} \cdot H_r + \frac{4 \cdot \pi}{3} \cdot \frac{D_r^2}{3} \quad \text{[Eq.28]}$$

$$H_r = \frac{3}{2} \cdot D_r \quad \text{[Eq.29]}$$

Table 54. Reactors R-401 and R-402 sizing

	R-401	**R-402**
V_{real} **(m^3)**	2.336	2.195
D_r **(m)**	0.91	0.89
H_r **(m)**	1.36	1.33

From the energy balance around both reactors, by the following equation it can be calculated the utility mass flow rate and the heat transfer area required for the refrigeration of the reactors. Cooling water (cw) at 30ºC from the cooling tower circuit is used as refrigerant fluid, as it will extract the necessary heat at a lower cost compared to other refrigerant fluids, exiting the system at 50ºC.

$$Q = m_{cw} \cdot C_p \cdot \Delta T = U \cdot A \cdot \Delta T \qquad \text{[Eq.30]}$$

Table 55. R-401 and R-402 heat transfer design

	R-401	**R-402**
Q (kW)	-390.9	-49.6
m_{cw} (kg/h)	16832.36	2134.99
ΔT (°C)	140	140
U (W/m°C)	400	400
A (m^2)	6.98	0.89

Stirring is needed in the reactor equipment in order to homogenize the content of the vessel so that the concentrations and the temperature are the same through the volume of the reactor as well as mass and heat transfer are favoured.

The agitator type selection depends on the type of mixing required, the capacity of the vessel and the physical properties of the fluid, mainly the viscosity. Paddle, anchor and helical ribbon agitators are commonly suitable for viscous liquids. The following Figure 29 can be used to make a preliminary selection of the agitator type, based on the viscosity and the reactor volume. (Towler et al., 2013)

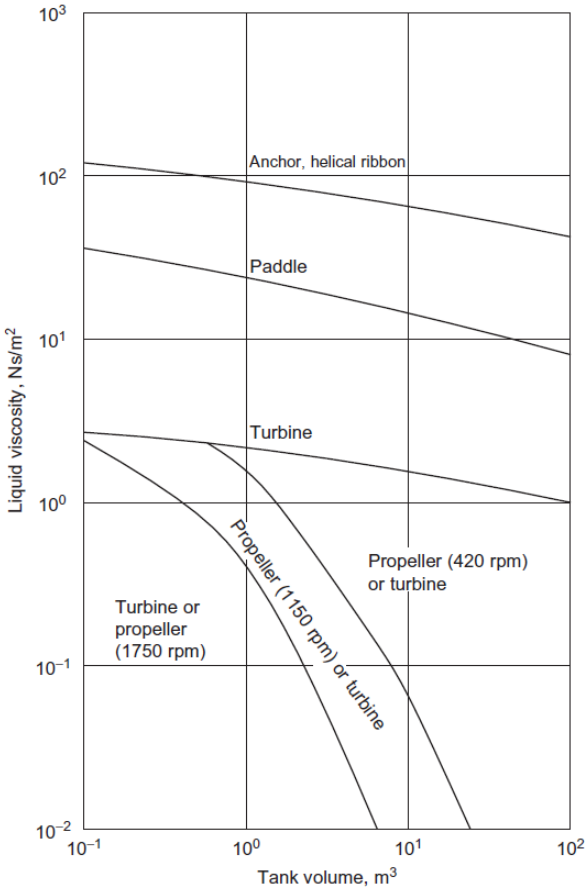

Figure 29. Impeller selection guide (Sinnot, 2005)

Table 56. Impeller selection parameters

	R-401	**R-402**
μ_L (Ns/m^2)	580.8	881.6
V (m^3)	2.336	2.195

By following Figure 29, anchor agitators with a configuration as shown in Figure 30 are selected for both R-401 and R-402, being this a suitable type use for this kind of systems. Anchor agitators are used with close clearance between the blades and vessel wall so anchor to tank diameter ratios are of 0.95 or higher.

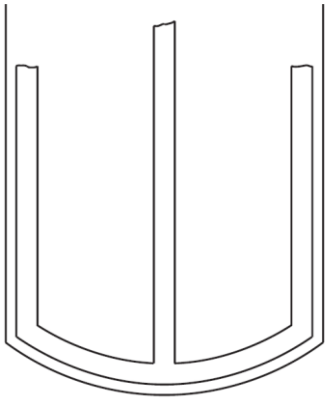

Figure 30. Anchor type of agitator (Sinnot, 2005)

3.4. Hold tank

The sizing of the equipment is estimated by equations 28 and 29 with a similar procedure for the CSTR R-401 and R-402. Again, a 10% oversizing over the tank volume will be increased as a safety measure against expansion.

Table 57.HT-201 sizing

Q (m^3/h)	10.92
τ (h)	0.167
V_{real} (m^3) (+10%)	2.00
D_t (m)	0.85
H_t (m)	1.28

From the energy balance around the hold tank, the following Table 58 shows the utility mass flow rate and the heat transfer area required in order to maintain the hold tank at 160ºC . Cooling water (cw) at 30ºC from the cooling tower circuit is used as refrigerant fluid, as it will extract the necessary heat at a lower cost compared to other refrigerant fluids, exiting the system at 50ºC.

Table 58.HT-201 heat transfer design

Q (W)	9350.89
m_{cw} (kg/s)	0.11
ΔT (ºC)	130
U (W/m^2ºC)	250
A (m^2)	0.29

Stirring is needed in the tank in order to homogenize the content of the vessel as well as mass and heat transfer are favoured.

The agitator type selection depends on the type of mixing required, the capacity of the vessel and the physical properties of the fluid, mainly the viscosity. The same procedure than the CSTRs will be followed by using Figure 29 for the selection of the agitator type.

Table 59.Agitator selection parameters

μ_L (Ns/m^2)	0.0305
V (m^3)	2.00

A turbine impeller type of agitator with a speed of 1750 rpm is selected, being this type suitable at high Reynolds numbers, this is, low viscosity fluids. For turbine agitators, impeller to tank diameter ratios of 0.6 are recommended. (Towler et al., 2013). Baffles are used to improve the mixing and reduce problems of vortex formation. An estimation of the power requirement for baffled agitated tanks is given by Tower et al., with a value of 1.5 kW/m^3 for the hold tank system.

3.5. Heat Exchangers

The general equation for heat transfer across a surface in order to carry out the exchangers design is the following one.

$$Q = U \cdot A \cdot \Delta T_m \qquad \text{[Eq.31]}$$

Where Q is the heat transferred per unit time, U is the overall heat transfer coefficient, A is the heat transfer area and ΔT_m is the mean temperature difference or driving force of the system.

Heat exchangers of the process will be assumed to be shell and tubes heat exchangers with negligible pressure drop. As a rule of thumb, corrosive and fouling fluids, or with the lowest pressure drop allowable should be allocated to the tube side, while viscous fluids or when condensation takes places, shell side should be used. Besides, condensers and thermosiphons will be used when phase change takes place.

The mean temperature difference is estimated by the logarithmic mean temperature difference corrected by a temperature correction factor F_t that accounts for the flow to be a mixture of co-current, counter-current and cross flow.

$$\Delta T_m = F_t \cdot \Delta T_{lm} \qquad \text{[Eq.32]}$$

If it is assumed there is no change in specific heats nor heat losses and the overall heat-transfer coefficient is constant, the logarithmic mean temperature difference for counter-current flow is expressed as:

$$\Delta T_{lm} = \frac{(T_1 - t_2) - (T_2 - t_1)}{\ln\left(\frac{T_1 - t_2}{T_2 - t_1}\right)} \qquad \text{[Eq.33]}$$

Where T_1 and T_2 is for the hot fluid inlet and outlet temperature and t_1 and t_2 is for the cold fluid inlet and outlet temperate, respectively.

The overall heat transfer coefficient will be estimated by taking typical values provided by Sinnot (Sinnot, 2015) for various types of heat exchanger based on hot and cold fluid properties. These coefficients already include an allowance for fouling.

Heat exchanger E-102 preheats the fluid process from 80ºC to 130ºC previous to its entrance to the prepolymer reactor E-103. Low pressure steam (lps) at 151.9ºC and 5 bar is used as heating fluid. The following Table 60 sums up the results obtained.

Table 60.E-102 heat transfer design

Tube side		**Shell side**	
$\boldsymbol{m_{stream4}}$ **(kg/h)**	16445.73	$\boldsymbol{m_{lps}}$**(kg/h)**	1074.12
$\boldsymbol{C_P \cdot \Delta T}$ **(J/kg)**	137712.0	$\boldsymbol{\lambda}$ **(kJ/kg)**	2108.5
Q (kW)		629.10	
U (W/m^{2}ºC)		750	
A (m^2)		19.94	
$\boldsymbol{\Delta T}$ **(ºC)**		42.1	

Heat exchanger E-201 heats stream 11 coming from the hold tank from 160ºC to 180ºC previous to its entrance to the lactide reactor. Medium pressure steam (mps) at 198.3ºC and 15 bar is used as heating fluid. The following Table 61 sums up the results obtained.

Table 61.E-201 heat transfer design

Tube side		**Shell side**	
$\boldsymbol{m_{mps}}$ **(kg/h)**	17.34	$\boldsymbol{m_{stream11}}$ **(kg/h)**	12228.63
$\boldsymbol{\lambda}$ **(kJ/kg)**	1940.7	$\boldsymbol{C_P \cdot \Delta T}$ **(J/kg)**	2752.8
Q (kW)		9.35	
U (W/m^{2}ºC)		600	
A (m^2)		0.58	
$\boldsymbol{\Delta T}$ **(ºC)**		27.1	

Condenser E-301 partially condensates stream 17 coming as vapour from the lactide reactor to a mass vapour fraction of 0.212. Cooling water (cw) at 30ºC from the cooling tower circuit is used as refrigerant fluid as it will extract the necessary heat at a lower cost compared to other refrigerant fluids, exiting the system at 50ºC

Table 62.E-301 heat transfer design

Tube side		**Shell side**	
$\boldsymbol{m_{stream17}}$ **(kg/h)**	11242.38	$\boldsymbol{m_{cw}}$ (kg/h)	80851.83
$\boldsymbol{C_P \cdot \Delta T}$ **(J/kg)**	54378.9	$\boldsymbol{C_P}$ (J/kgºC)	4180.0
$\boldsymbol{\lambda}$ **(kJ/kg)**	492.5	$\boldsymbol{\Delta T}$ (ºC)	20
Q (kW)		1877.60	
U (W/m^{2}ºC)		1250	
A (m^2)		10.80	
$\boldsymbol{\Delta T}$ **(ºC)**		139.04	

Heat exchanger E-401 heats stream 24 coming from the purification section from 146ºC to 180ºC previous to its entrance to the polymerization reactor. Medium pressure steam (mps) at 198.3ºC and 15 bar is used as heating fluid. The following table 63 sums up the results obtained.

Table 63.E-401 heat transfer design

Tube side		**Shell side**	
$m_{stream24}$ **(kg/h)**	8809.36	m_{mps}(kg/h)	21.24
$C_P \cdot \Delta T$ **(J/kg)**	4679.8	λ (kJ/kg)	1940.7
Q (kW)		11.45	
U (W/m^{2}ºC)		500	
A (m^2)		0.71	
ΔT **(ºC)**		32.4	

Condenser E-302 is the condenser of the packed column T-301 which operates at 50 mmHg and at a condenser temperature of 126ºC. Cooling water (cw) at 30ºC from the cooling tower circuit is used as refrigerant fluid as it will extract the necessary heat at a lower cost compared to other refrigerant fluids, exiting the system at 50ºC

Table 64.E-302 heat transfer design

m_{cw} **(kg/h)**	53981.20
$C_P \cdot \Delta T$ **(J/kg)**	83600
Q (kW)	1253.56
U (W/m^{2}ºC)	350
A (m^2)	41.84
ΔT **(ºC)**	85.6

Thermosiphon E-303 is the reboiler of the packed column T-301 which operates at 50 mmHg and at a bottom temperature of 158ºC. Medium pressure steam (mps) at 179.9ºC and 10 bar is used as heating fluid.

Table 65.E-303 heat transfer design

m_{mps} **(kg/h)**	42.17
λ **(kJ/kg)**	2015.3
Q (kW)	800.31
U (W/m^{2}ºC)	1118
A (m^2)	21.12
ΔT **(ºC)**	33.9

Condenser E-304 is the condenser of the packed column T-302 which operates at 10 mmHg and at a condenser temperature of 137ºC. Cooling water (cw) at 30ºC from the cooling tower circuit is used as refrigerant fluid as it will extract the necessary heat at a lower cost compared to other refrigerant fluids, exiting the system at 50ºC

Table 66.E-304 heat transfer design

m_{cw} **(kg/h)**	167632.27
$C_P \cdot \Delta T$ **(J/kg)**	83600
Q (kW)	3892.79
U (W/m^{2}ºC)	350
A (m^2)	115.07
ΔT **(ºC)**	96.7

Thermosiphon E-305 is the reboiler of the packed column T-302 which operates at 10 mmHg and at a bottom temperature of 146ºC. Medium pressure steam (mps) at 179.9ºC and 10 bar is used as heating fluid.

Table 67.E-305 heat transfer design

m_{mps} (kg/h)	300.88
λ (kJ/kg)	2015.3
Q (kW)	3688.76
U (W/m^{2}ºC)	1731
A (m^2)	97.33
ΔT (ºC)	21.9

3.6. Pumps

Pumps in the process have the main objective of stablishing an energy supply necessary for liquid impulsion through pipes between process vessels. Taking into consideration operating conditions of the process and physical properties of the fluids, centrifugal and positive displacement pumps are selected. Centrifugal pumps provide simple construction with low cost compared to others and, in addition, is the most common type in the industry given its versatility to operate with different types of fluids. On the other side, positive displacement pumps will be used when dealing with viscous fluids. (Mott et al., 2006)

Prior to pump power estimation, suction and discharge conductions will be detailed based on the volumetric flow over the pipe and an initially estimating the velocity within recommended values. Liquid velocities recommended values in pipes range from [1-3] m/s. (Turton et al.,2012) Steel pipes Schedule selection will be based on temperature conditions and corrosive properties of the liquid to be pumped and diameters are standardized according to ASME Code B 36.19.

Pipe lengths has been estimated based on safety distances between equipment in the plant and the height of each equipment. Minimum safety distances for chemical plants recommendations provided by GE Global Asset Protection Services GAP 2.5.2. will be followed. Since pipe accessories are not object of study, an equivalent length of 15% will be added. (Global asset protection services LLC., 2015)

Table 68.Pipe sizing results

Stream	Q (m^3/h)	v_{ass} (m/s)	D_i (mm)	Sch	$D_{i,st}$ (mm)	t (mm)	D_e (mm)	DN	v_{real} (m/s)	L (m)
3	14.883	1.5	59.24	80	60.3	5.54	71.4	50	1.45	11.97
4	14.883	1.5	59.24	80	60.3	5.54	71.4	50	1.45	23.73
7	10.240	1.5	49.14	80	48.3	5.08	58.5	40	1.55	23.73
8	10.240	1.5	49.14	80	48.3	5.08	58.5	40	1.55	11.30
15	0.630	1.5	12.18	40	13.7	2.24	18.2	8	1.19	39.55
16	0.630	1.5	12.18	40	13.7	2.24	18.2	8	1.19	11.30
18	8.453	1.5	44.64	40	48.3	3.68	55.7	40	1.28	12.02
19	8.453	1.5	44.64	40	48.3	3.68	55.7	40	1.28	20.21
23	6.045	1.5	37.75	40	42.2	3.56	49.3	32	1.20	18.53
24	6.045	1.5	37.75	40	42.2	3.56	49.3	32	1.20	12.02

The supply energy required for incompressible fluids movement thought a conduit between two points depends on its properties and the flow rate to be treated and the difference in height and pressure between the two points. If a mechanical energy balance is stablished, the power of a pump W (W) can be determined by the following equation 34.

$$W = \frac{v_2^2 - v_1^2}{2 \cdot \alpha} + g \cdot (z_2 - z_1) + \frac{P_2 - P_1}{\rho} + \sum F \qquad \text{[Eq.34]}$$

Where the subscripts 1 and 2 refer to the suction and discharge points, respectively and

- v = Fluid velocity (m/s)
- α = 0.5 for laminar regime / 1 for turbulent regime
- g = gravity acceleration (m/s^2)
- z = Height (m)
- P = Pressure (Pa)
- ρ = Fluid density (kg/m^3)
- ΣF = Friction loss through conduction (m^2/s^2)

Redefining the equation in terms of the total load h_w (m):

$$\frac{v_1^2 - v_2^2}{2 \cdot g \cdot (\alpha_1 - \alpha_2)} + (z_1 - z_2) + \frac{P_1 - P_2}{g \cdot \rho} + h_w - \sum h_f = 0 \qquad \text{[Eq.35]}$$

The head loss due to friction in pipelines h_f is proportional to the fluid velocity and the length to diameter ratio of the conduit. Mathematically, this expression is given by Darcy's equation.

$$h_f = f \cdot \frac{L}{D} \cdot \frac{v^2}{2 \cdot \rho} \qquad \text{[Eq.36]}$$

Where f is the friction factor. For turbulent flow it can be estimated by the following equation 37.

$$f = \frac{0.25}{\left[\log\left(\frac{1}{3.7 \cdot \left(\frac{D}{\varepsilon}\right)} + \frac{5.74}{Re^{0.9}}\right)\right]} \qquad \text{[Eq.37]}$$

Where ε is the roughness, which for a commercial steel pipe has a value of $4.6 \cdot 10^{-5}$ m. (Sinnot, 2005)

The theoretical power pump required is therefore determined by the following equation 38. Taking into consideration that there are energy losses inside the pump due to the effect of friction and turbulence, a value of 75 % of efficiency is assumed, so that the real power of the pump is calculated by equation 39.

$$P_{th} = h_w \cdot \rho \cdot g \cdot Q \qquad \text{[Eq.38]}$$

$$P_{real} = \frac{P_{th}}{\eta} \qquad \text{[Eq.39]}$$

The A / B identifier refers to the arrangement of two pumps in parallel with the same characteristics, so that one of them is in reserve and its use is intended for occasions in which the pump in use is undergoing maintenance or cannot operate properly.

Table 69.Pump power estimation

Pump	P-101 A/B	P-102 A/B	P-201 A/B	P-301 A/B	P-401 A/B
z_1 (m)	1.50	6.71	5.00	2.00	1.50
z_2 (m)	6.71	1.28	1.28	3.19	2.00
ΔP (Pa)	40300	-94625	-97925	-3300	-99992
Re (-)	42296.9	2753.5	584.3	42337.0	703.2
f (-)	0.024	0.047	0.085	0.025	0.078
L (m)	35.71	35.03	50.85	32.23	30.54
h_f (m)	0.014	0.036	0.204	0.010	0.028
h_w (m)	1.505	3.221	5.591	1.449	7.522
P_{th} (W)	67.43	100.68	10.52	44.39	180.58
P_{real} (W)	89.91	134.24	14.02	59.18	240.77

3.7. Vacuum pumps

Vacuum pumps are needed for equipment that operate under vacuum. The type of vacuum pump selection depends on the degree of the vacuum required, as well as the capacity of the system and the rate of air in leakage.

As aqueous solutions are to be treated, steam-jet ejectors are a versatile and economic type of vacuum pump frequently used in the industry, as they can handle high vapour flow rates and produce low pressures down to about 0.1 mmHg. (Sinnot, 2005) Its design is out of the scope of the project.

APPENDIX 4: DETAILED DESIGN – PREPOLYMER REACTOR

4.1. Heat transfer design

The general equation for heat transfer across a surface in order to carry out the evaporator design is the following equation 40.

$$Q = U \cdot A \cdot \Delta T_m \quad \text{[Eq.40]}$$

Where Q is the heat transferred per unit time calculated in previous *Appendix 2*, U is the overall heat transfer coefficient, A is the heat transfer area and ΔT_m is the mean temperature difference or driving force of the system.

The mean temperature difference is estimated by the logarithmic mean temperature difference corrected by a temperature correction factor F_t that accounts for the flow to be a mixture of co-current, counter-current and cross flow.

$$\Delta T_m = F_t \cdot \Delta T_{lm} \quad \text{[Eq.41]}$$

As the fluid is being vaporized, tube side temperature will be isothermal once it reaches the saturation temperature and thus the mean temperature difference should be based on the liquid boiling point. The quantity of heat required to bring the feed to its boiling point is included in the total duty, but it will be neglected for the mean temperature difference calculation as the feed will rapidly mix with the boiling pool of liquid. The mean temperature difference for co-current flow is then expressed by equation 42.

$$\Delta T_{lm} = \frac{(t_2 - t_1)}{\ln\left(\frac{T_{sat} - t_1}{T_{sat} - t_2}\right)} \quad \text{[Eq.42]}$$

Where T_{sat} is the saturation temperature of the fluid that is vaporized and t_1 and t_2 is for the cold fluid inlet and outlet temperate, respectively.

Since both sides are not isothermal, the logarithmic temperature difference must be corrected for departures from true cross- or counter-current flow. The correction factor can be expressed as a function of the shell and tube fluid temperatures and the number of tube and shell passes. A value close to 1 means the terminal temperature differences are large while a value close to 0 means there is a temperature cross between the hot and cold fluids. A limit value of 0.75 is stablished to define an economic exchanger design, thus below this point another type of exchanger should be proposed. For a 1:1 exchanger, the following equation 43 is deduced:

$$F_t = \frac{\sqrt{(R^2+1)} \cdot \ln\left[\frac{1-S}{1-RS}\right]}{(R-1) \cdot \ln\left[\frac{2-S\cdot\left[R+1-\sqrt{(R^2+1)}\right]}{2-S\cdot\left[R+1+\sqrt{(R^2+1)}\right]}\right]} \quad \text{[Eq.43]}$$

Where R represents the shell-side fluid flow-rate times the fluid mean specific heat divided by the tube-side fluid flow-rate times the tube-side fluid specific heat and S is a measure of the temperature efficiency of the exchanger.

$$R = \frac{T_1 - T_2}{t_2 - t_1} \quad \text{[Eq.44]}$$

$$S = \frac{t_2 - t_1}{T_1 - t_1} \qquad \text{[Eq.45]}$$

Table 70. Mean temperature difference parameters

ΔT_{lm} (ºC)	139.8
F	0.82

The overall heat transfer coefficient for a falling film evaporator can be expressed as the overall resistance to heat transfer by the sum of several individual resistances as shown below in equation 46.

$$\frac{1}{U_o} = \frac{1}{h_o} + \frac{1}{h_{id}} + \frac{d_o \cdot \ln\left(\frac{d_o}{d_i}\right)}{2 \cdot k_w} + \frac{d_o}{d_i} \cdot \frac{1}{h_{id}} + \frac{d_o}{d_i} \cdot \frac{1}{h_i} \qquad \text{[Eq.46]}$$

Where U_o is the overall coefficient based on the outside area of the tube, h_o and h_{id} are the outside fluid film and dirt coefficient, h_i and h_{id} are the inside fluid film and dirt coefficient, k_w is the thermal conductivity of the tube wall material and d_i and d_o are the inside and outside tube diameter. In order to calculate the overall heat transfer coefficient, a trial and error procedure needs to be carried out, starting with an assumed value function of the type of evaporator and fluid conditions. The results shown below are the final ones, obtained once the following expression is satisfied and an optimisation of the design has been carried out.

$$0 < \frac{U_{o.calc} - U_{o.ass}}{U_{o.ass}} < 30\% \qquad \text{[Eq.47]}$$

Table 71.Heat transfer parameters E-103

Q (kW)	535.64
$U_{o.ass}$ (W/m^{2}ºC)	34.58
ΔT (ºC)	114.1
A (m^2)	166.24

4.1.1. Physical properties

The following Table 72 collects the physical properties of the different compounds involved in the system required for the design of the falling film evaporator E-103. It has been assumed a constant value with no variation along the evaporator evaluated at the mean temperature in order to ease the design procedure.

Table 72. Physical properties in E-103

	Liquid Tube-side	**Vapour Tube-side**	**Cooling water Shell-side**
ρ (kg/m^3)	1120.2	4.8	991.8
μ (kg/ms)	$3.05 \cdot 10^{-2}$	$1.50 \cdot 10^{-5}$	$6.71 \cdot 10^{-4}$
v (m^2/s)	$2.723 \cdot 10^{-5}$	$3.125 \cdot 10^{-6}$	$6.765 \cdot 10^{-7}$
k (W/mK)	0.195	0.039	0.618
C_p (J/kgK)	137.6	1927.5	4180.0

4.1.2. Shell and tubes definition

Tube dimensions are also estimated by a trial and error procedure and the values selected are the optimal standard values in order to satisfy design requirements. Tube outside diameter (d_o) of 20 mm and 1.6 mm wall thickness (δ_w) has been chosen in order to assure a compact and therefore cheaper equipment for heat transfer required and to withstand the internal pressure and give an adequate corrosion allowance.

Tube length (L) is of 16 ft (4.88 m). This length is the optimum value for the reduction in shell diameter, which results in lower cost of the equipment.

As pressure drop is not a limiting variable in the equipment design, a triangular pitch pattern is stablished for the tubes arrangement, which will provide a higher heat-transfer rate through the surface. Therefore the distance between the tube centres, defined as tube pitch (p_t), will be the recommended value of $p_t = 1.25 \cdot d_o$.

An internal floating head is selected as it is more versatile than fixed head and U-tube shapes. This configuration is suitable for the high-temperature differentials of the system, as well as the tubes can be rodded from end to end and the bundle removed, providing an easiness in cleaning for fouling liquids.

The shell-bundle diameter (D_b) is estimated as a function based on the tube layouts, where K_1 and n_1 are 0.319 and 2.142, respectively, for a triangular pattern and 1 tube passes. (Sinnot. 2005)

$$D_s = d_o \cdot \left(\frac{N_t}{K_1}\right)^{\frac{1}{n_1}} \quad \text{[Eq.48]}$$

$$A_{tube} = \pi \cdot d_o \cdot L \quad \text{[Eq.49]}$$

$$N_t = \frac{A}{A_{tube}} \quad \text{[Eq.50]}$$

The number of tubes (N_t) is rounded to the nearest even number. The shell-bundle diameter needs to sum the bundle diametrical clearance, which can be obtained by the following Figure 31 as a function of the shell-bundle diameter.

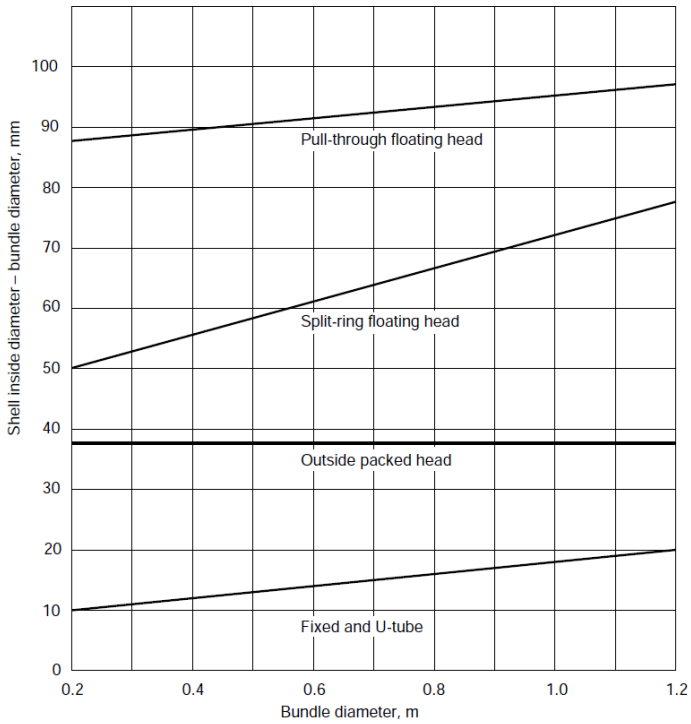

Figure 31. Shell-bundle clearance

For a split-ring floating head is of 0.062 m, and the shell diameter is rounded to the nearest standard pipe size, as well as the shell thickness. The following Table 73 collects the results for the equipment.

Table 73.Shell and tubes sizing

A_{tube} (m^2)	0.307
N_t (tubes)	544
D_b (m)	0.645
Bundle clearance (m)	0.062
D_s (m)	0.707
D_s (m) (Standardized)	0.7112

The use of single segmental baffles is needed in order to direct the cooling water across the tubes and so increase velocity while improving the rate of transfer. Recommended dimensions for baffle cut ranges from 15-45% and a value of 25% is selected. Baffle spacing (l_B) will be dimensioned as the 20% of the standardized shell diameter. Recommended values range from $[0.2 - 1.0] \cdot D_s$ to assure high transfer coefficients without higher pressure drops.

4.1.3. Tube side heat transfer coefficient

The resistance to heat transfer in a system equals the sum of individual resistances. In this case, as a gas-liquid system is to be considered, the overall heat transfer coefficient can be determined by the equation 51, where h_{iG} and h_{iL} are the heat transfer coefficient referred to the gas and the liquid, respectively.

$$\frac{1}{h_i} = \frac{1}{h_{iG}} + \frac{1}{h_{iL}} \qquad \text{[Eq.51]}$$

4.1.3.1. Liquid heat transfer coefficient

It is necessary to define the circulation of the liquid through the evaporator in order to determine the heat transfer coefficient of the liquid through the tubes. It can be distinguished three different regimes for the liquid circulation: laminar, with waves and turbulent; and the Reynolds number defines the transition among them.

$$Re = \frac{\Gamma}{\upsilon} \qquad \text{[Eq.52]}$$

Where υ is the kinematic viscosity and Γ is the flow rate per unit of wet perimeter, defined by the following expression for a falling film evaporator. (Gutiérrez, 1984)

$$\Gamma = \frac{g \cdot \delta^3}{3 \cdot \upsilon} \cdot sen(\theta) \qquad \text{[Eq.53]}$$

Being δ the film thickness, υ the kinematic viscosity and θ the inclination angle of the wall, in radians, which for a vertical wall is the equivalent to 90º.

The kinematic viscosity is calculated based on liquid density and dynamic viscosity. Liquid density is determined by the following equation 54 proposed by Winztke et al., based on a reference temperature of 150 ºC for which density is 1.145 g/cm^3 and based on the thermal coefficient of expansion at that reference temperature. (Winztke et al.. 1997)

$$\rho\left(\frac{g}{cm^3}\right) = \frac{1.145}{1+0.0007391(T(^{\circ}C)-150)} \qquad \text{[Eq.54]}$$

Dynamic viscosity at 180ºC is determined by equation 55 proposed by Dorgan et al. (Safrit et al., 2013) and based on the polymer molecular weight (Mw), the critical entanglement molecular weight (Mc) with a value of 9211 g/mol, the parameter B which corresponds to zero shear rate constant of -4.87 and the parameter p which corresponds to the chain packing length with a value of 3.5.

$$\eta_0 = 10^B \cdot M_w \left[1 + \left(\frac{M_w}{M_c}\right)^{p-1}\right] \qquad \text{[Eq.55]}$$

Table 74.Liquid characterization

υ (m^2/s)	$2.72 \cdot 10^{-5}$
δ (mm)	4
Γ (m^2/s)	0.00768
Reynolds (-)	282.2

The Navier-Stokes equation allows to describe the flow of a liquid film in laminar regime. Once integrated and applied to the system considered for a vertical wall, the velocity profile can be expressed by the following equation 56, being y the transversal coordinate. Cartesian coordinates are used instead of cylindrical since the correction in thickness due to curvature effects can be negligible because of the difference in film thickness with respect to the tubes radius.

$$v_z = \frac{g}{\upsilon} \cdot sen(\theta)\left(\delta y - \frac{y^2}{2}\right) \qquad \text{[Eq.56]}$$

The following expressions for the maximum and mean velocity are then determined:

$$v_{max} = \frac{g \cdot \delta^2}{2 \cdot \upsilon} \cdot sen(\theta) \quad \text{[Eq.57]}$$

$$v = \frac{g \cdot \delta^2}{3 \cdot \upsilon} \cdot sen(\theta) \quad \text{[Eq.58]}$$

Table 75. Maximum and mean liquid velocity

v_{max} (m/s)	2.88
v (m/s)	1.92

Note that linear velocity is in the range recommended for liquids through tubes which is [1-3] m/s.

The inlet and outlet hydrodynamic effects of the evaporator should be taken into account as there is an inlet length Le until the flow becomes uniform. However, Cerro and Whitaker (1974) demonstrates that this length at the inlet can be neglected except for systems that operate under moderate pressures. The outlet effect, where the film thick widens due to the presence of surfactants forming a film on the surface of the liquid, does not depend on the column height and it can also be neglected for laminar regimes.

A laminar flow is to be considered for a Reynolds number below 2000, and the following equation 59 can be used in order to estimate the film-heat transfer coefficient.

$$Nu = 1.86 \cdot (Re \cdot \mathrm{Pr})^{0.33} \cdot \left(\frac{d_e}{L}\right)^{0.33} \cdot \left(\frac{\mu}{\mu_w}\right)^{0.14} \quad \text{[Eq.59]}$$

Where Nu is the Nusselt number$\left(Nu = \frac{h \cdot d_e}{k_f}\right)$, Pr is the Prandtl number $\left(Pr = \frac{c_p \cdot \mu}{k_f}\right)$, d_e is the hydraulic mean diameter, equivalent to the internal diameter for tubes configuration, and μ and μ_w stand for the fluid viscosity at the bulk fluid temperature and at the wall, respectively. This effect will be assumed to be negligible for the system considered. It needs to be taken into account if the Nusselt number is less than 3.5, this value should be taken.

Table 76.Tube-side liquid heat transfer coefficient

Re (-)	282.2
Pr (-)	21.53
d_e (m)	0.016
Nu (-)	4.99
h_{iL} (W/m^{2}K)	60.84

4.1.3.2. Gas heat transfer coefficient

As well as the liquid, it is necessary to define the circulation of the gas through the evaporator tubes in order to determine the heat transfer coefficient through the tubes. It is assumed gas circulation in a wet-walled column to be similar to circulation through an empty tube taking into account the laminar regime of the liquid and the high differences in velocity, viscosity and density between both phases gas and liquid. It is also assumed to be negligible the

flow density that is exerted by the gas on the liquid (τ_G) as it can be considered that the water vapour does not exert any important pressure over the polymer surface.

$$Re = \frac{\rho \cdot u_t \cdot d_e}{\mu} \quad \text{[Eq.60]}$$

Gas velocity through the tubes (u_t) is calculated by considering the cross sectional area of one tube, multiplied by the number of tubes, as only 1 pass tubes is taken.

$$S_{tube} = \frac{\pi \cdot (d_o - 2 \cdot \delta_t)^2}{4} \quad \text{[Eq.61]}$$

$$S_{flow} = N_t \cdot S_{tube} \quad \text{[Eq.62]}$$

$$u_t = \frac{W_g}{\rho \cdot S_{flow}} \quad \text{[Eq.63]}$$

As a turbulent flow is considered, the general equation 64 for an exchanger design can be used, where C has a value of 0.021 for gases.

$$Nu = C \cdot Re^{0.8} \cdot Pr^{0.33} \cdot \left(\frac{\mu}{\mu_w}\right)^{0.14} \quad \text{[Eq.64]}$$

Table 77. Tube-side gas heat transfer coefficient

S_{flow} (m^2)	$2.01 \cdot 10^{-4}$
u_t (m/s)	10.57
Re (-)	53909
Pr (-)	0.739
Nu (-)	115.96
h_{iG} (W/m^{2}K)	283.37

Note that linear velocity is in the range recommended for gases and vapours through tubes which is [10-30] m/s.

4.1.4. Shell side heat transfer coefficient

Kern's method is used to estimate the shell-side heat transfer coefficient. The Reynolds number is defined to estimate the Nusselt number.

$$Re = \frac{\rho \cdot u_s \cdot d_e}{\mu} \quad \text{[Eq.65]}$$

Where u_s is the linear velocity and d_e is the equivalent diameter.

The linear velocity is calculated by defining the mass velocity $G_s = \frac{W_s}{A_s}\left(\frac{kg}{s \cdot m^2}\right)$, where the cross flow area (A_s) is estimated by using the flow area between the tubes taken in the axial direction and the wetted perimeter of the tubes, as shown in Figure 32.

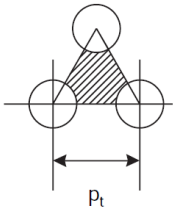

Figure 32. Equivalent cross-sectional area and wetted perimeter (Sinnot, 2005)

$$A_s = \frac{(p_t - d_o)\cdot D_s \cdot l_B}{p_t} \quad \text{[Eq.66]}$$

$$u_s = \frac{G_s}{\rho} \quad \text{[Eq.67]}$$

The hydraulic diameter, for an equilateral triangular pitch arrangement is expressed as follows:

$$d_e = \frac{4\cdot\left(\frac{p_t}{2}\cdot 0.87\cdot p_t - \frac{1}{2}\pi\cdot\frac{d_o^2}{4}\right)}{\frac{\pi\cdot d_o}{2}} = \frac{1.10}{d_o}\cdot(p_t^2 - 0.917\cdot d_o^2) \quad \text{[Eq.68]}$$

Table 78. Shell-side liquid characterization

A_s (m^2)	0.0198
u_s (m/s)	0.326
d_e (m)	0.0146
Re (-)	7037

Note that linear velocity is in the range recommended for shell side liquids which is [0.3-1] m/s. Therefore, the Nusselt can be estimated by the following equation 69.

$$Nu = \frac{h_s\cdot d_e}{k_f} = j_h\cdot Re\cdot Pr^{\frac{1}{3}}\cdot\left(\frac{\mu}{\mu_w}\right)^{0.14} \quad \text{[Eq.69]}$$

The following Figure 33 relates the Reynolds number with the value of the heat transfer factor j_h as a function of the baffle cut and the tube arrangement.

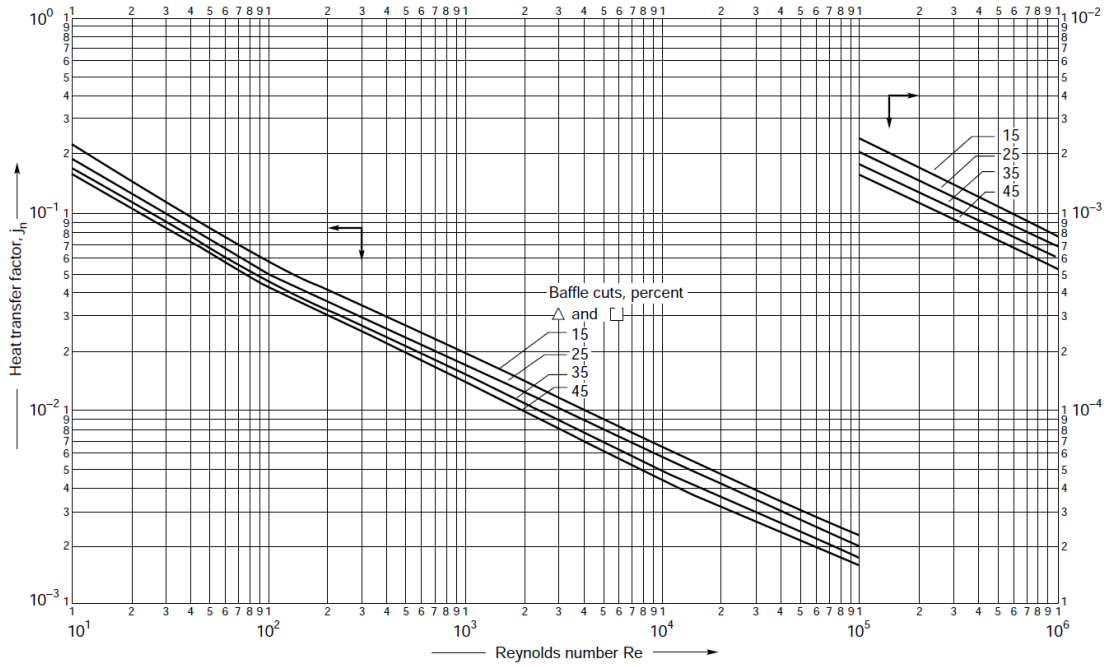

Figure 33. Shell-side heat-transfer factors - segmental baffles (Towler, 2013)

Table 79. Shell-side liquid heat transfer coefficient

Baffle cut (%)	25
j_h (-)	0.007
Pr (-)	4.538
Nu (-)	81.55
h_s (W/m^{2}K)	3448.17

4.1.5. Overall heat transfer coefficient

Retaking equation 46, parameters that are still missing are determined in this section. Fouling factors are necessary in order to oversize the evaporator so as to allow for the reduction in performance during operation due to process and service fluids fouling. Charring or fooling will end in a low thermal conductivity and thus reducing the overall coefficient. An estimation of the fouling coefficients is provided by Sinnot based on common process and service fluids for shell and tube exchangers with plain tubes. (Sinnot, 2005)

Table 80.Fouling factor coefficients

h_{id} (W/m^{2}K)	6000
h_{od} (W/m^{2}K)	4500

Material selection is critical for an adequate design of the evaporator and will be discussed in Section 4.2 of this Appendix. The thermal conductivity of the selected material (k_w) and a summary of the parameters that has been estimated in order to calculate the overall heat transfer coefficient are shown in the following Table 81.

Table 81.Overall heat transfer coefficient

h_o (W/m^{2}K)	3448
h_{od} (W/m^{2}K)	4500
h_i (W/m^{2}K)	50
h_{id} (W/m^{2}K)	6000
d_o (m)	0.020
d_i (m)	0.016
k_w (W/m^{2}K) (Stainless steel)	16
$U_{o.ass}$ (W/m^{2}K)	34.57
$U_{o.calc}$ (W/m^{2}K)	38.74

$$\frac{U_{o.calc} - U_{o.ass}}{U_{o.ass}} = 12.0\ \% < 30\%$$

4.1.6. Tube-side pressure drop

Pressure drop needs to be estimated in order to assure it stands within specifications for this type of equipment. The tube friction loss is calculated by equation 70 for pressure-drop losses in pipes:

$$\Delta P_t = 8 \cdot j_f \cdot \left(\frac{L}{d_i}\right)\left(\frac{\mu}{\mu_w}\right)^{-m} \cdot \frac{\rho \cdot u_t^2}{2} \qquad \text{[Eq.70]}$$

Where *m* is 0.25 for laminar flow and 0.14 for turbulent flow. The value of the friction factor j_f is estimated as a function of the Reynolds number by following Figure 34.

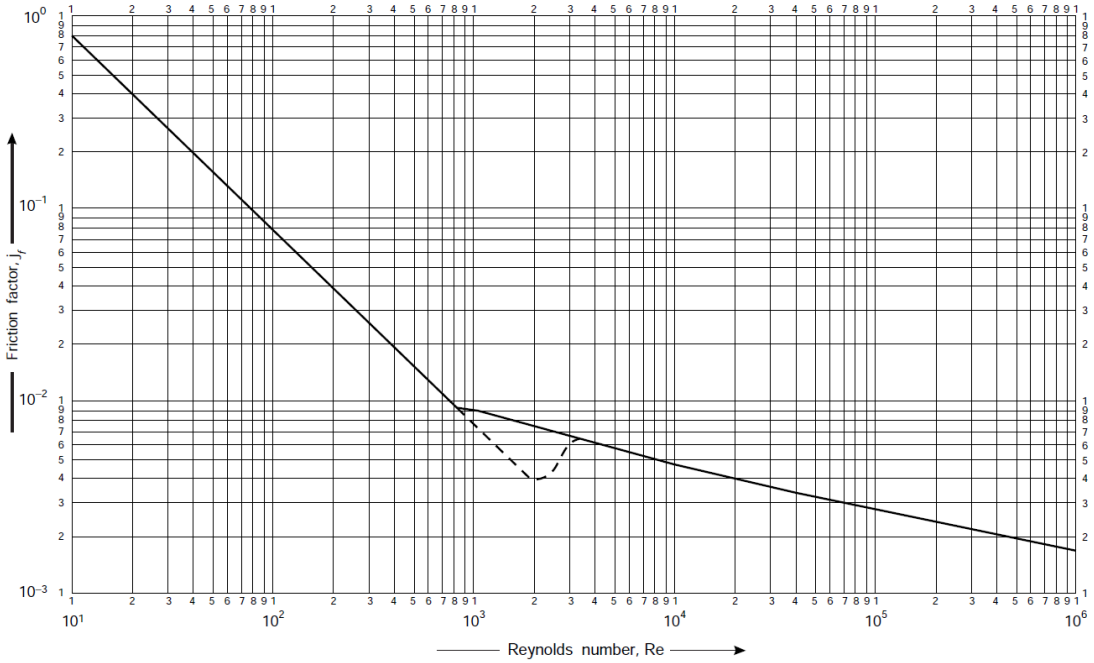

Figure 34. Tube-side friction factors (Towler, 2013)

Table 82. Tube-side liquid pressure drop

j_{fL} (-)	0.015
ΔP_{tL} (kN/m^2)	75.67

Pressure drop recommended values for liquids which viscosity is in the range [1-10] mNs/m^2, which is the case of the system considered, are in the range of [50-70] kN/m^2 for an optimum design of the equipment. The estimated pressure drop is a little over the recommended range, but it will be assume to be valid for the design.

Table 83. Tube-side gas pressure drop

j_{fG} (-)	0.003
ΔP_{tG} (kN/m^2)	1.95

Pressure drop recommended values for gases and vapours which operate under vacuum, which is the case of the system that is considered, are of 0.1·Absolute pressure (6.66 kN/m^2) for an optimum design of the equipment. The estimated pressure drop is below the recommended value so it is acceptable for the design of the equipment.

4.1.7. Shell-side pressure drop

The shell pressure drop is estimated by the following equation 71, where j_f is the friction factor estimated by the Figure 35.

$$\Delta P_s = 8 \cdot j_f \cdot \left(\frac{D_s}{d_e}\right) \cdot \left(\frac{L}{l_B}\right) \cdot \frac{\rho \cdot u_s^2}{2} \cdot \left(\frac{\mu}{\mu_w}\right)^{-0.14} \qquad \text{[Eq.71]}$$

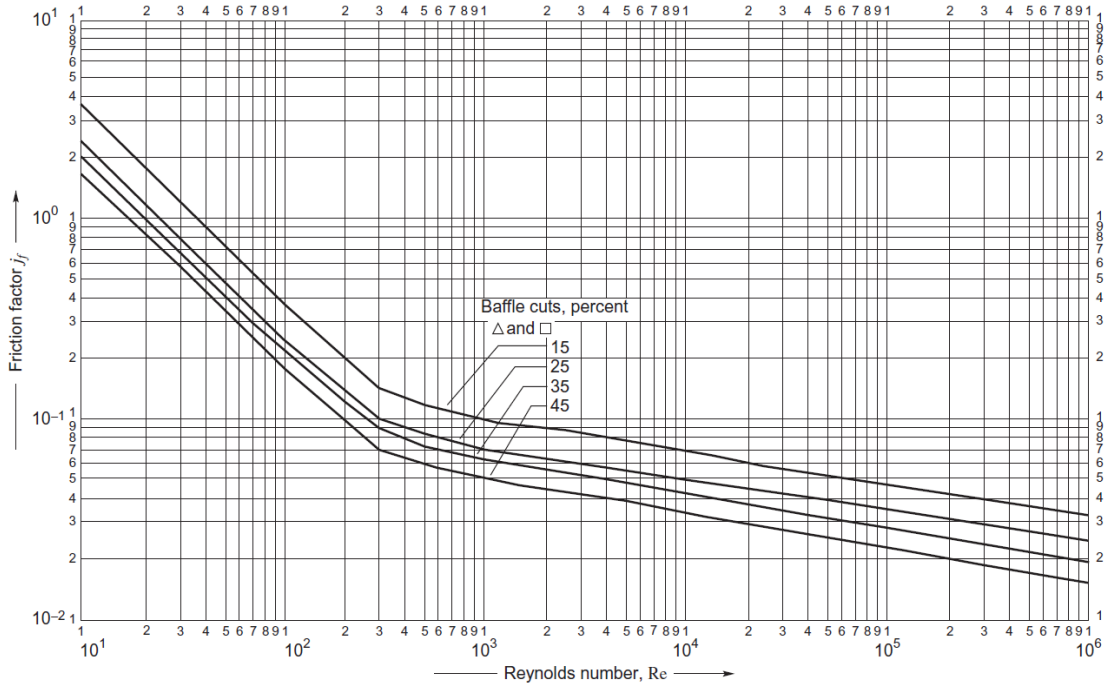

Figure 35. Shell-side friction factor - segmental baffles (Towler, 2013)

Table 84.Shell-side pressure drop

Baffle cut (%)	25
j_f **(-)**	0.052
ΔP_t **(kN/m^2)**	36.53

Pressure drop recommended values for liquids which viscosity is lower than 1 mNs/m^2, which is the case of the system that is considered, are of 35 kN/m^2 for an optimum design of the equipment. The estimated pressure drop is therefore considered acceptable for the design of the equipment.

4.2. Mechanical design

The mechanical design of the evaporator E-103 follows the design for pressure vessels specified in ASME BPV Section VIII Division 1. (Towler et al., 2013)

4.2.1. Design pressure

The design of a pressure vessel must be able to withstand the maximum pressure at which it can operate. Generally, the design pressure is oversized by [5-10]% above the operating pressure.

Table 85.Design pressure

$P_{op.max}$ **(psia)**	14.696
P_d **(psia)**	16.165

4.2.2. Design temperature

Likewise, since the resistance of metals decreases as the temperature increases, the design must be made based on the design temperature at which the maximum allowable stress must be evaluated.

- The maximum design temperature corresponds to the maximum operating temperature plus 50ºF.
- The minimum design temperature corresponds to the minimum operating temperature minus 25ºF

Table 86.Minimum and maximum design temperature

$T_{op.max}$ (ºF)	356
$T_{op.min}$ (ºF)	266
$T_{d.max}$ (ºF)	406
$T_{d.min}$ (ºF)	241

4.2.3. Construction material

The construction material selected in the design of a pressure vessel must be such that it adapts to the different process conditions such as temperature, pressure or resistance to corrosion, among other factors, while satisfying mechanical requirements such as high resistance and ease of construction. The chosen material will be the one that represents the lowest cost of equipment and that satisfies both process and mechanical requirements.

Ashby diagrams allows to select the adequate material for a system by choosing a material index M, which is intended to be maximized. One of the main objectives in the design of process units is to maximize the resistance of the vessel so that it supports the mechanical stresses to which it may be subjected. The material index is given by equation 72 where σ_f is the yield strength (resistance to elasticity for metals) and ρ the density.

$$M = \frac{\sigma_f}{\rho} \qquad \text{[Eq.72]}$$

The following Ashby diagram in Figure 36 relates both parameters. By drawing a line parallel to the reference line of the M index intended to be maximized, the appropriate type of material is determined.

It is obtained that the suitable materials for construction are steels, alloys, certain ceramics and composites. The selection of the chosen material will be justified according to the process environment. Generally, the materials used in process vessels are carbon steels, low and high steel alloys, other alloys, coated plates and reinforced plastics.

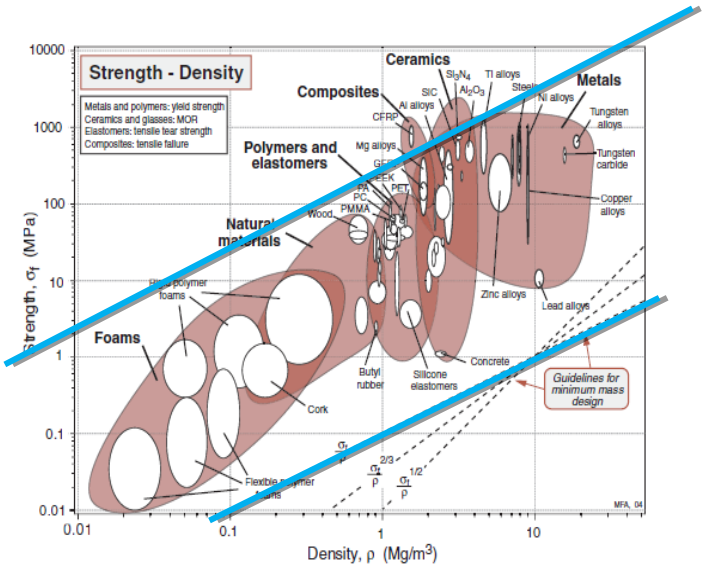

Figure 36. Yield strength vs density for different materials (Ashby, 2005)

As mentioned in previous sections, lactic acid has a high corrosion capacity against certain materials, and therefore a material whose corrosion resistance is adequate needs to be selected. SANDVIKD Advanced Materials Company provides materials tailored to lactic acid based on corrosion rate, temperature, and substance concentration, as shown in Table 87. A caption is provided in Table 88 to ease the interpretation of Table 87.

Table 87. Corrosion rate for different lactic acid concentrations and temperatures (Sandvik, 2020)

Conc. %	50	50	75	75	75	80	80	80	90	90	90	90
Temp. °C	75-90	95-104	20-90	100	110	20-95	100	117	20	40	50-100	127
Carbon steel	2	2	2	2	2	2	2	2	2	2	2	2
13 Cr	2	2	2	2	2	2	2	2	2	2	2	2
Sandvik 1802	0	1	0	0	0	0	0	1	0	0	0	1
Sandvik 3R12	1	2	0	1	1	0	1	2	0	1	2	2
Sandvik 3R60	0	1	0	0	0	0	0	1	0	0	0	1
Sandvik 2RK65	0	1	0	0	0	0	0	0	0	0	0	0
Sanicro 28	0	0	0	0	0	0	0	0	0	0	0	0
254 SMO	0	0	0	0	0	0	0	0	0	0	0	0
654 SMO	0	0	0	0	0	0	0	0	0	0	0	0
Sandvik SAF 2304	0	0	0	0	0	0	0	0				1
Sandvik SAF 2205	0	0	0	0	0	0	0	0	0	0	0	0
Sandvik SAF 2507	0	0	0	0	0	0	0	0	0	0	0	0
Titanium (CP Ti)	0	1	0	0	1	0	0	1	0	0	0	1

Table 88. Corrosion rate identification (Sandvik, 2020)

Symbol	Corrosion rate	Description
0	< 0.1 mm/year	The material is corrosion proof
1	[0.1-1.0] mm/year	The material is not corrosion proof, but useful in certain cases
2	> 1 mm/year	Serious corrosion problems. The material is not usable.

Based on Table 87 and operating conditions, the optimal material that satisfies these conditions is SANDVIK 2RK65^{TM} , which is a high-alloy austenitic stainless steel intended for use under severe corrosive conditions within the process industry.

The maximum allowable stress is the maximum stress that a vessel construction material is capable of withstand. This value varies depending on the temperature and the material used. For the selected material, the maximum allowable stress at the design temperature is of 22.27 ksi.

4.2.4. Shell thickness

The minimum shell thickness for cylindrical vessels under internal pressure must be the highest value of the thicknesses calculated by equations 73 and 74, following the ASME BPV Sec. VIII D.1 code.

- Minimum thickness for radial stress:

$$t_R = \frac{P_i \cdot D_i}{2 \cdot S \cdot E - 1.2 \cdot P_i} \quad \text{[Eq.73]}$$

- Minimum thickness for longitudinal stress:

$$t_L = \frac{P_i \cdot D_i}{4 \cdot S \cdot E - 0.8 \cdot P_i} \quad \text{[Eq.74]}$$

Where P_i is the internal pressure design (psi), D_i is the internal shell diameter (in), S is the maximum allowable stress (psi) and E is the welded joint efficiency.

However, a minimum wall thickness should be considered in order to ensure that the vessel is resistant enough to support its weight and possible loads. This minimum thickness includes the 2 mm of corrosion and is given as a function of the shell diameter.

Table 89. Minimum shell thickness for pressure vessels (Sinnot, 2005)

Shell diameter (m)	Minimum thickness (mm)
1	5
1-2	7
2-2.5	9
2.5-3.0	10
3-3.5	12

The strength of a welded joint depends mainly on the type of joint as well as the quality of the weld. To evaluate this, visual inspections are carried out using non-destructive

techniques, such as visual inspections or radiographic examinations that determine the welding efficiency.

The mechanical design of a pressure vessel must consider a welding factor that takes into account the type of joint and the radiography required. Table 90 shows different welding efficiencies depending on the type of joint and degree of inspection.

Table 90.Maximum allowable joint efficiency (Towler, 2013)

Joint description	**Joint category**	**Degree of radiographic examination**		
		Full	**Spot**	**None**
Double-welded butt joint or equivalent	A. B. C. D	1.0	0.85	0.7
Single-welded butt joint with backing strip	A. B. C. D	0.9	0.8	0.65
Single-welded butt joint without backing strip	A. B. C	NA	NA	0.60
Double full fillet lap joint	A. B. C	NA	NA	0.55
Single full fillet lap joint with plug welds	B. C	NA	NA	0.50
Single full fillet lap joint without plug welds	A. B	NA	NA	0.45

The need for a minimum thickness is important to avoid material losses through corrosion or erosion. For carbon steels or low alloy steels, when the corrosion conditions are not severe, an additional minimum thickness of 2 mm should be used. When the corrosion conditions are more severe, which is the case considered, the additional thickness should be increased by 4 mm. (Sinnot, 2005)

Table 91.Shell thickness

P_i (psi)	16.165
D_i (in)	28
S (psi)	22266
E	1
t_R (in)	$1.016 \cdot 10^{-2}$
t_L (in)	$0.508 \cdot 10^{-2}$
t_R (mm) +4 mm corrosion	4.26
t_L (mm) +4 mm corrosion	4.13

The minimum thickness calculated for both radial stress and longitudinal stress give similar values but both less than the minimum thickness shown in Table 89. Therefore, the thickness chosen is the minimum indicated in said table for recipients of 1 meter diameter. Note that said minimum thickness already includes 2 mm of corrosion, and an extra 2 mm is added for corrosion due to the presence of lactic acid. It is concluded that the minimum shell thickness is 7 mm.

4.2.5. Head types and thickness

For cylindrical vessels, there are 3 common head types whose selection depends on various factors. The torispherical head, figure 37 c), is the type of head most used for pressures lower than 15 bar, mainly due to its low cost. For pressures greater than 15 bar, however, the use of ellipsoidal heads as shows figure 37 b) may be more economical. Figure 37 a) shows a hemispherical head, which provides a greater internal volume and is capable of withstanding higher pressures for the same thickness than a torispherical head. However, their manufacturing cost is higher and their use is generally reduced to high pressures.

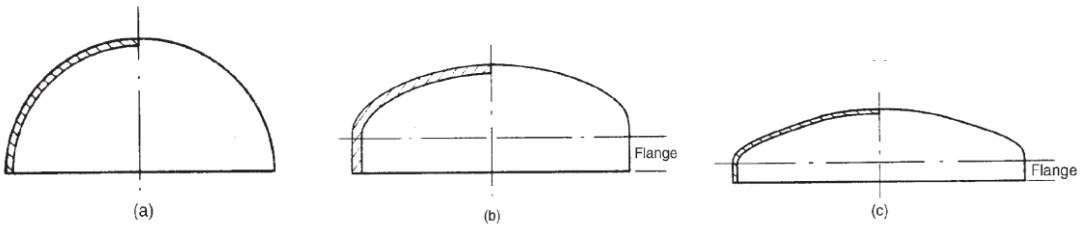

Figure 37. Head types (Sinnot, 2005)

The following equations 75 – 77 allows to obtain the minimum thickness in the different types of heads based on the ASME BPV Sec. VIII D.1 code.

- Hemispherical head:

$$t = \frac{P_i \cdot D_i}{4 \cdot S \cdot E - 0.4 \cdot P_i} \quad \text{[Eq.75]}$$

- Ellipsoidal head:

$$t = \frac{P_i \cdot D_i}{2 \cdot S \cdot E - 0.2 \cdot P_i} \quad \text{[Eq.76]}$$

- Torispherical head:

$$t = \frac{0.885 \cdot P_i \cdot R_c}{S \cdot E - 0.1 \cdot P_i} \quad \text{[Eq.77]}$$

Table 92.Head thickness for different types

Head type	Torispherical	Ellipsoidal	Hemispherical
t (in)	0.0180	0.0102	0.0051
t (mm) + 4 mm corrosion	4.4570	4.3582	4.1291

Table 92 shows the minimum thickness necessary for the three types of heads. It can be seen that the minimum thickness is that of the hemispherical head. However, as mentioned above, the hemispherical head entails a higher manufacturing cost and therefore its use is reduced to recipients that operate at high pressures. Evaporator E-103 does not operate at higher pressures than 15 bar and therefore the ellipsoidal head would also entail a higher cost compared to the torispherical head despite having a higher thickness.

In this way the torispherical head is selected for evaporator E-103. The minimum thickness necessary for the torispherical head is again less than the minimum necessary thickness indicated in Table 91 so thickness of the chosen head will be 7 mm.

The torispherical head dimensions are estimated using equations 78 to 82, referring to the parameters shown in Figure 38, where D_e correspond to the external diameter of the evaporator and s to the shell thickness.

$$R = D_e \quad \text{[Eq.78]}$$

$$r = 0.1 \cdot D_e \quad \text{[Eq.79]}$$

$$h = 3.5 \cdot s \quad \text{[Eq.80]}$$

$$H_i = 0.1935 \cdot D_e + h \quad \text{[Eq.81]}$$

$$H_t = H_i + s \quad \text{[Eq.82]}$$

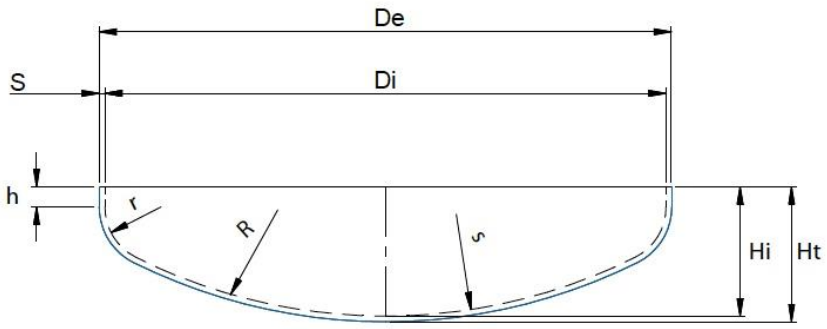

Figure 38. Torispherical head sizing

Table 93. Torispherical head sizing

R (mm)	711.2
r (mm)	71.12
h (mm)	24.50
H_i (mm)	162.12
H_t (mm)	169.12

4.2.6. Design loads

The main loads to which a process vessel can be subjected to are:

- Pressure loads.
- Loads due to the weight of the evaporator and internal accessories, in operating conditions.
- Loads due to the weight of the evaporator and internal accessories, under hydraulic test conditions.
- Wind load.
- Seismic loads.
- Loads supported or reacting in the evaporator.

The combination of possible loads that causes the worst case scenario must be estimated and a design must be based on that scenario in order to satisfy mechanical requirements. The thickness estimated in the previous section will be used to estimate the following loads, assuring the resulting stresses are below the maximum allowed for the selected material.

4.2.6.1. Pressure loads

The longitudinal stress (σ_L) and circumferential stress (σ_h) due to pressure, both internal and external, is given respectively by the following equations 83 and 84.

$$\sigma_h = \frac{P \cdot D_i}{2 \cdot t} \quad \text{[Eq.83]}$$

$$\sigma_L = \frac{P \cdot D_i}{4 \cdot t} \quad \text{[Eq.84]}$$

Table 94. Longitudinal and circumferential stresses.

$\boldsymbol{P_i}$ $\boldsymbol{(N/mm^2)}$	0.111
$\boldsymbol{D_i}$ **(mm)**	711.2
t (mm)	7
$\boldsymbol{\sigma_L}$ $\boldsymbol{(N/mm^2)}$	2.83
$\boldsymbol{\sigma_H}$ $\boldsymbol{(N/mm^2)}$	5.66

4.2.6.2. Dead weight of vessel and contents load

The stress due to the weight of the evaporator can be traction (+) or compression (-) depending on whether we are above or below the evaporator support. The usual support for vertical equipment is the skirt type support, which is allocated at the base of the evaporator, so the stress due to the weight is considered compressive and therefore negative.

$$\sigma_W = \frac{W_{total}}{\pi \cdot (D_i + t) \cdot t} \quad \text{[Eq.85]}$$

Where W is the total weight of the vessel, which it can be estimated by the following equation 86, including internal accessories. The total weight does not include the weight of the liquid inside the evaporator, as in skirt-type supports this weight is transferred directly to the support.

$$W_v = C_v \cdot \pi \cdot \rho_v \cdot D_m \cdot g \cdot (H_v + 0.8 \cdot D_m) \cdot t \cdot 10^{-3} \quad \text{[Eq.86]}$$

C_v is a correction factor that accounts for the weight of nozzles, manways, internal supports, etc., and can be taken a value of 1.15 for this type of vessels. H_v is the height of the cylindrical section, ρ_v is the density of the vessel material and D_m ($D_m = D_i + t$) is the mean diameter of the vessel.

For a steel vessel, equation 86 can be reduced to the following equation 87.

$$W_v = 240 \cdot C_v \cdot D_m \cdot (H_v + 0.8 \cdot D_m) \cdot t \quad \text{[Eq.87]}$$

The height of the evaporator will be estimated as the sum of the length of the tubes plus the inferior part of the evaporator.

$$H_v = H_{tubes} + H_{inferior} \quad \text{[Eq.88]}$$

At the bottom, the height must be high enough to allow a liquid sump at the bottom of the evaporator as well as a decoupling space that the vapour may require. Recommended values are between 5 to 10 ft. In addition, it is recommended the height to be less than 53 m and the H/D ratio below 30. For 20 < H/D < 30, special design should be considered. (Towler et al., 2013)

Table 95. Height of evaporator E-103

H_{tubes} (m)	4.88
$H_{inferior}$ (m)	1.83
H_v (m)	6.71
H/D	9.43

It is verified that height of the vessel is within the recommended values as it is under 53 m and a H/D ratio below 20.

Table 96. Weight load

C_v	1.15
D_m (m)	0.718
H_v (m)	6.71
t (mm)	7
W_v (N)	10106.1
σ_w (N/mm^2)	0.64

4.2.6.3. Wind load

For the calculation of the wind load, the evaporator will be considered as a cantilever beam and the wind as a uniformly distributed load acting along the vessel. Thus, the bending moment M_x is given by the following equation 89, varying parabolically from 0 at the top of the equipment to reaching the maximum value at the base, as shown in Figure 39.

$$M_x = \frac{F_w \cdot {H_v}^2}{2} \qquad \text{[Eq.89]}$$

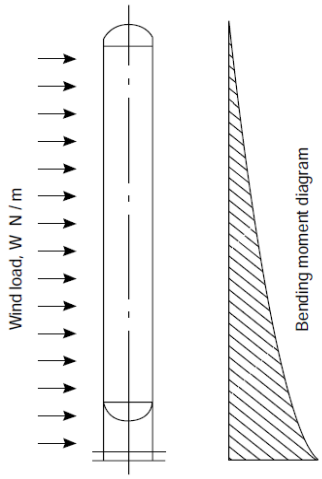

Figure 39. Wind load in vertical vessel

The load due to the wind action depends on both the shape of the evaporator and the speed of the wind, as shown by the equation 90, where Cd is the Drag coefficient, ρ_a is the air density and u_w is the wind velocity.

$$P_w = \frac{1}{2} \cdot C_d \cdot \rho_a \cdot u_w^2 \qquad \text{[Eq.90]}$$

For cylindrical structures, the wind load can be estimated using the following semi-empirical equation 91, where P_w is in N/m^2 and u_w in km/h.

$$P_w = 0.05 \cdot u_w^2 \quad \text{[Eq.91]}$$

Wind speed should be considered as the maximum speed that can occur at the location during the life of the plant. Thus, the load per unit length of the evaporator is calculated using equation 92 where the effective diameter D_{eff} is considered as the outer diameter plus an excess for thermal insulation and accessories, generally a value of 0.4 m.

$$F_w = P_w \cdot D_{eff} \quad \text{[Eq.92]}$$

$$\sigma_b = \pm \frac{M_v}{I_v} \cdot \left(\frac{D_i}{2} + t\right) \quad \text{[Eq.93]}$$

Where M_v is the total bending moment in the plane considered and I_v is the second moment of area of the vessel in the bending plane, estimated as a function of the external and internal diameter of the vessel.

$$I_v = \frac{\pi}{64} \cdot \left(D_0^4 - D_i^4\right) \quad \text{[Eq.94]}$$

The positive and negative sign of σ_b is due to whether it is tensile or compressive stress, depending on the point of the evaporator that is being considered. Both values must be taken into account.

For the wind load, a maximum speed of 120 km/h is considered. Table 97 collects the results obtained, as well as the necessary parameters for its estimation.

Table 97. Wind load

$\boldsymbol{u_w}$ **(km/h)**	120
$\boldsymbol{P_w}$ $\boldsymbol{(N/m^2)}$	360
$\boldsymbol{D_{eff}}$ $\boldsymbol{(m)}$	1.12
$\boldsymbol{F_w}$ **(N/m)**	405.07
$\boldsymbol{M_x}$ **(N·m)**	9115.74
$\boldsymbol{I_v}$ $\boldsymbol{(mm^4)}$	$1.02 \cdot 10^9$
$\pm\boldsymbol{\sigma_b}$ $\boldsymbol{(N/mm^2)}$	3.24

4.2.6.4. Combined loads

Taking into account the major loads to be considered, the principal stresses to consider will be given by the following equations 95 to 97.

$$\sigma_1 = \frac{1}{2} \cdot \left[\sigma_h + \sigma_z + \sqrt{(\sigma_h - \sigma_z)^2 + 4 \cdot \tau^2}\right] \quad \text{[Eq.95]}$$

$$\sigma_2 = \frac{1}{2} \cdot \left[\sigma_h + \sigma_z - \sqrt{(\sigma_h - \sigma_z)^2 + 4 \cdot \tau^2}\right] \quad \text{[Eq.96]}$$

$$\sigma_3 = 0.5 \cdot P \quad \text{[Eq.97]}$$

Where the torsional stress τ can be considered non-significant, σ_3 is negligible in thin-walled vessels and σ_z is the total longitudinal stress calculated as:

$$\sigma_z = \sigma_L + \sigma_w \pm \sigma_b \quad \text{[Eq.98]}$$

In this way, using the theory of maximum shear stress, the maximum intensity of stress allowed at any point of the evaporator for its design is given by the maximum value calculated by means of the equations 99 to 101.

$$\sigma_1 - \sigma_2 \quad \text{[Eq.99]}$$

$$\sigma_1 - \sigma_3 \quad \text{[Eq.100]}$$

$$\sigma_2 - \sigma_3 \quad \text{[Eq.101]}$$

And the thickness of the shell, initially assumed, must ensure that the maximum stress intensity does not exceed the maximum stress allowed for the chosen construction material at any point in the vessel.

Moreover, when the longitudinal stress σ_z is compressive, the design of the evaporator must ensure that the maximum value of the resultant of the axial stress does not exceed the critical value at which the vessel can fail due to buckling, in addition to the maximum stress allowed for the material of construction, which value is given by the following equation 102.

$$\sigma_c = \frac{E}{\sqrt{3 \cdot (1-\upsilon^2)}} \cdot \left(\frac{t}{R_p}\right) \quad \text{[Eq.102]}$$

Where R_p is the curvature radius and υ is the Poisson coefficient. For a value of υ of 0.3, and cylindrical steel vessel at room temperature, with E = 200 N/mm^2 and a safety factor of 12, the equation, in N/mm^2, is reduced to:

$$\sigma_c = 2 \cdot 10^4 \cdot \left(\frac{t}{D_0}\right) \quad \text{[Eq.103]}$$

Table 98.Combined load verification

$\boldsymbol{\sigma_z}$ $\boldsymbol{(N/mm^2)}$	5.44
$\boldsymbol{\sigma_c}$ $\boldsymbol{(N/mm^2)}$	193.05
$\boldsymbol{\sigma_1 - \sigma_2}$ $\boldsymbol{(N/mm^2)}$	11.10
$\boldsymbol{\sigma_1 - \sigma_3}$ $\boldsymbol{(N/mm^2)}$	5.66
$\boldsymbol{\sigma_2 - \sigma_3}$ $\boldsymbol{(N/mm^2)}$	5.44
S $\boldsymbol{(N/mm^2)}$	153.52

It is verified that the maximum stress intensity ($\sigma_1 - \sigma_2$) is well below the maximum allowable stress S. It is also verified that the compressive longitudinal stress σ_z does not exceed the critical value at which the vessel can fail due to buckling σ_c. The shell thickness is the minimum recommended for vertical vessels with a diameter of less than 1 meter. If this were not the case, the option of reducing the thickness in order to reduce costs could be considered.

4.2.7. Support design

The selection of the type of support depends on several factors such as the size, shape and weight of the vessel, the design temperature and pressure, the location and the internal and external accessories of the evaporator. For vertical recipients, skirt-type supports are generally

used, designed in such a way that it is capable of supporting the loads at which the recipient is subjected, in addition to allowing easy access to the vessel and to accessories for inspection and maintenance.

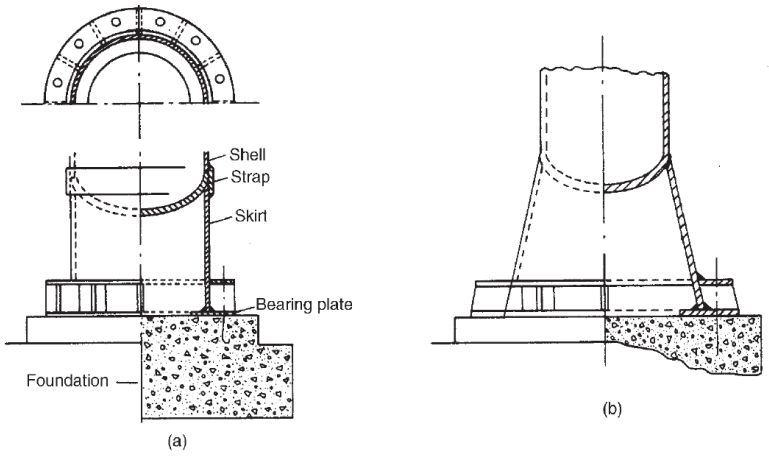

Figure 40. Skirt-type support a) Straight skirt. b) conical skirt. (Sinnot, 2005)

The skirt-type support consists on a cylindrical or conical shell welded to the base of the evaporator so that the load is transmitted to its foundations. Skirt thickness must be high enough to support the dead weight loads and the bending moments to which it is subjected. The resulting stresses are calculated by the following equations 104 and 105, where σ_{bs} is the bending stress and σ_{ws} the stress due to the dead weight on the skirt.

$$\sigma_s(traction) = \sigma_{bs} - \sigma_{ws} \quad \text{[Eq.104]}$$

$$\sigma_s(compression) = \sigma_{bs} + \sigma_{ws} \quad \text{[Eq.105]}$$

σ_{bs} and σ_{ws} are estimated by equations 106 and 107 where M_s is the maximum bending moment, evaluated at the base of the support, D_s is the internal diameter of the support base, t_s the thickness of the support and W the total weight of the evaporator, including the weight of the liquid.

$$\sigma_{bs} = \frac{4 \cdot M_s}{\pi \cdot (D_s + t_s) \cdot t_s \cdot D_s} \quad \text{[Eq.106]}$$

$$\sigma_{ws} = \frac{W}{\pi \cdot (D_s + t_s) \cdot t_s} \quad \text{[Eq.107]}$$

$$W_{liquid} = \frac{\pi \cdot D_i^2}{4} \cdot H_v \cdot \rho_L \cdot g \quad \text{[Eq.108]}$$

Table 99. Bending stress and stress due to the dead weight on the skirt

$\boldsymbol{W_{liquid}}$ **(N)**	29286.56
$\boldsymbol{W}$ **(N)**	39392.67
$\boldsymbol{D_s}$ **(m)**	0.7112
$\boldsymbol{t_s}$ $\boldsymbol{(m)}$	0.007
$\boldsymbol{\sigma_{ws}}$ $\boldsymbol{(N/mm^2)}$	0.640
$\boldsymbol{H_s}$ $\boldsymbol{(m)}$	1.50
$\boldsymbol{F_w}$ $\boldsymbol{(N/m)}$	405.07
$\boldsymbol{M_s}$ $\boldsymbol{(N \cdot m)}$	13647.77
$\boldsymbol{\sigma_{bs}}$ $\boldsymbol{(N/mm^2)}$	4.86

The minimum thickness of the support must not be less than 6 mm, not including the corrosion thickness, and must be such that it satisfies the following design conditions:

$$\sigma_s(tracción) \not> S_s \cdot E \cdot \sin(\theta_s) \quad \text{[Eq.109]}$$

$$\sigma_s(compresión) \not> 0.125 \cdot E \cdot \left(\frac{t_s}{D_s}\right) \cdot \sin(\theta_s) \quad \text{[Eq.110]}$$

Being S_s the maximum stress allowed for the support construction material and θ_s the angle of the base of the conical skirt, generally between 80º and 90º.

Table 100. Verification of design conditions

$\boldsymbol{\sigma_s(traction)(N/mm^2)}$	2.36
$\boldsymbol{\sigma_s(compression)\ (N/mm^2)}$	7.35
$\boldsymbol{\theta_s}$ **(°)**	90
$\boldsymbol{E_y\ (N/mm^2)}$	210000
$\boldsymbol{S_s\ (N/mm^2)}$	88.94
Condition 109 $\boldsymbol{(N/mm^2)}$	OK
Condition 110 $\boldsymbol{(N/mm^2)}$	OK

It is verified that both stresses satisfy design conditions and therefore the angle of the base, the thickness, and the height of the support initially assumed is considered as valid for the support design.

4.2.8. Openings and openings compensation

The process vessels have accessories and openings that can cause concentration of specific stresses. That is why the wall thickness is increased at these points in order to compensate for stress differences.

The compensation type is the use of a welded collar around the openings as it is the simplest and most common type of compensation, with an external diameter of 1.5 to 2 times the diameter of the opening. This diameter corresponds to the standardized external diameter of each stream, which will be calculated based on the flow to be treated, its density and its velocity.

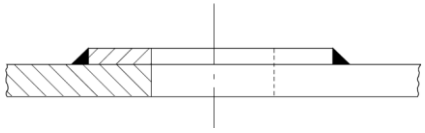

Figure 41. Welded collar around openings. (Sinnot, 2005)

The openings diameter is estimated based on the volumetric flow over the pipe and an initially estimated velocity within recommended values. Velocities recommended values in pipes range from [1-3] m/s and [10-30] m/s for liquids and vapour and gases, respectively. (Turton et al., 2012) Openings sizing is shown in the following Table 101, which diameters has been standardized according to the ASME Code B.36.19 for stainless steel. The selected external diameter of the aperture compensation is 1.5 times the standardized diameter of the stream

Table 101. Openings sizing

Stream	Q (m^3/h)	v_{ass} (m/s)	D_i (mm)	Sch (-)	$D_{i,st}$ (mm)	t (mm)	D_e (mm)	DN	v_{real} (m/s)
5	14.4	1.5	58.30	80	60.3	5.54	71.38	50	1.40
6	1036.5	20	135.39	80	141.3	9.53	160.36	125	18.36
7	10.2	1.5	49.14	80	48.3	5.08	58.46	40	1.55
cw	23.2	1.5	73.92	40	73.0	5.16	83.32	65	1.54
cwr	23.3	1.5	74.11	40	73.0	5.16	83.32	65	1.55